Particle Size Analysis by Laser Diffraction Spectrometry: Application to Cementitious Powders

Vincent A. Hackley
Lin-Sien Lum
Vadas Gintautas
Chiara F. Ferraris

NIST

National Institute of Standards and Technology
Technology Administration, U.S. Department of Commerce

Particle Size Analysis by Laser Diffraction Spectrometry: Application to Cementitious Powders

Vincent A. Hackley
Lin-Sien Lum
Vadas Gintautas
Materials Science and Engineering Laboratory
National Institute of Standards and Technology

Chiara F. Ferraris
Building and Fire Research Laboratory
National Institute of Standards and Technology

March 2004

FORWARD

Particle size distribution (PSD) measurements are now routinely employed to characterize cement powders. A variety of techniques are available for this purpose. However, at present, an industry standard does not exist for PSD analysis, nor do uniform methods exist for sample preparation. Two recent international round-robin tests sponsored by ASTM committee C01.25.01 revealed high variability in reported PSDs, even among participants using similar instruments. The round-robin studies also identified laser diffraction spectrometry (LDS) as the most common technique used by the cement community for routine determination of PSD. Therefore, studies were conducted to identify and examine the factors that significantly influence the determination of the PSD in cement powder by LDS. Potentially, the single most significant influence on measurement of the PSD arises from the requirement that powders be dispersed prior to analysis by LDS; dispersion efficiency will depend on factors such as solids concentration, choice of dispersion medium, and the application of chemical and/or mechanical deagglomeration methods. Another potentially significant source of error originates from the conversion of the measured optical spectrum to a PSD, a process that requires application of an appropriate optical model. The Mie model requires input of optical constants (real and imaginary refractive index) for the solid phase. The choice of optical constants can greatly influence the PSD, especially the ultrafine fraction (below about 1 µm diameter). The current work was undertaken with the objective of improving the precision, and therefore the degree of confidence, associated with the LDS technique in its application to cement characterization, and to assess the overall measurement precision of LDS under controlled conditions. We report all relevant experimental data gathered in the course of these studies, and briefly summarize each set of results pertaining to a specific influence or parameter.

ACKNOWLEDGEMENTS

TABLE OF CONTENTS

LIST OF FIGURES

LIST OF TABLES

TERMS, SYMBOLS AND ABBREVIATIONS

Frequently used and/or critical terms, symbols and abbreviations are defined below. Where applicable, terminology relating to dispersion and particulate systems follows NIST recommended practice guide 960-3.[1] In general, definitions relating to optical aspects are consistent with ISO 13320-1:1999(E).[2]

absorption Reduction of intensity of a light beam traversing a medium through energy conversion in the medium (e.g., conversion to heat). Although absorption does not contribute directly to scattering or diffraction, it nevertheless impacts diffraction spectra by reducing the angle-dependent intensity of diffracted light. Absorption is a function of the size and complex refractive index of the absorbing particles.

aerosol Particles dispersed in a gaseous phase.

agglomerate An aggregation of particles held together by physical forces, and which can be dispersed (deagglomerated) by mechanical and/or chemical treatment.

coefficient of variation Relative measure (%) for precision; standard deviation divided by mean value of population and multiplied by 100 (for normal distributions of data the median is equal to the mean).

complex refractive index, $m = n + ik$ There are two so-called optical constants for a material phase at a given wavelength (i.e., the real, n, and imaginary, k, components of the complex refractive index). The real component determines refraction and reflection, while the imaginary component accounts for absorption. The optical constants are not directly measurable, but must be derived from measurable quantities such as reflectance and transmittance, or angles of refraction. The optical constants are critical parameters for accurate measurements using the Mie optical model.

cumulative volume PSD A function that shows the cumulative volume of particles characterized by particle sizes below a specified size and plotted over a range of specified sizes. This function rises from 0 % at small sizes and approaches 100 % at large sizes, often exhibiting a sigmoidal shape.

differential volume PSD A function giving the fractional volume of particles falling within a series of specified size intervals versus the characteristic size for the interval. This method of presenting size data has been adopted by most instrument companies, but it leads to certain limitations on the interpretation and comparison of size data that are described in detail in Appendix A.

diffraction Spreading of light around the contour of a particle beyond the limits of its geometrical shadow with a small deviation from rectilinear propagation. Diffraction is independent of the refractive index of the particles.

dispersion In general, a two-phase system in which discontinuities of any kind (solid, liquid, gas) are dispersed in a continuous phase of a different composition or state; more specifically in regard to laser diffraction, the term dispersion is used to describe solid particles suspended in a liquid medium or stream of air. Also refers to the actual process of dispersing a powder into a continuous medium.

dispersion medium A continuous liquid or gas phase into which a powder is dispersed prior to analysis by LDS.

IPA Isopropyl alcohol (isopropanol).

isoelectric point (IEP) The pH at which particles in an aqueous dispersion have an electrokinetic potential of zero. The IEP generally indicates the pH of lowest stability against agglomeration for particles stabilized by electrostatic charge, and is typically determined by measurement of the zeta potential.

laser diffraction spectrometry (LDS) Refers to a general technique by which particle size is determined from an analysis of the laser scattering spectrum of a dilute dispersion of particles.

median diameter (d_{50}) The particle diameter representing the 50th percentile of a mass or volume weighted PSD: 50 % of the total mass or volume of particles in a PSD will fall below the median diameter and 50 % will exceed that value. Similarly, d_{10} and d_{90} represent the 10th and 90th percentiles, respectively. These diameters are used to characterize various fractions within a PSD.

obscuration Percentage of incident light that is attenuated due to extinction (scattering and/or absorption) by the particles.

optical constants see complex refractive index

optical model A mathematical construct used to convert an experimental laser diffraction spectrum into a PSD based on a specific optical scattering theory and input parameters.

particle size distribution (PSD) A function that describes the size dependency of the frequency of particles falling within a specified size increment or below a specified size.

relative refractive index (n_R) Ratio of the refractive index of the dispersed phase to the refractive index of the dispersion medium.

residual agglomerate An agglomerate of primary particles that persists beyond the normal dispersion process.

polarization intensity differential scattering (PIDS) A proprietary multi-wavelength technology designed to improve the analysis of sub-micrometer particles by LDS.

powder A relatively dry accumulation of particulate matter with a macroscopic consistency.

primary particle In a powder or suspension, the finest particulate phase achievable without comminution (i.e., using chemical and/or moderate mechanical/ultrasonic means of dispersion, but not high-energy milling). Primary particles generally constitute the finest subunits in agglomerates. Primary particles are not necessarily monosize, and may be characterized by a distribution of sizes. A suspension in which the solid phase exists entirely as discrete primary particles would yield the absolute PSD for that powder. LDS cannot differentiate between large primary particles and agglomerates consisting of smaller primary particles.

reflection Return of radiation by a surface without change in wavelength.

refraction Change in the direction of propagation of light determined by a change in the velocity of propagation in passing from one medium to another, where the refractive index varies between the two media.

scattering General term describing the change in propagation of light at the interface of two media..

surfactant A substance that lowers the interfacial tension between the solution in which it is dissolved, and other phases that are present (e.g., solid particles in a liquid dispersion), and, accordingly, is positively adsorbed at the interface.

suspension A liquid in which solid particles have been dispersed. Generally synonymous with the term *dispersion* for the purpose of this document.

well-dispersed Describes a stable dispersion (suspension) in which the primary particle size has been achieved.

Terms relating to the statistical comparison of LDS data

sample Single-batch powder suspension prepared for LDS wet method analysis. In the case of dry method LDS, *sample* refers to a single batch of dry powder loaded onto the instrument for analysis.

subsample For LDS wet method, an aliquot removed from a *sample* and subsequently diluted into a volume of clear liquid for LDS analysis. Subsamples do not apply to the LDS dry method.

run Individual LDS test or measurement performed on a subsample (for wet method) or sample (for dry method) and generating a single PSD.

INTRODUCTION

The Blaine air permeability test[3] has been widely used for almost 50 years by the cement industry to assess the fineness of cement powders. Its utility arises from the close correlation between surface area and the rate of cement hydration. However, the Blaine method is somewhat cumbersome, does not lend itself to automation, and requires application of a correction factor based on analysis of a reference material.[4] Powder surface area can also be calculated based on measurement of the particle size distribution (PSD). PSD measurements may offer a rapid, more direct and user-simplified approach to fineness measurement. Although PSD measurements are increasingly employed to characterize the fineness of cement powders and to determine a Blaine-equivalent value, there is presently no standard method for determining the PSD of cement.

Two recent international round-robin studies sponsored by ASTM committee C01.25.01 revealed high variability in reported PSDs, even among participants using similar instruments.[5,6,7] The round-robin tests also identified laser diffraction spectrometry (LDS) as the most commonly used technique for routine determination of cement PSD throughout the industry. LDS instruments support two approaches to PSD analysis, namely *wet* and *dry*. In the wet method, the powder sample must first be dispersed into a non-reactive liquid carrier such as alcohol. This can be achieved by various chemical and/or mechanical means, including use of surfactants and ultrasonic treatment. In the dry method, the sample is introduced as a dry powder directly via a vacuum or compressed air stream, which then disperses and transports the material through the sensing zone. The round-robin studies indicate that the majority of cement testing laboratories use the wet method, with isopropyl alcohol (IPA) being the most common dispersion medium. However, there is significant variation, both amongst round-robin participants and in the published literature, in regard to the choice of medium and the specific procedures used to disperse cementitious powders.

Since laser diffraction is not able to differentiate between primary particles and agglomerates, the dispersion process is probably the single most critical issue impacting accuracy and precision of PSD analysis. The degree of dispersion achieved in dry aerosol methods will likely vary depending on particle size, geometry of the dispersing device, residence time in the sensing zone, and level of applied shear force. Similarly, wet dispersion methods are subject to variations in surface chemistry of the powders, solids concentration, nature of the dispersion medium, and amount and type of mechanical energy expended to break up agglomerates. An additional complicating factor is the multiphase nature of cementitious materials, which leads to varying surface chemistries and particle geometries, a highly agglomerated state, and a very broad PSD, all of which contribute to the difficulty of obtaining a consistently well-dispersed state.

Another potential source of uncertainty arises from the mathematical analysis of the measured diffraction spectrum. This analysis requires that an appropriate optical model be chosen for the test material, a choice that depends on both the particle size range and optical properties of the solid phase.[2] This is often a complex issue for cementitious materials, which typically exhibit PSDs containing a very broad range of sizes and multiple solid phases. For a PSD limited to large particles (greater than a few micrometers), the choice is simple; Fraunhofer diffraction theory provides an accurate analysis and does not require input of the optical constants (refractive indices) for the sample material. For finer particles, and depending upon the refractive index of the material, significant artifacts and errors can occur if the Fraunhofer model is applied. In this case, Mie scattering theory is warranted. The Mie optical model requires knowledge of the optical constants for both the particle and liquid phases. Since pure transparent liquids are generally used as dispersion media, optical constants are well known and present no impediment. Furthermore, optical constants for many common monophasic solids can be easily found in published sources. However, for multiphase cementitious powders, the selection of appropriate constants can be problematic. Thus, published or vendor-supplied approximate values are typically chosen, or "mean" values are

7

calculated based on the known optical constants for each constituent pure mineral phase. Cyr and Tagmit-Hamou[8] give an example of this type of calculation for a typical portland cement, and they also report the refractive index values (real component) or a range of values for each constituent phase (reproduced below in Table 1). Due to such practices, a lack of uniformity exists in the application of optical models for cement characterization, and this has no doubt contributed to variability and uncertainty in PSD measurements for cementitious materials.

Table 1. Refractive index values (real) for constituent phases in a typical portland cement powder.

mineral phase[¶]	refractive index,[§] n
C_3S	1.72
C_2S	1.73
C_3A	1.71
C_4AF	2.03
sulfates	1.56
free lime	1.84
limestone filler	1.58

[¶] C=CaO, S=SiO_2, A=Al_2O_3, F=Fe_2O_3
[§] mean value from reported range in Ref. 8

Accurate and reproducible measurement of the PSD of a cementitious powder is therefore an important practical issue for the cement industry, and it is likewise a key limiting factor in on-going computational efforts to simulate the microstructure and predict the performance of cement-based materials.[9,10,11] An analysis of the factors affecting powder dispersion and measurement by LDS should lead to a higher degree of confidence in reported data and a more efficient system of sample preparation for laboratory or industry purposes. It is also believed that such studies are necessary to identify potential significant sources of error for the development of a standard method for cement PSD measurement based on the LDS technique.

We have investigated the influence of the dispersion medium and the method of particle dispersion, and have examined the effect of variations in the optical constants and choice of optical model. In addition, we have examined the influence of dispersion methods and media on discrete size fractions using a series of high-purity aluminum oxide powders characterized by relatively narrow PSDs. As a surrogate, aluminum oxide has a density and refractive index similar to portland cement, but it is chemically stable in water unlike the latter. We report here all relevant data obtained in the course of these studies, with brief summaries of each set of data and an executive summary with conclusions at the end. The purpose of this report is to organize and present the results for further consideration and analysis. More detailed interpretation is planned for future publications.

All reported data is provided with appropriate statistical uncertainty in the form of error bars that correspond to the estimated standard deviation (combined standard uncertainty).[†] The standard deviation is calculated from replicate measurements, and is equal to the positive square root of the estimated variance for a given set of replicate measurements. No attempt has been made to identify or isolate systematic or non-random errors.

[†] see NIST Technical Note 1297, *Guidelines for Evaluating and Expressing the Uncertainty of NIST Measurement Results*, B.N. Taylor and C.E. Kuyatt (U.S. Government Printing Office, Washington, DC), 1994.

METHODS AND MATERIALS

Laser Diffraction Spectrometry

In the LDS technique, the angular distribution of light is measured after passing through an optically dilute dispersion of suspended particles (see Figure 1). The intensity of the detected signal is determined by three processes: scattering, diffraction and absorption.[12] Scattered light consists of reflected and refracted waves, and is influenced by the form, size, and composition of the particles. Diffracted light arises from edge phenomena, and is dependent only on the geometric cross-section of the particle; thus diffraction is independent of the composition and refractive properties. Absorption occurs when light is converted to other forms of energy by interaction with the particles, thereby attenuating the intensity. Absorption is influenced by both particle size and composition. LDS is sensitive to all three of these phenomena, but is often limited to light detected at the forward (low) scattering angles. More recently, instruments have incorporated wide angle and backscatter detection to aid in the analysis of finer size particles.
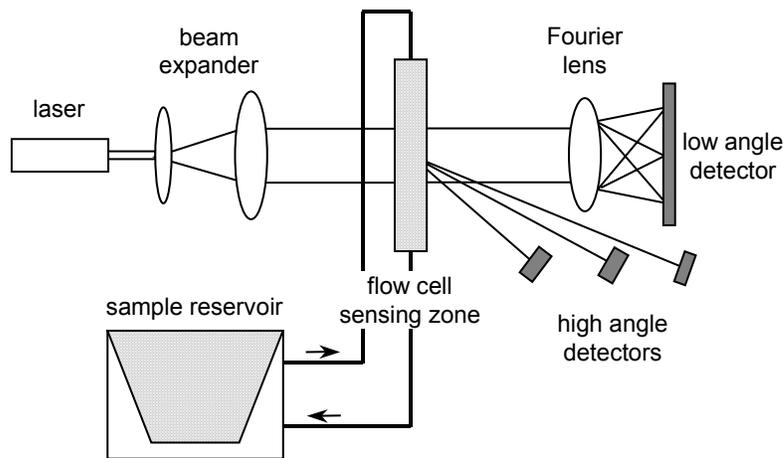
Figure 1. Schematic of the optical system for a typical laser diffraction spectrometer with a liquid flow cell. For a dry powder system, the sample reservoir is replaced by a powder loading module with an air flow handling system without a return loop.

The key material property (other than size and shape) that impacts LDS is the complex refractive index $m = n - ik$. The parameters n and k, often referred to as the optical constants, are the real and imaginary (absorptive) components, respectively, of the complex refractive index. Often, the *relative* refractive index is used, which is simply the ratio of the complex refractive index of the particulate phase relative to the dispersion medium. Scattering arises due to differences in the refractive index (real component) between the particle and the medium. Values of n have been published for many bulk monophasic materials.[13] Values used for portland cement typically range from 1.6 to 1.8.[5] Absorption becomes important primarily for the fine fraction, below about one micrometer in diameter, where it can have a large impact on the PSD. Portland cement is typically gray to off-white in color, and thus a finite, but relatively low value for the imaginary component is predicted. The value $k = 0.1$ is often reported for cement, although its appropriateness for general use has not, to our knowledge, been established.

9

There are two principal optical models for analysis of diffraction spectra: Mie and Fraunhofer. Mie theory describes scattering by homogeneous spheres of arbitrary size, and is the most rigorous optical scattering model currently available. For non-spherical particles, Mie provides a volume-weighted equivalent-spherical diameter. Mie theory has been applied with mixed success to the analysis of powders with diameters from several 100s of micrometers down to about 100 nm. An accurate representation of the "true" size distribution by Mie scattering is dependent on the input of an accurate value for the complex refractive index. For particles much larger than the wavelength of light, the Fraunhofer approximation can be used without knowledge of the refractive index, since it is based on the diffraction effect only. The range of validity for Fraunhofer is limited at the fine end to diameters a few times greater than the wavelength of light (λ) for particles that are opaque or have a large refractive index contrast with the medium.[2] For transparent particles, or particles with a moderate refraction contrast, the lower limit is raised to about 40λ; for the visible wavelengths used in most LDS instruments, this corresponds to about 25 µm. The benefit of using the Fraunhofer model is that the interpretation is not dependent on the absorptive or refractive properties of the material. The drawback is that use of the Fraunhofer approximation beyond the valid range can lead to large systematic errors in the calculated PSD.[2]

One must also consider that only narrow PSDs can show the fine-structure in an angular scattering spectrum that is characteristic of homogeneous, monodisperse spheres. For broad PSDs, this fine-structure in the spectrum is lost due to smoothing of the angle-dependent ripples that are characteristic of monosize scatterers. As a result of this smoothing, high resolution with respect to size can not be expected for materials with broad PSDs like portland cement.[2]

Materials can be analyzed by LDS using either wet or dry sampling methods. Differences between the wet and dry methods arise primarily from the different ways in which the powders are dispersed in each case. In a liquid, it is possible to modify solution chemistry, for example by changing pH or adding chemical dispersing agents. Deagglomeration can also be achieved by ultrasonic disruption. Thus, for the finest fractions, a better state of dispersion can usually be achieved in an appropriately selected liquid medium. Water is an excellent dispersing medium for most inorganic powders; however, due to the reactive nature of cement in water, alcohols are commonly used as a dispersing medium for this material. In dry powder measurements, a stream of compressed air (or a vacuum) is used to disperse the particles and to transport them through the sensing zone. This method of dispersion works best for the coarser size fractions, where interparticle contacts are weaker. For particles smaller than about 1 µm, aerosol dispersion is generally not very efficient for sizing, as will be subsequently demonstrated by studies on aluminum oxide powder.

Materials and Instrumentation

Portland cement proficiency powder #135 (for property data see Appendix B) was obtained from the Concrete and Cement Reference Laboratory (CCRL) at NIST. Six high-purity α-phase aluminum oxide powders (AKP-30, AA-07, AA-2, AA-5, and AA-10) manufactured by Sumitomo Chemical Co. (Tokyo, Japan)[†] were used as discrete size fractioned surrogate powders. Table 2 lists physical and purity data provided by the manufacturer.

---

† Certain trade names and company products are mentioned in the text or identified in illustrations in order to specify adequately the experimental procedure and equipment used. In no case does such identification imply recommendation or endorsement by National Institute of Standards and Technology, nor does it imply that the products are necessarily the best available for the purpose.

Table 2. Aluminum oxide property data from manufacturer.

Property	AKP-30	AA-07	AA-2	AA-5	AA-10
phase	α	α	α	α	α
mean particle size (μm)¶	0.3	0.6 to 0.8	1.8 to 2.2	4 to 6	8 to 11
specific surface area (m^2/g)	5 to 10	2 to 2.6	0.8 to 1.1	0.3 to 0.5	0.2 to 0.5
purity (%)	>99.99	>99.99	>99.99	>99.99	>99.99

¶ measured by x-ray gravimetric sedimentation

Aqueous solutions were prepared using high-purity deionized water (18 MΩ-cm resistance). Analytical reagent grade NaOH and HNO_3 were used to adjust the pH of aqueous aluminum oxide suspensions. Alcohol suspensions were prepared using analytical reagent grade isopropyl alcohol and n-butyl alcohol (Mallinckrodt, Paris, KY), anhydrous methyl alcohol (Mallinckrodt, Paris, KY) and 200 proof anhydrous ethyl alcohol (Warner-Graham, Cockeysville, MD). The surfactant Aerosol OT (sodium 1,4-Bis (2-ethylhexyl) sulfosuccinate) was obtained from Cytec Industries (West Paterson, NJ). The chemical additive WRDA-19 (naphthalene sulfonate, 43 % solids content), was obtained from W.R. Grace & Co., Construction Products Division (Cambridge, MA). All suspensions were prepared in Pyrex glass beakers.

All wet method LDS measurements were performed using a LS-230 spectrometer (Beckman Coulter, Hialeah, FL) with a variable-speed recirculating fluid module and software version 3.00.41. The fluid module contains a built-in low-intensity bath ultrasonication system. This instrument includes a proprietary multi-wavelength technology based on Polarization Intensity Differential Scattering (PIDS) to improve the analysis of submicrometer particles. The optical system uses a solid state 750 nm laser source and a tungsten lamp with band-pass filters at 450 nm, 600 nm and 900 nm. All cement samples were analyzed using PIDS. Aluminum oxide samples were analyzed both with and without incorporation of PIDS technology.

All dry method LDS measurements were performed using a Mastersizer 2000 (Malvern Instruments Inc., Southborough, MA) with a Scirocco 2000 dry module and version 5.1 software. This system uses a variable feed-rate vibrating tray to control powder flow into a compressed air stream, where the air flow can be controlled to ± 0.002 MPa. Dispersion occurs in the air stream due to shear forces applied during particle acceleration and through particle-wall collisions. The optical system uses two laser light sources: a He-Ne laser (633 nm) and a solid state diode laser with an unspecified wavelength in the blue spectrum.

A Sonifier 450 ultrasonicator (Branson Ultrasonics, Danbury, CT) with an immersible 1.25 cm titanium horn and a maximum output power of 450 W was used to aid dispersion of powders in liquid media. Ultrasonication was applied at an amplitude of 40 % for a specified period of time.

The zeta potential of aluminum oxide powders in aqueous media was determined using a ESA 9800 electroacoustic analyzer (Matec Applied Sciences, Hopkinton, MA).

Procedures

Basic procedure for preparing stock cement-alcohol suspensions

A 20 % mass fraction suspension was prepared by adding 20 g of powder to 80 g of alcohol. Physical property data for the alcohols used in this study are provided in Table 3. The dispersion was

mixed using a magnetic stirrer for several minutes. Using an immersion type ultrasonicator, the dispersion was ultrasonicated at 40 % amplitude for a specified period of time (1 to 5 min), using an ice bath to prevent overheating of the sample. The base-line procedure included a 5 min ultrasonic treatment.

Base-line procedure for measurement of cement-alcohol suspensions by LDS

Stock cement dispersion was added drop-wise to a circulating alcohol solution previously loaded into the instrument, until the vendor recommended obscuration level was obtained (average obscuration level 52 %, 9 % for PIDS). Cement optical constants used for the Mie analysis were $n = 1.7$ and $k = 0.1$, unless otherwise indicated. The refractive index used for each alcohol medium is listed in Table 3. Because these alcohols are optically transparent, only the real component is reported.

Table 3. Physical and optical parameters for alcohol suspending media. Values refer to 20 °C where applicable.[¶]

medium (abbrev.)	refractive index, n	density (g/cm^3)	viscosity $(mPa\ s)$	molar mass (g/mol)	SPP[§]
methyl alcohol (MeOH)	1.329	0.7914	0.597	32.042	0.857
ethyl alcohol (EtOH)	1.361	0.7893	1.200	46.07	0.853
isopropyl alcohol (IPA)	1.378	0.7855	2.31	60.096	0.848
n-butyl alcohol (BuOH)	1.399	0.8098	2.948	74.12	0.837

[¶] From Ref. 14, or calculated from relationships provided therein
[§] Solvent polarity scale. From Ref. 15.

Sample preparation procedures for alumina suspensions

A 100 mL alcohol stock suspension was prepared at a 1 % solid volume fraction using IPA as the medium. After the powder was introduced to the IPA, the suspension was equilibrated with magnetic stirring for 30 min, and then ultrasonicated in an ice bath for 4 min at 40 % amplitude and 50 % duty cycle (resulting in an actual treatment time of 2 min). The test sample was then stirred for an additional 30 min. Two alcohol suspensions were prepared for each powder.

Similarly, a 100 mL aqueous stock suspension was prepared at a 1 % solid volume fraction using deionized water as the medium. The pH of the suspension was then adjusted to pH 5.5 ± 0.1 using dilute HNO_3, following which the suspension was equilibrated with magnetic stirring for 30 min. The suspension was then ultrasonicated for 4 min at 40 % amplitude and 50 % duty cycle (resulting in an actual treatment time of 2 min). The test sample was then stirred for an additional 30 min. Before analysis, the pH was checked and readjusted if necessary. Two aqueous suspensions were prepared for each powder.

Two additional sets of samples were prepared to test the efficacy of ultrasonic treatment. In the first set, IPA suspensions for AKP-30 and AA-07 were prepared following the previously described procedure but in the absence of ultrasonication. The suspensions were equilibrated 60 min using a magnetic stirrer and then analyzed. In the second set, IPA suspensions were again prepared for these two powders following the base-line procedure, but with an actual ultrasonication treatment of 4 min (again using 40 % amplitude and 50 % duty cycle). One sample suspension per powder per condition

was prepared, and three subsamples from each sample were each analyzed, for a total of six PSD analyses per powder (three for each powder per treatment condition).

For zeta potential measurements using the electrokinetic sonic amplitude (ESA) technique, aqueous suspensions were prepared at a 2 % solid volume fraction and adjusted to pH 5.5, stirred 30 min, ultrasonicated at 40 % amplitude and 50 % duty cycle for a total treatment time of 3 min, stirred an additional 30 min, and then analyzed. Sample temperature during measurements was (30 ± 0.4) °C.

Procedure for analysis of aluminum oxide suspensions by LDS

The reservoir-recirculator on the LS-230 fluid module was loaded with either IPA or deionized water adjusted to pH 5.5 ± 0.1, after which the background spectrum was measured according to the manufacturer's instructions. Stock suspension was then added drop-wise to the reservoir until the recommended obscuration range was achieved (average obscuration level 46 %, 8 % for PIDS), after which measurements were commenced. Three subsamples were taken from each suspension, and each subsample was analyzed once, for a total of six PSD measurements per powder. This process was performed for both IPA and aqueous suspensions. Table 4 lists the optical constants used in the Mie optical model for the analysis of aluminum oxide.

Table 4. Optical constants used in the analysis of aluminum oxide with the LS-230 spectrometer.

Wavelength (nm)	Dispersion Medium		α-Al_2O_3	
	H_2O (n)	IPA (n)	n	k
750	1.332	1.377	1.762	0
PIDS 450	1.332	1.377	1.779	0
PIDS 600	1.332	1.377	1.768	0
PIDS 900	1.332	1.377	1.758	0

Procedure for analysis of aluminum oxide powders by dry-method LDS

Each powder sample was loaded into the feeder bin of the Mastersizer 2000 dry powder module. Manufacturer recommended settings and protocols were used where appropriate. A vibration level of 75 % was used in the feeder. The air stream pressure was set at 0.4 MPa. Three runs were performed for each powder sample. The refractive index for aluminum oxide was set at $n = 1.762$ with $k = 0$. The suspending medium, air, is assigned a refractive index $n = 1$ by default.

EXPERIMENTAL RESULTS

Analysis of Cement PSD by LDS

Background

In this study, the effects of various factors thought to influence the analysis of the PSD in cement powder by the LDS technique were examined using a typical portland cement (CCRL 135 – see Appendix B) as test material. The study focused on wet (alcohol-based) dispersion methods. The overall objective is to develop a strategy for PSD analysis that would result in improvements in both accuracy and precision relative to existing industry practices. In developing best practice guidelines, two key issues were identified: sample preparation (i.e., the dispersion process) and choice of optical model. The experiments published here were designed to address these issues. First, a series of alcohols are examined to determine the influence of the medium on dispersion. As an extension to this exercise, an aqueous-based alternative procedure for PSD analysis is presented. Next, the application of high-energy ultrasonic treatment and surfactant addition are examined as methods for improving dispersion. Following this, a detailed analysis of measurement repeatability (sample-to-sample) and precision (subsample-to-subsample and run-to-run) is provided. Finally, the sensitivity of the calculated PSD to variations in the choice of optical constants for the cement phase is examined in detail. Unless otherwise noted, graphs of PSDs show the mean differential volume % (line) and one standard deviation (vertical error bar) determined from the analysis of replicate runs.

Choice of medium

The choice of suspending medium for cement powder is limited by several factors. Optically, the medium must be transparent with a refractive index that is relatively low (1 to 1.4). The liquid must be chemically inert with regard to hydration and/or dissolution of the solid phase, yet sufficiently polar to allow complete wetting of the powder surface. The viscosity of the medium should be low enough that the liquid flows easily during analysis and sample mixing (i.e., under moderate shear conditions), but high enough to avoid rapid segregation or settling of particles during liquid sampling and analysis. For ceramic materials, water is often the medium of choice. For cementitious powders, however, water is generally avoided due to the reactivity issue (i.e., hydration of calcium silicate phase), and alcohol (typically isopropyl) is used instead.

Therefore we examined the dispersion of CCRL 135 in a series of four alcohols: methyl (MeOH), ethyl (EtOH), isopropyl (IPA) and n-butyl (BuOH). These liquids have nearly identical refractive indices, densities and polarities (see Table 3 for a list of optical and physical properties), but exhibit a wide range of room temperature viscosities differing by a factor of 5 from lowest to highest. We also present results from a new aqueous-based procedure that is designed to circumvent the reactivity issue by using a chemical admixture to inhibit hydration.

Figure 2 compares the mean differential volume PSDs measured in each of four alcohol media. The curves for MeOH, EtOH and IPA have been offset in the y-direction in order to facilitate comparison. The samples were prepared using the base-line procedure, except for an ultrasonication time of 2 min, and analyzed using the Mie optical model with the base-line refractive index values (n=1.7, k=0.1) and including PIDS analysis. Sequentially analyzed subsamples consisting of 3 runs each were averaged for each of two separately prepared samples to generate the pairs of curves shown in Figure 2.[§] It was observed that the low viscosity of MeOH (see Table 3) caused difficulties

---

§ Tests were run about 1 year after the completion of all other reported CCRL 135 measurements. Portland cement is known to undergo aging effects over time, including hydration, which may impact the PSD. Therefore, fresh IPA measurements were made for comparison with measurement data collected during the same time period in other alcohol media, and should not be compared to CCRL 135 data shown elsewhere in this report.

during transfer of the stock suspension for dilution prior to measurement; significant leakage from the disposable pipette was noted during transfer. Furthermore, we attribute the sizable standard deviations (error bars) for PSDs measured in MeOH to poor mixing and/or sampling errors caused by the low fluid viscosity. The potential for sampling error and measurement artifacts is therefore, in our opinion, quite large for MeOH. As the medium viscosity increases from MeOH to BuOH, the precision and repeatability generally improve. IPA yields the best overall precision under the conditions of this experiment. EtOH yields a PSD that is somewhat finer compared to IPA, but the precision is poor as reflected by the large error bars in Figure 2. BuOH also yields a somewhat finer PSD, with slightly poorer precision relative to IPA. Both sample-to-sample repeatability and run-to-run precision are similar for EtOH, IPA and BuOH. It is possible that an optimum viscosity value exists, balancing material settling at low viscosity and hindered mixing/dispersion at high viscosity; however, it is not possible to determine this optimum from the present limited work. Another possibility is that IPA behaves differently due to its non-linear configuration and consequently different interaction properties with cement.[16]
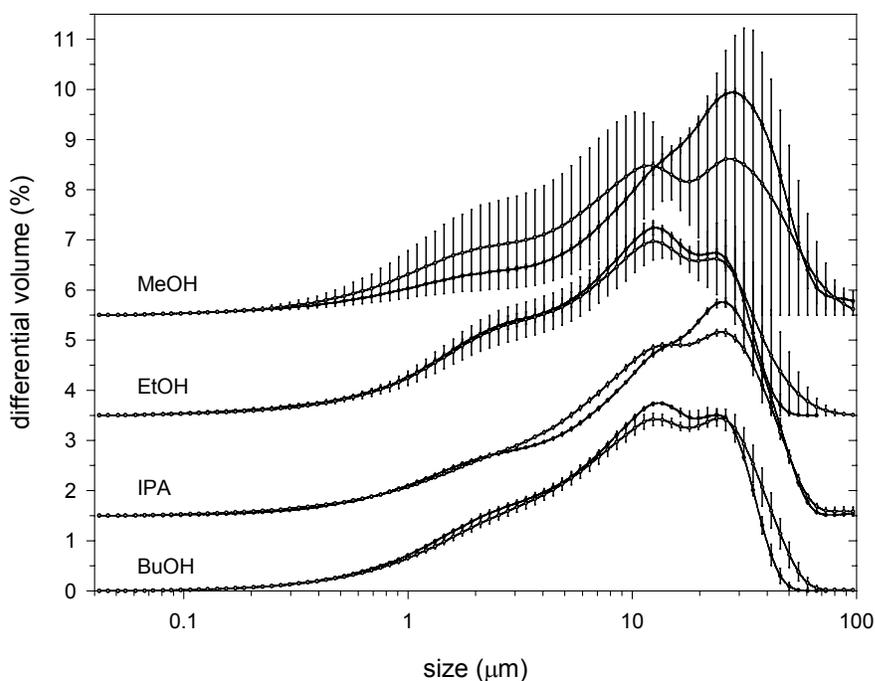
Figure 2. Effect of alcohol suspending medium on PSD for CCRL 135. Each curve represents the mean of 2 to 4 replicate subsamples derived from a single sample, with 3 runs per subsample. Two samples were analyzed in each medium. Except for n-butyl alcohol, each pair of PSDs has been offset in the y-direction for clarity; zero differential volume is identified by the intersection of each PSD with the y-axis.

Sampling error and poor precision/repeatability resulting from low viscosity might be reduced if the volume of stock suspension transferred to the instrument during the dilution process were increased. Presently, using a 20 % mass fraction solids content for the stock (an arbitrary choice based on input from some industry members), only 3 to 4 drops are necessary to achieve the required optical obscuration level on the instrument. By reducing the solids content in the stock suspension to 5 %, a four-fold increase in transfer volume would be achieved. On the other hand, if less powder is used in the preparation of the stock suspension, then this will increase the likelihood of sampling

15

errors at this stage. To compensate for the reduced solids concentration, the total volume of the stock suspension could be increased or riffling[†] could be used to insure a more homogeneous sampling of the cement powder. A lower solids concentration in the stock will probably mean that less ultrasonic energy is required to achieve the same level of dispersion. This may be an added benefit of lowering the solids content.

WRDA-19 is known in the cement industry as a high range water-reducer admixture (HRWRA) or superplasticizer. It is a naphthalene sulfonate (anionic) surfactant that adsorbs to the active sites of calcium silicate particles and bonds with dissolved mineral species, resulting in improved dispersion of the cement powder (thereby requiring less water) and a concurrent reduction in the rate of hydration. Typically used at low dosing levels, a sufficiently high concentration of the additive can cause strong inhibition of hydration. Prior experiments based on acoustic attenuation measurements indicated that a mass fraction addition of 1 % WRDA-19 to a 20 % mass fraction suspension of a typical portland cement resulted in the complete absence of hydration for a period of at least 6 h. A suspension of CCRL 135 was prepared according to the base-line procedure with an ultrasonication time of 2 min. Instead of deionized water, a solution containing WRDA-19 was used as the suspending medium. The concentration of the additive was such that the suspension contained 1 % WRDA-19 relative to the mass of the cement powder.
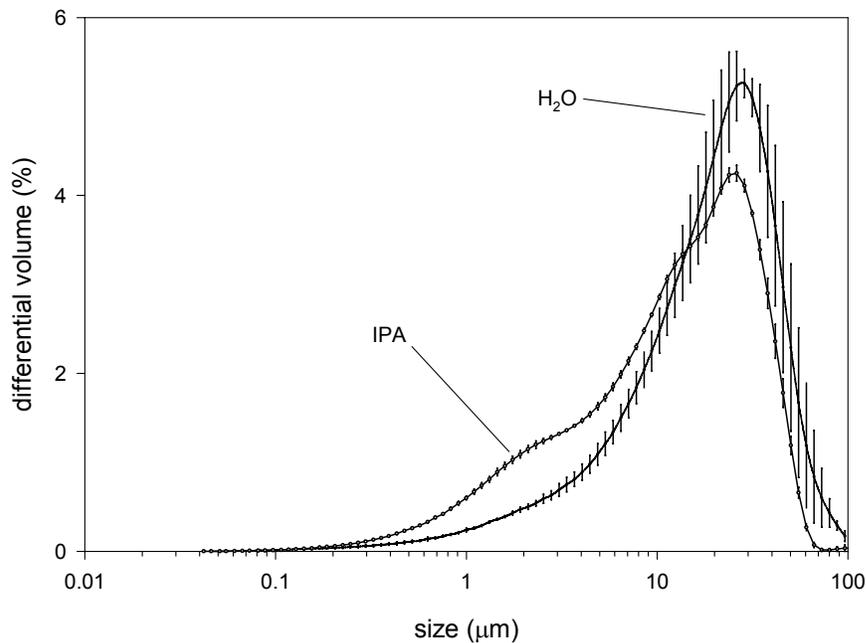
Figure 3. Comparison of differential volume PSDs for CCRL 135 measured in IPA and in water with 1 % naphthalene sulfonate, WRDA-19, added to inhibit hydration.

Figure 3 shows the differential volume PSD determined for CCRL 135 dispersed in a 1 % aqueous solution of the naphthalene sulfonate chemical admixture, WRDA-19. This curve is compared to the PSD measured in IPA. In both cases the base-line sample preparation procedure was used with an ultrasonication time of 2 min. For the aqueous dispersion, the stock suspension

---

† Mixing/sampling method in which a steady stream of powder flows into a rotating basket of containers. Applicable for subsampling large samples with good flow properties.

was diluted into a solution of WRDA-19 at the same liquid-phase concentration level. A blank measurement was performed on the solution, which is discolored and thus slightly absorptive. There are two significant observations regarding this data. First, the aqueous PSD is quite a bit coarser compared with IPA. In particular, the size fraction below about 10 µm is apparently underestimated in the aqueous dispersion. Second, the associated precision is much worse than IPA, keeping in mind that both sets of data represent the averaging of six measurement runs from two subsamples. Even in the presence of a saturating amount of the chemical admixture, which serves as both a dispersant and a hydration inhibitor, the fine size fraction in the aqueous sample is apparently not fully dispersed. Perhaps this is due to some limited hydration or dissolution of the colloidal phase upon initial contact with the aqueous medium. Regardless, it would appear that the aqueous-based method offers no advantage over using IPA or other alcohol media, but further tests may be warranted verify this conclusion. Possible advantages to using an aqueous-based dispersion method include reduced use of organic solvents, lowered material cost and closer correspondence with real cement applications.

Effect of ultrasonic treatment

The following data were obtained for dispersions of CCRL 135 in IPA using the standard (Mie) optical model with PIDS analysis. Figure 4 shows the effect of ultrasonic treatment time (for the stock suspension) on the measured PSD (mean of three replicate runs), while Figure 5 compares the resulting mean volume-weighted diameters (d_{10}, d_{50} and d_{90}) as a function of treatment time. There is a significant shift toward finer fractions at the expense of coarser sizes in the measured PSD following the initial application of ultrasonic energy. However, above 1 min the effect appears to saturate and no further dispersive improvement is observed. Therefore, we conclude that some minimum amount of ultrasonic treatment should contribute to an improvement in cement dispersion, but that this effect is relatively moderate in IPA.
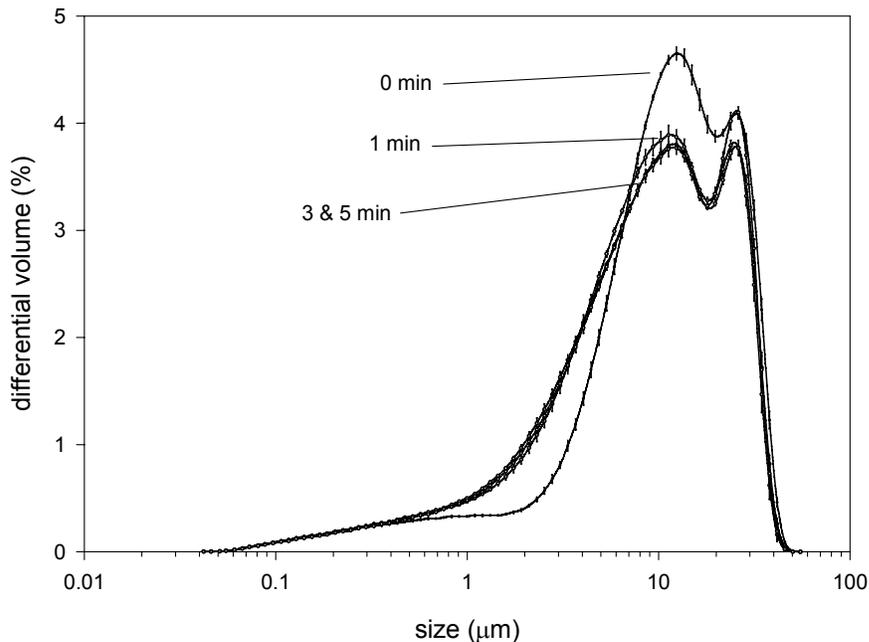
Figure 4. Effect of ultrasonic treatment time on the measured PSD for CCRL 135 in IPA. Each curve represents the mean of three runs at each condition. Vertical error bars represent one standard deviation.

17
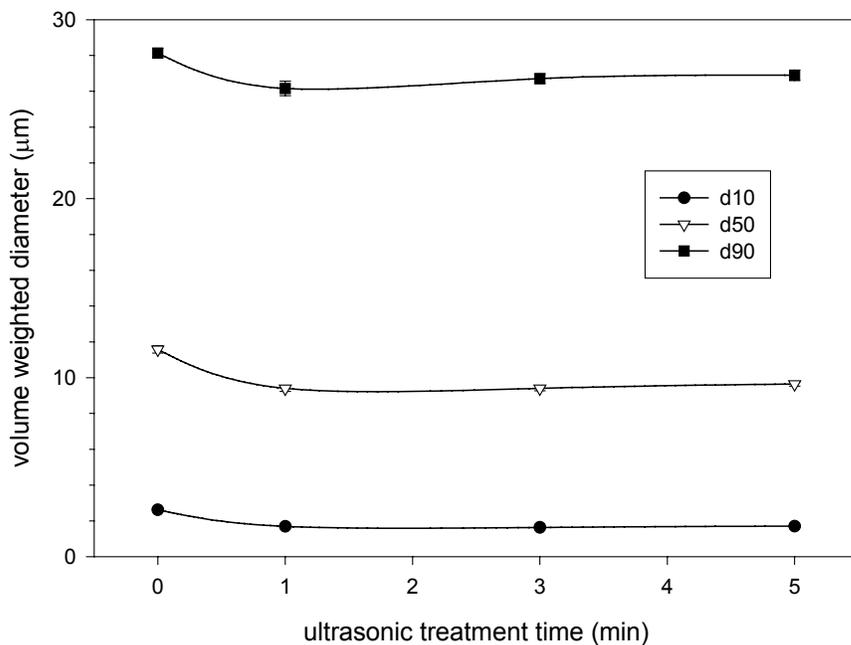
Figure 5. Effect of ultrasonic treatment time on the mean characteristic diameters for CCRL 135 in IPA. Vertical error bars are smaller than the symbol dimension.
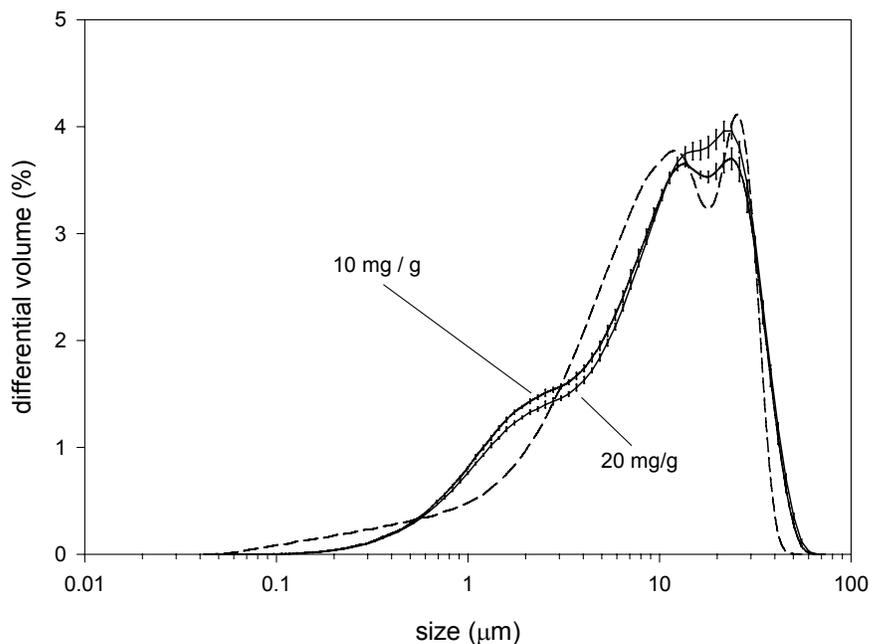
Figure 6. The effect of AOT surfactant on the measured PSD for CCRL 135 in IPA. The dashed line shows the PSD measured in IPA without addition of AOT.

Effect of anionic surfactant addition

The following data were obtained for dispersions of CCRL 135 in IPA using the standard (Mie) optical model with PIDS analysis. Figure 6 shows the effect of AOT surfactant on the measured PSD for two concentrations of AOT (based on the mass of the solid phase). AOT is an all-purpose

surfactant and wetting agent used throughout the drug, cosmetic and food industries. It is evident that the surfactant has only a moderate effect on the dispersion of cement in IPA. There is a small increase in the size range from 0.5 μm to 3 μm, which is accompanied by reductions in both the sub-0.5 μm fraction and some of the coarser fractions. There may be some advantage to using AOT or similar anionic surfactants, but further research would be required to explore this possibility.

Repeatability and precision

The following data were obtained for dispersions of CCRL 135 in IPA using the standard (Mie) optical model with PIDS analysis. Samples were prepared according to the base-line procedure with an ultrasonication treatment time of 5 min. In all, three replicate samples (i.e., stock suspensions) were prepared separately by this procedure (identified as Sample 1, 2 and 3). Multiple subsamples were then taken from each sample in order to prepare a test suspension. For selected subsamples, multiple runs (single PSD measurements) were performed. Table 5 shows the organization of test samples for the purpose of analyzing measurement precision.

Table 5. Hierarchical Organization of Test Samples.

Sample	Subsample	No. Runs
1	1	3
	2	1
	3	1
2	1	1
	2	1
	3	1
3	1	1
	2	1
	3	3
	4	1

Three levels of precision were examined: run, subsample and sample. The run-to-run variation was examined across three individual runs (measurements) from each of two subsamples, each of which was in turn associated with a different sample (i.e., Sample 1 and Sample 2 in Table 5). An average run-to-run coefficient of variation (CV) was then calculated for three characteristic diameters (d_{10}, d_{50} and d_{90}) based on these two sets of runs. PSDs for the individual runs used in these calculations are shown in Figure 7 and Figure 8, while Figure 9 shows the mean PSDs determined from these two sets of runs.

The subsample-to-subsample variation was examined across multiple subsamples within each of the three samples. In the case where multiple runs were associated with a subsample, only the first run was used for subsample statistics. The three sets of CV values were then averaged to obtain the mean subsample-to-subsample CV for each characteristic diameter. PSDs for the individual subsample runs are shown in Figure 10, Figure 11 and Figure 12. Figure 13 compares the mean PSDs calculated for each set of subsample runs.

The sample-to-sample (repeatability) variation was determined across the three samples listed in Table 5. In this case, the characteristic diameters were extracted from the same sequentially numbered subsample within each of the three samples and then averaged. Thus there are three sets of

sample-to-sample CV values corresponding to the three sequentially numbered subsamples within each sample (subsample 4 of sample 3 was not included). These three sets of data were then averaged to determine the mean sample-to-sample CV values for each characteristic diameter. The individual sample runs are not shown. The mean PSDs corresponding to each set of runs belonging to a sequentially numbered subsample are shown in Figure 14.

Finally, the CV values for each characteristic diameter representing the three statistical populations are compared in histogram format in Figure 15.

The precision of replicate sequential runs within a single subsample is very good, with CVs near 1 %. The subsample-to-subsample and sample-to-sample variations are similar in magnitude, with CVs ranging from about 5 % for d_{10} up to 16 % for d_{90}. This seems to indicate that the most significant contribution to uncertainty in the measured PSDs arises during the process of diluting the stock sample prior to analysis or in sampling the stock suspension itself. An examination of the individual subsample runs in Figure 10, Figure 11 and Figure 12 does not show a systematic trend, such as coarsening, that might indicate an aging effect in the sequentially analyzed subsamples. The CV values generally increase with increasing characteristic diameter, indicating that the poorest precision is associated with the coarser fractions. This may be due simply to the smaller number of large particles sampled compared with finer particles. Although the coarse particles represent the largest fraction on a volume or mass basis, their number density in the sensing zone is small compared to the finer size particles and this could be reflected in the precision. Another possible source of variation may be due to segregation within the stock sample due to variations in the stirring rate or liquid sampling technique prior to dilution.
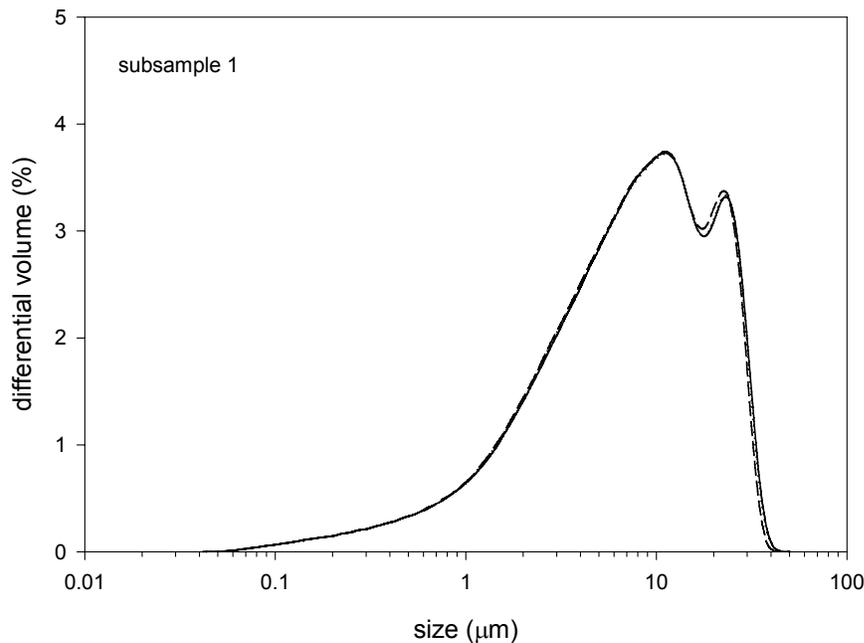
Figure 7. PSDs for CCRL 135 in IPA determined from three sequential replicate measurements (runs) on subsample 1 of sample 1.
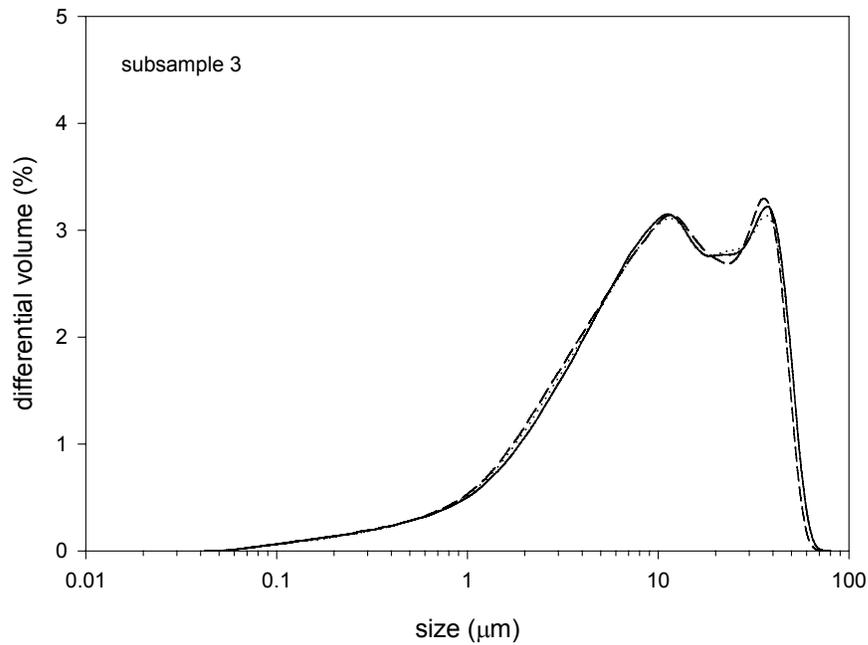
Figure 8. PSDs for CCRL 135 in IPA determined from three sequential replicate measurements (runs) on subsample 3 of sample 3.
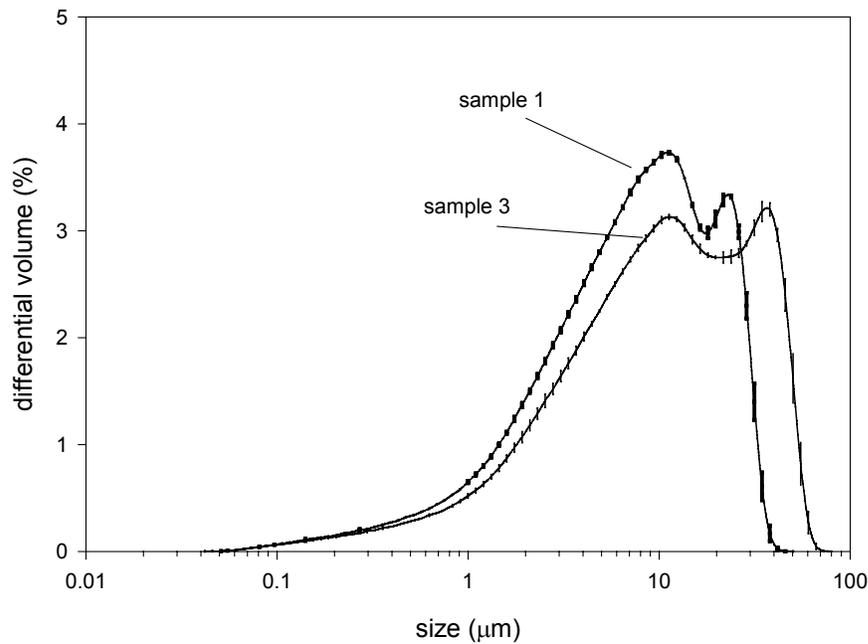
Figure 9. Mean (run-to-run) PSDs determined from each of two samples/subsamples. Vertical error bars represent one standard deviation from the mean.
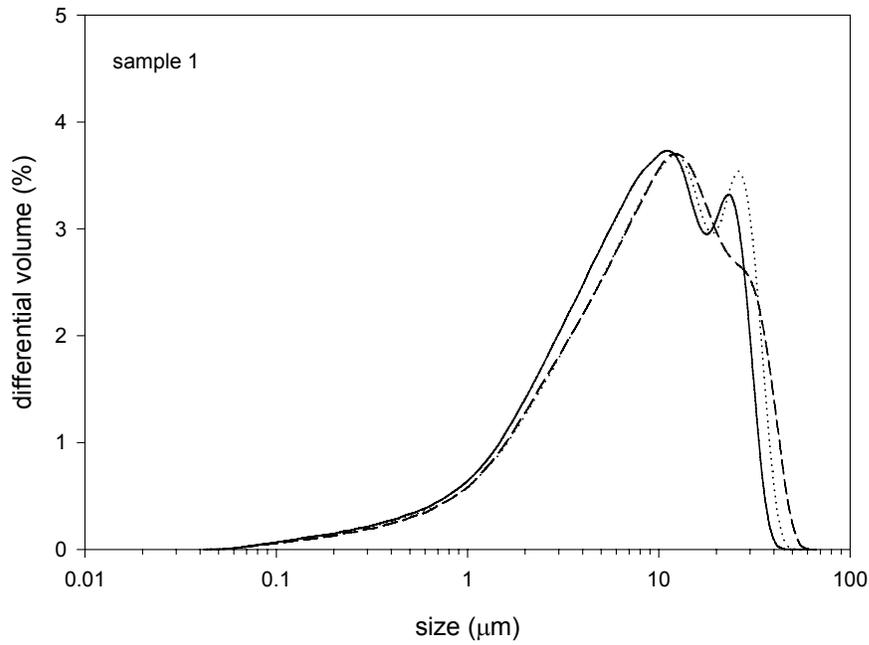
Figure 10. PSDs for CCRL 135 in IPA determined from three sequential replicate subsamples of sample 1. Each curve represents a single measurement (run) from that subsample.
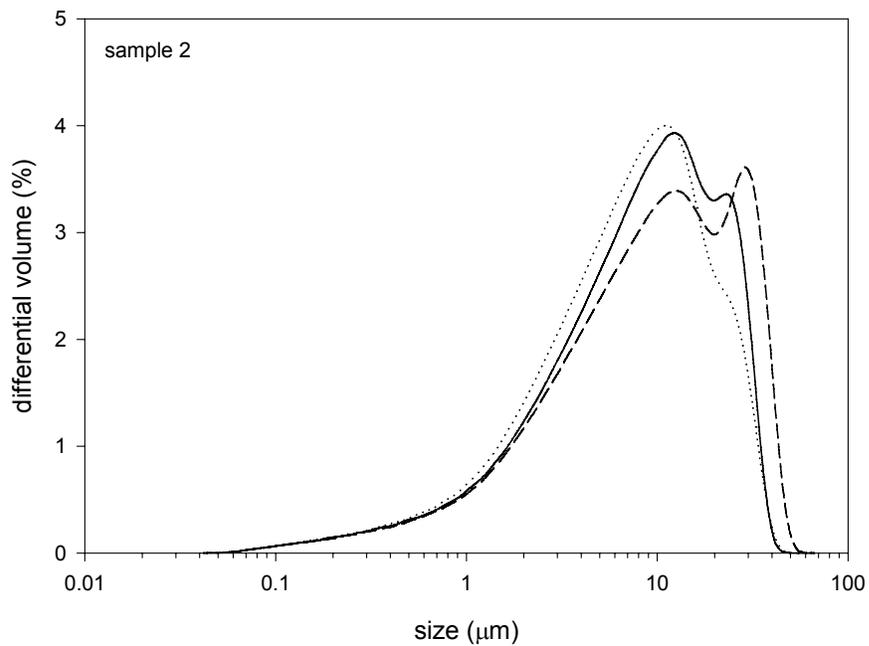
Figure 11. PSDs for CCRL 135 in IPA determined from three sequential replicate subsamples of sample 2. Each curve represents a single measurement (run) from that subsample.
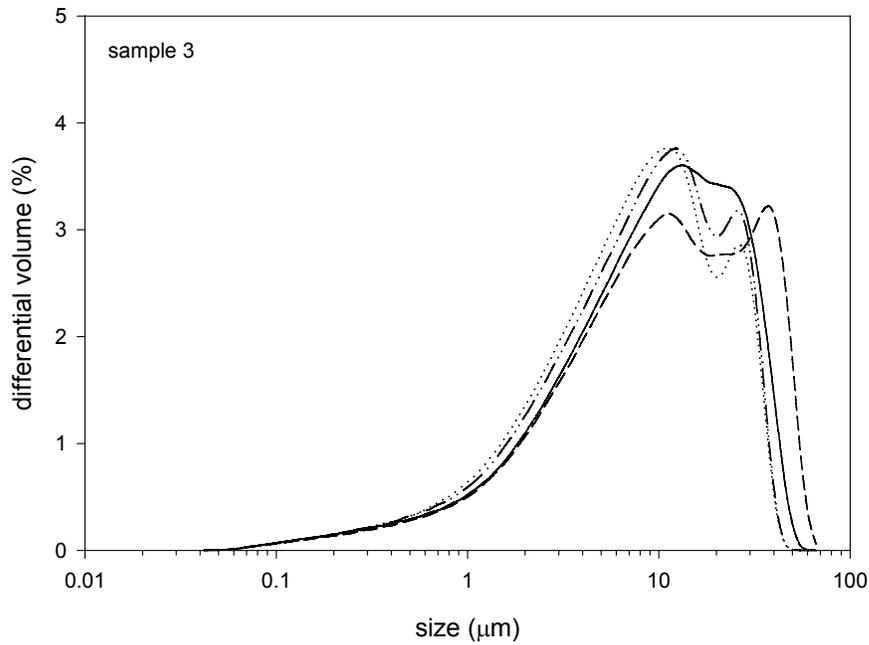
Figure 12. PSDs for CCRL 135 in IPA determined from three sequential replicate subsamples of sample 3. Each curve represents a single measurement (run) from that subsample.
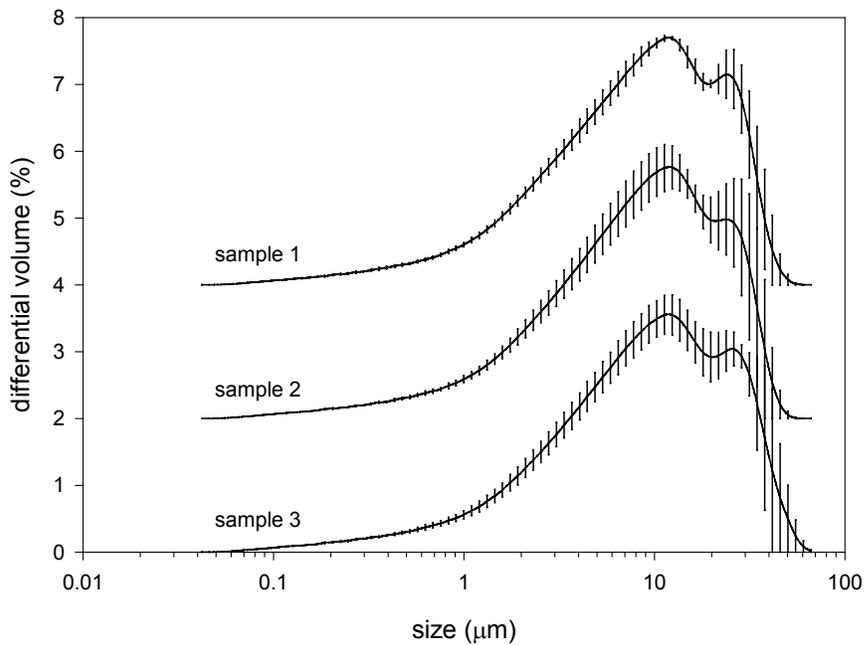
Figure 13. Mean PSDs representing the subsample-to-subsample variation in each sample. Vertical error bars represent one standard deviation about the mean. The PSDs for sample 1 and sample 2 are vertically offset by +4 % and +2 %, respectively.
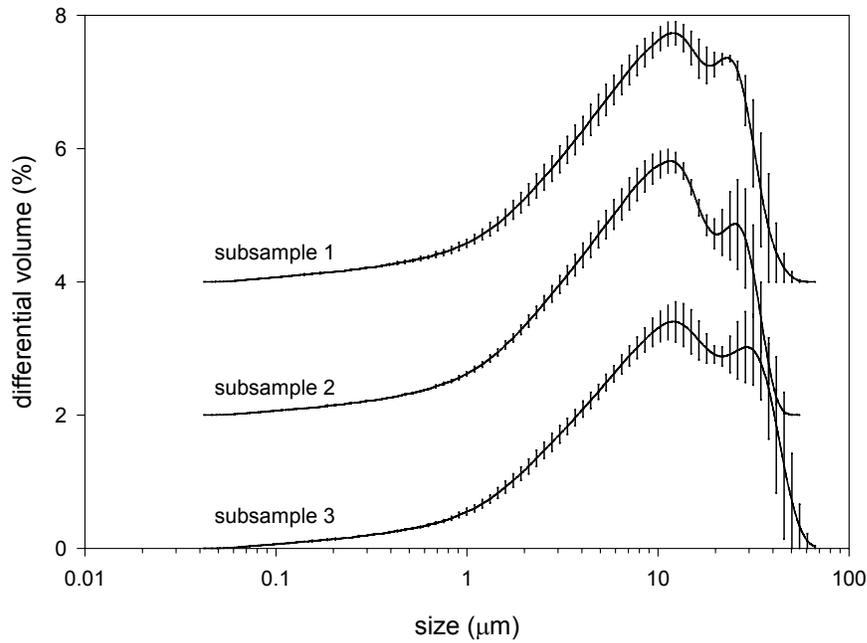
Figure 14. Mean PSDs representing the sample-to-sample variation calculated using sequentially numbered subsamples with one measurement (run) each. Vertical error bars represent one standard deviation about the mean. The PSDs for subsample 1 and subsample 2 are vertically offset by +4 % and +2 %, respectively.
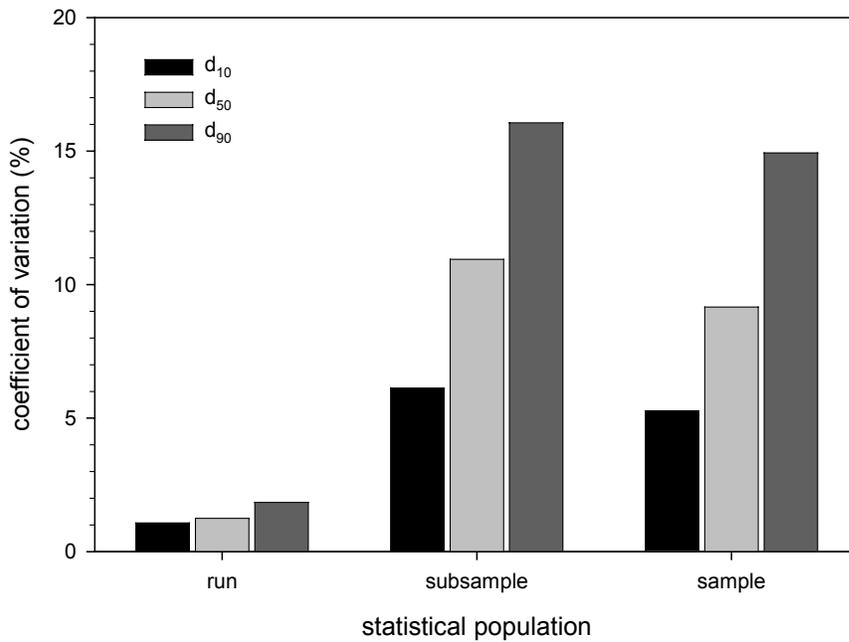
Figure 15. Histogram comparing the coefficients of variation for the characteristic diameters at the three statistical levels of analysis.

Sensitivity to variations in the optical model

We have determined that the most significant factor, post-sample-preparation, impacting PSD determination is the choice of optical model used for inversion of the measured diffraction spectrum. In particular, the optical constants or complex refractive index ($m = n + ik$) for the solid phase must be correctly assigned if the Mie scattering model is used for spectral analysis. We have examined the sensitivity of the calculated PSD to variations in the real (n) and imaginary (k) components of the complex refractive index over a range of values that encompasses reasonable estimates for portland cement. The scattering spectrum used for these model calculations was chosen from the experimental base-line measurements of CCRL 135, and is considered representative of that data set. The m-independent PSD, calculated using the Fraunhofer approximation, is included for comparison in selected figures.

Figure 16, Figure 17 and Figure 18 show the variation in the calculated differential volume PSD as a function of the real component of the complex refractive index for each of three fixed imaginary component values: 0 (transparent), 0.01 (weakly absorbing) and 0.1 (moderately absorbing), respectively. For $n \geq 1.6$ (i.e., fairly refractive materials), the model is not very sensitive to the choice of n for weakly absorbing or transparent materials (i.e., $k < 0.1$). It is only moderately sensitive at $k = 0.1$. The range of n values from 1.6 to 1.8 is thought to bracket the most likely volume-average value for a typical portland cement,[6,8] while the most commonly cited value of k for portland cement is 0.1. The Fraunhofer model generates a PSD that is nearly equivalent to the Mie calculation for optical constants $n = 1.6$ and $k = 0.1$. Comparing the Fraunhofer curve to the Mie curve corresponding to $n = 1.7$ (i.e., the average value cited for portland cement)[6,7] in Figure 16 to 18 should provide a reasonable indication of the expected magnitude of variations between the two optical models as applied to cement. Here we see that for any value of k selected, the Fraunhofer model by comparison presents a much greater fine fraction below 1 μm with a slight reduction in the 2 to 40 μm size range.

The sensitivity of the Mie model to a variation in k for a series of fixed values of n is shown in Figure 19 through Figure 25. These sets of curves can be used as a guide to understand the influence of the imaginary component on the inversion of diffraction spectra for a given value of n. As noted above for the case of $n = 1.7$, the Fraunhofer model tends to overestimate the submicrometer range. Here we see that this statement can be extended to $n \geq 1.7$. Except for highly refractive particles ($n > 2$), where absorption is largely irrelevant, the magnitude of the calculated submicrometer fraction depends on the choice of k, with the dependence becoming stronger as n becomes smaller. By contrast, the portion of the PSD above 1 μm is largely insensitive to the value of k for values of $n \geq 1.7$. For $n \geq 1.5$, the coarse fraction above 40 μm is unaffected by the choice of optical model, and both Mie and Fraunhofer yield identical results.

Figure 26 shows the dependence of the calculated cumulative PSD on the value of k for three material types that vary in their real refractive index. Portland cement probably lies within the middle set of curves, with $n = 1.7$. This is simply a different way of viewing the sensitivity of the PSD to k. Clearly, if 1.7 is close to the correct value for cement, then only about 10 % (on a mass or volume basis) of the PSD is likely to be affected by the value chosen for k. In other words, only the fraction below d_{10} will be highly sensitive to k.

Figure 16. Sensitivity of calculated PSD to variation in real component of complex refractive index for *k* = 0. Diffraction spectrum of CCRL 135 analyzed using Mie optical model.
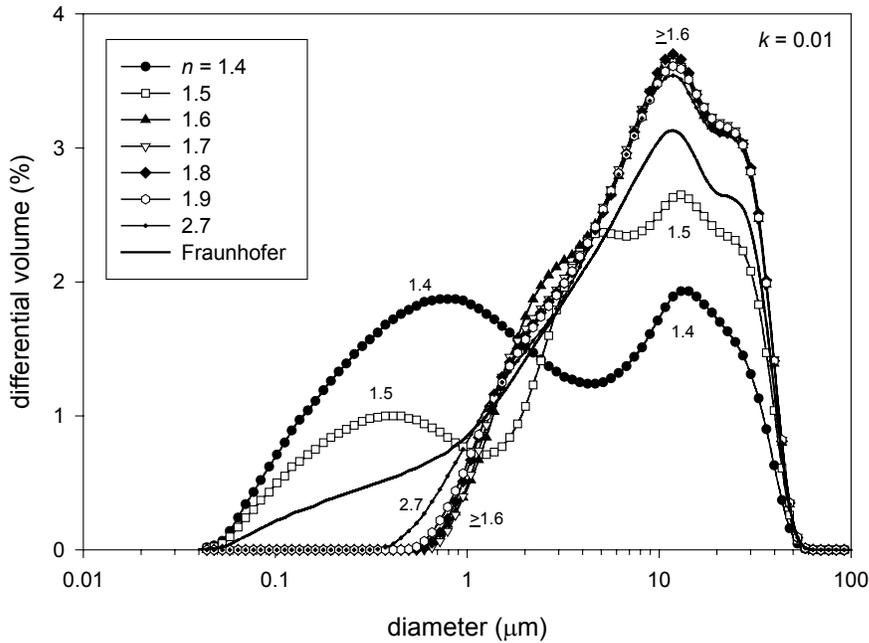
Figure 17. Sensitivity of calculated PSD to variation in real component of complex refractive index for *k* = 0.01. Diffraction spectrum of CCRL 135 analyzed using Mie optical model.

26
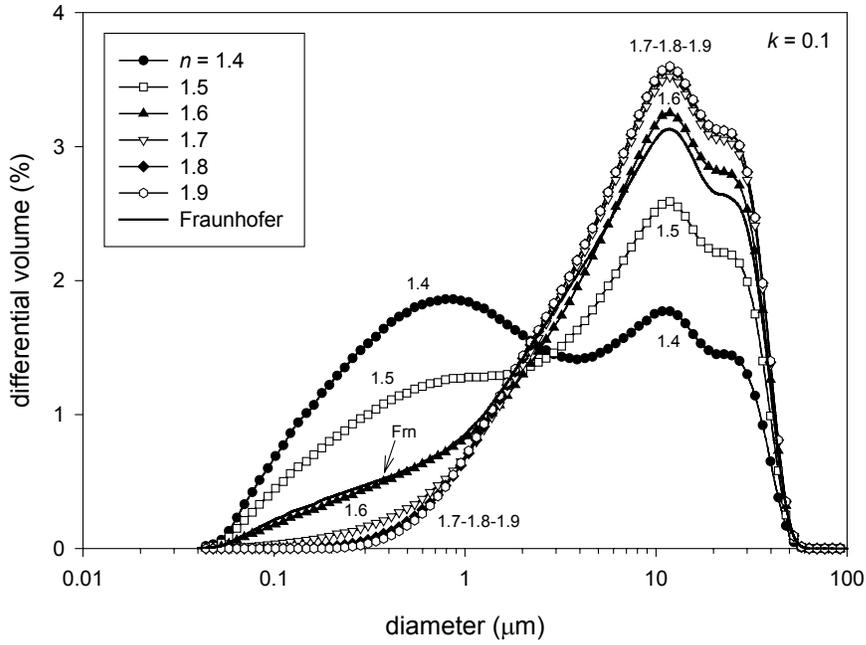
Figure 18. Sensitivity of calculated PSD to variation in real component of complex refractive index for *k* = 0.1. Diffraction spectrum of CCRL 135 analyzed using Mie optical model.
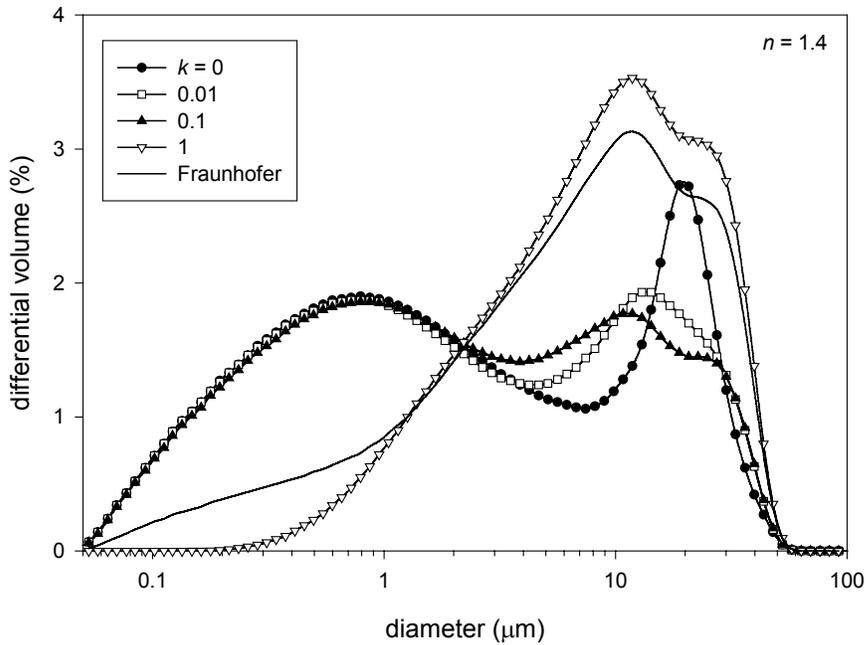
Figure 19. Sensitivity of calculated PSD to variation in imaginary component of complex refractive index for *n* = 1.4. Diffraction spectrum of CCRL 135 analyzed using Mie optical model.
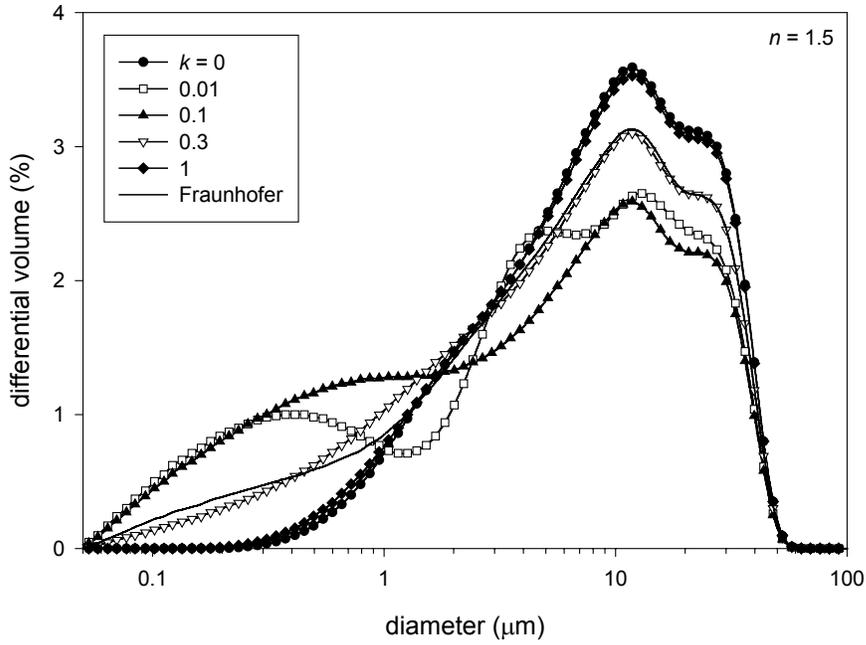
Figure 20. Sensitivity of calculated PSD to variation in imaginary component of complex refractive index for *n* = 1.5. Diffraction spectrum of CCRL 135 analyzed using Mie optical model.
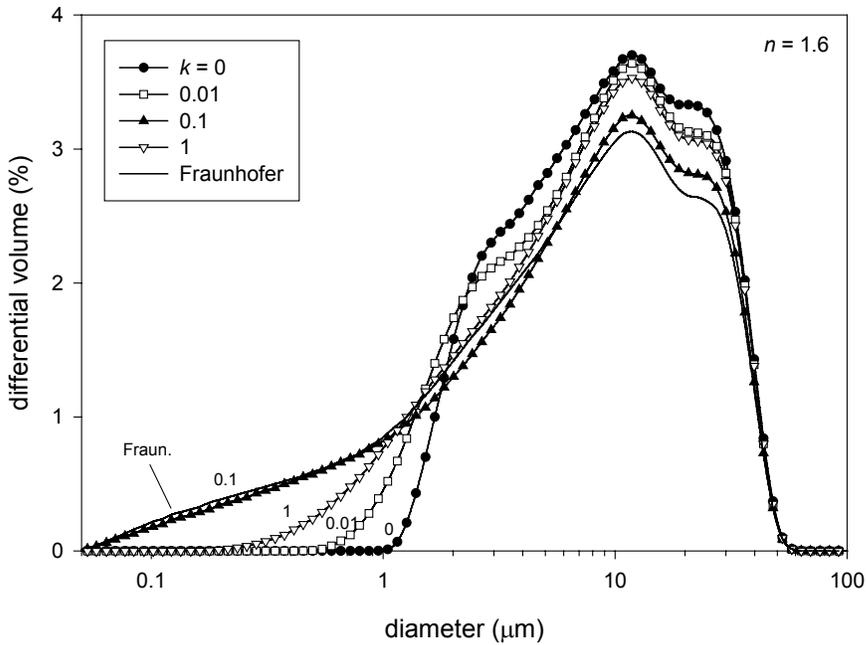
Figure 21. Sensitivity of calculated PSD to variation in imaginary component of complex refractive index for *n* = 1.6. Diffraction spectrum of CCRL 135 analyzed using Mie optical model.
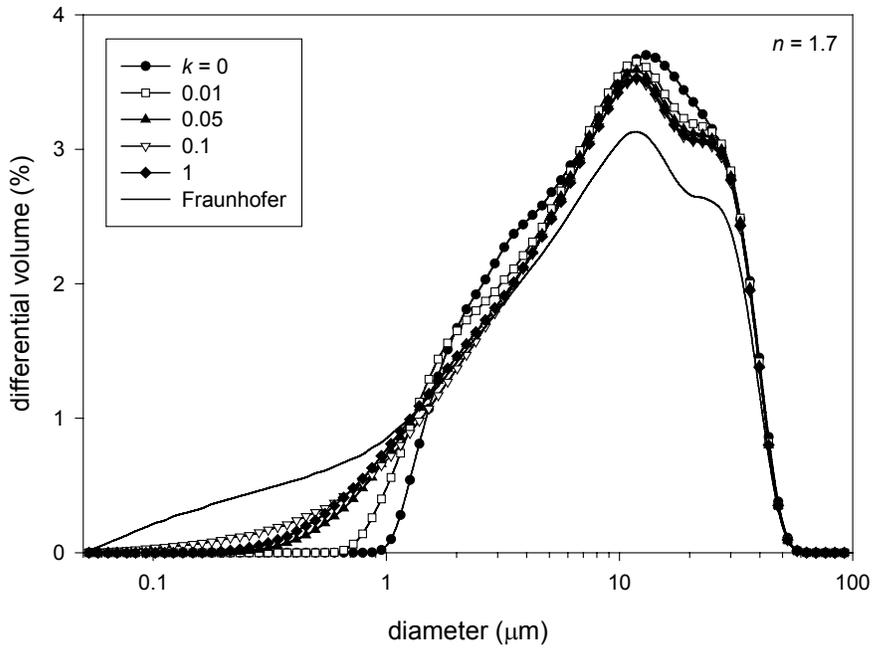
Figure 22. Sensitivity of calculated PSD to variation in imaginary component of complex refractive index for *n* = 1.7. Diffraction spectrum of CCRL 135 analyzed using Mie optical model.
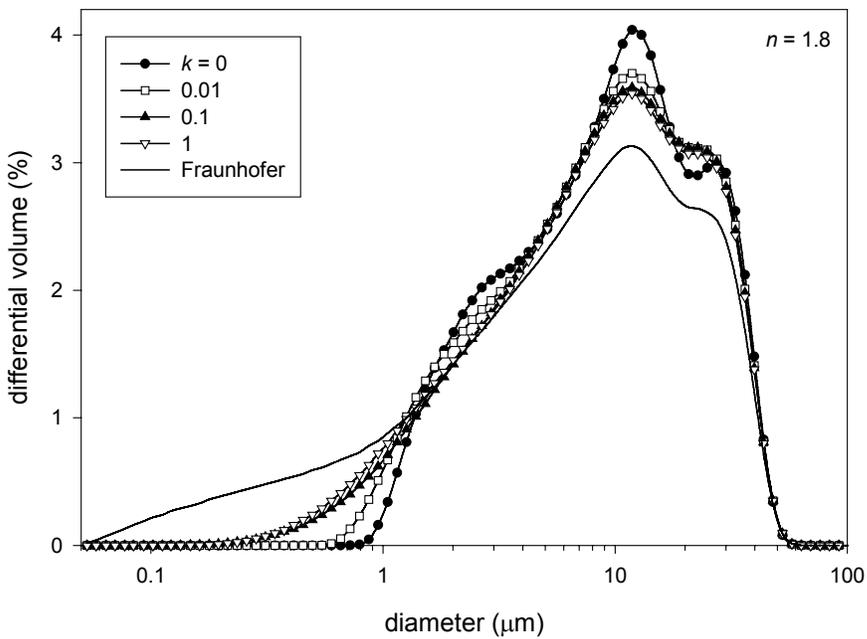
Figure 23. Sensitivity of calculated PSD to variation in imaginary component of complex refractive index for *n* = 1.8. Diffraction spectrum of CCRL 135 analyzed using Mie optical model.
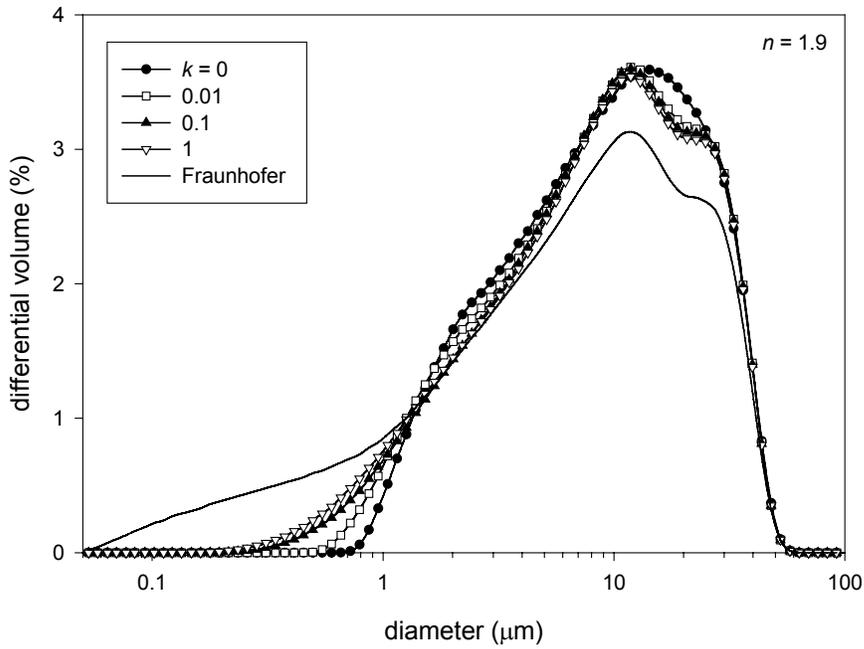
Figure 24. Sensitivity of calculated PSD to variation in imaginary component of complex refractive index for *n* = 1.9. Diffraction spectrum of CCRL 135 analyzed using Mie optical model.

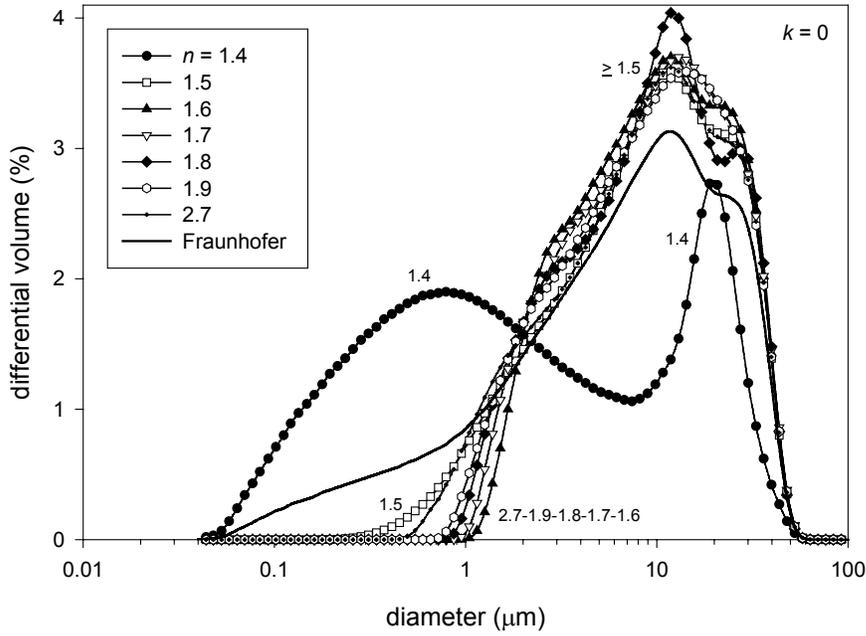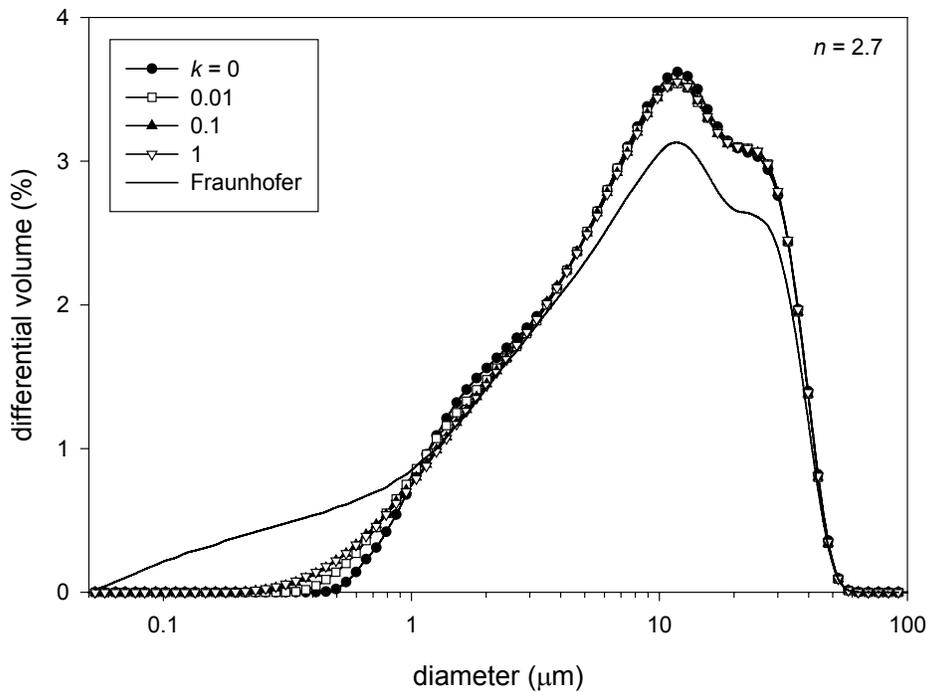**Figure 25. Sensitivity of calculated PSD to variation in imaginary component of complex refractive index for *n* = 2.7. Diffraction spectrum of CCRL 135 analyzed using Mie optical model.**
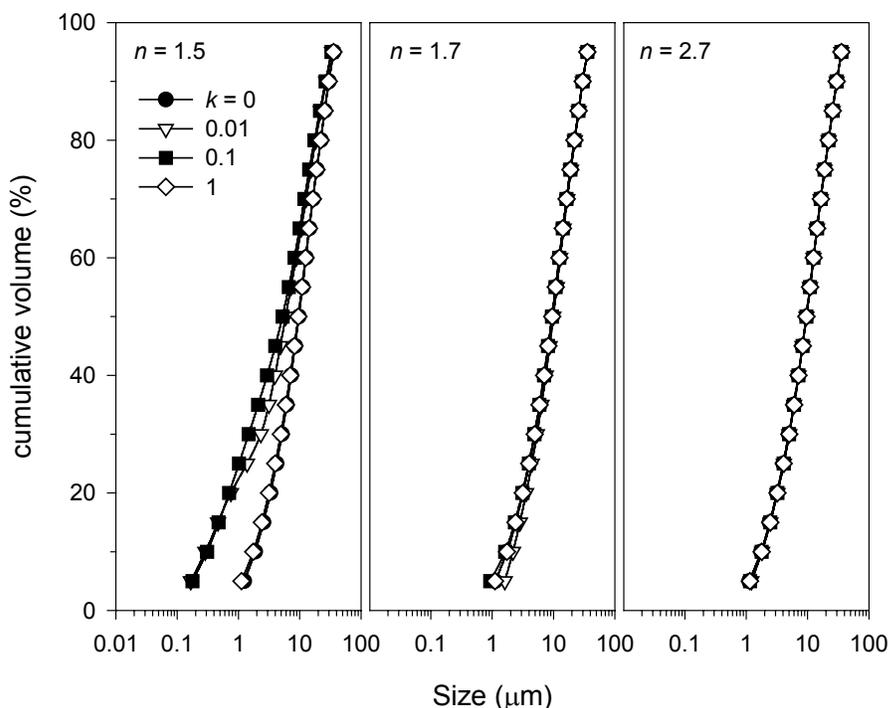
Figure 26. Sensitivity of calculated cumulative PSD to variation in imaginary component of complex refractive index for three values of *n*: left, glass; middle, typical cement; right, TiO$_2$ pigment (rutile). Diffraction spectrum of CCRL 135 analyzed using Mie optical model.

Analysis of Aluminum Oxide Discrete Size Fractions

Background

In this study, two dispersion methods (wet and dry) were compared for a series of aluminum oxide powders characterized by relatively narrow PSDs. In addition, two different wet dispersion media were evaluated and compared, namely water (aqueous solution) and alcohol (IPA).

Based on previous studies and published literature on aluminum oxide, it was anticipated that an aqueous medium would provide the best possible conditions for dispersion of this material. In aqueous-based metal oxide suspensions, dispersion arises from repulsive electrostatic interactions between like-charged particles. The particles develop a charge due to adsorption and desorption of protons at reactive surface sites, and thus charge and dispersion are pH-dependent. Optimal dispersion conditions exist when the pH of the medium is ≈ 3 pH units or more removed from the isoelectric point (IEP)[†] and the ionic strength is low (< 0.01 mol/L) . For (α-phase) aluminum oxide, the IEP is typically found near pH 9.[17] With this in mind, a nominal pH of 5.5, without additional electrolyte and accompanied by intense ultrasonic treatment, was chosen as the base-line condition for maximizing powder dispersion in this system. All other measurement results will be compared to the base-line PSDs.

[†] The IEP is the pH value in a suspension at which point the electrical potential (i.e., zeta potential) of the constituent particles, measured by electrokinetic methods, is equal to zero. A zeta potential of zero indicates that the positive and negative surface sites just compensate each other, and particle charge no longer exhibits a stabilizing influence on the suspension. As the pH moves away from the IEP, the zeta potential increases in magnitude, but the sign depends on whether the pH is above (negative) or below (positive) the IEP.

ESA data (zeta potential in aqueous medium)

Electrokinetic sonic amplitude (ESA) measurements were used to assess the surface charge state of each aqueous aluminum oxide suspension at a nominal pH of 5.5. Simultaneous conductivity measurements provide a relative measure of the soluble ionic species originating on the powder surface. Results are shown in Figure 27 for each powder. As expected, the zeta potential is positive for all suspensions, but the magnitude varies systematically. These variations are not critical for the purposes of this study, as they depend somewhat on solution conductivity (which varies between powders) and particle size (which increases from left to right in Figure 27). Although the ESA data has been corrected for particle size,[†] the correction factor is a rough estimate and does not quantitatively compensate for the effect. This leads to an apparent inverse dependence of zeta potential on particle size. An increase in conductivity, which reflects ionic concentration in solution, tends to reduce the zeta potential by screening the particle charge.

Most importantly, in all cases the zeta potential exceeds 60 mV, indicating the presence of a strong repulsive electrostatic barrier leading to excellent dispersion conditions. Typically, zeta potentials above about 30 mV are considered necessary to prevent significant agglomeration from occurring. In subsequent LDS measurements, the solid phase will be diluted prior to analysis and this will reduce the conductivity and particle concentration, and thus further increase the stability.
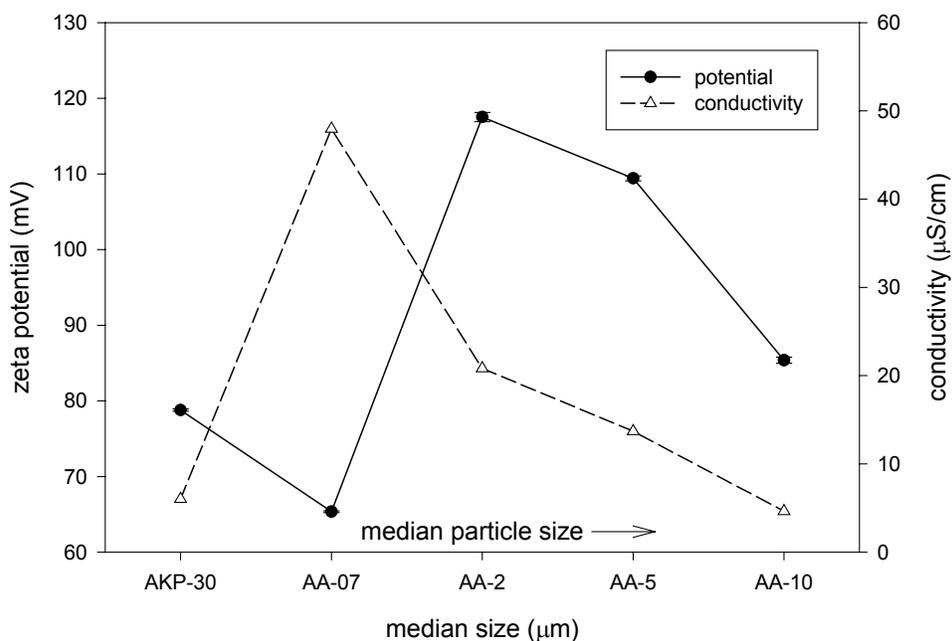
Figure 27. Zeta potential and conductivity of aluminum oxide powders in aqueous media at pH 5.5 and 2 % solid volume fraction.

---

† Particle size influences the measured ESA signal (from which zeta potential is subsequently calculated) through its effect on the inertial response of the particles in the applied ac field. As particle size increases, the induced particle motion tends to lag behind the field causing a phase shift and resulting in a reduced signal magnitude. The change in phase and magnitude can be calculated if the particle size is known a priori. The application of an inertial correction term is complicated by the presence of a distribution of sizes and/or by changes in the state of aggregation during analysis. The inertial effect vanishes at particle diameters below about 0.1 μm.

Wet dispersion method - aqueous data

The following data were obtained for aqueous dispersions of aluminum oxide at pH 5.5, using the standard (Mie) optical model with PIDS analysis. PSD data represents the mean (line) and standard deviation (error bar) calculated from the analysis of 3 individual subsamples (one run each) from each of 2 separately prepared samples, for a total of 6 measurements (runs). PSD error bars therefore represent the effects of subsample variation in combination with sample-to-sample variation, unless otherwise noted. Individual differential volume PSDs are shown for each powder, followed by a single graph comparing the cumulative volume PSDs for all powders. Also shown is the calculated standard deviation (all powders plotted collectively) as a function of particle size, and the mean volume-weighted percentile diameters (d_{10}, d_{50} and d_{90}) for each powder. Finally, the coefficient of variation for percentile diameters is calculated for each powder based on run-to-run and sample-to-sample variations, thus yielding a measure of precision and repeatability, respectively.

With the exception of AA-07 (Figure 29), which presents a model log-normal distribution, all powders exhibit multimodal PSDs. The most extreme example is the trimodal AKP-30 (Figure 28), which contains a log-normal primary mode centered at ≈ 0.3 µm and two minor modes appearing near 0.07 µm and just above 1 µm. The large error bars associated with the finer secondary mode indicate poor precision; this is expected when operating at the extreme limits of the LDS technique (i.e., below 0.1 µm). The intensity of scattered light scales with d^6 when $d \ll \lambda$ (where d is the particle diameter),[12] so small populations of sub-0.1 µm particles will be difficult to detect and quantify with a high degree of precision in systems containing much larger particles. The coarser secondary mode in AKP-30, which is very small in magnitude and exhibits large error bars, is most likely due to the presence of a small number of residual (undispersed) agglomerates.

For the remaining powders, AA-2 (Figure 30), AA-5 (Figure 31) and AA-10 (Figure 32), the PSD can be roughly fit by a log-normal distribution function, except for a small shoulder on the coarse side of the primary mode in each case. Like AKP-30, the coarse-side shoulder suggests the presence of some residual agglomerates. In the case of AA-5 and AA-10, the shoulder exhibits at a size ratio of about 2:1 compared with the primary mode, whereas for AA-2 the ratio is closer to 3:1.

For all powders where a secondary peak or shoulder is present on the coarse side of the primary mode, the size ratio relative to the primary mode is in the range of 2 to 3. This suggests that residual agglomerates are most likely, on average, to be low-multiple assemblies of the primary particles (e.g., doublets, triplets, and so forth).

Repeatability and precision (sample-to-sample and run-to-run, respectively) improve dramatically for powders lacking a substantial submicrometer (ultrafine) fraction. This is apparent in both the individual differential volume PSD graphs and the comparison of cumulative PSDs (Figure 33). A plot of the absolute errors (standard deviations) for all PSDs combined (Figure 34) also indicates a trend toward decreasing uncertainty with increasing particle size.

The percentile diameters are shown for reference in Figure 35. We can use these diameters as a metric for quantifying the relative precision and repeatability of the fine (d_{10}), median (d_{50}) and coarse (d_{90}) fractions of a PSD. Although the run-to-run precision (Figure 36 and Figure 37) and sample-to-sample repeatability (Figure 38), calculated for the three characteristic percentile diameters, are generally high for all powders with few exceptions, the CV shows a decreasing trend with increasing nominal particle size. The run-to-run CV (calculated relative to the percentile diameter value) exceeds 5 % in only one instance (i.e., d_{10} for AKP-30). It is notable that the minimum CV (i.e., best precision) is most commonly associated with the median percentile diameter. This is to be expected, since all test powders are characterized by a prominent log-normal mode. Examining repeatability (Figure 38), we see that the sample-to-sample CV exceeds 4 % only once (i.e., d_{10} for AKP-30). Again, the median percentile exhibits the lowest overall relative error,

exceeding 1 % only for AKP-30. The generally high repeatability emphasizes the benefit of averaging multiple LDS runs, rather than relying on a single measurement, particularly in the case of powders with a significant ultrafine phase. We will use the CVs calculated for aqueous suspensions as a bench mark for subsequent comparisons of precision and repeatability.
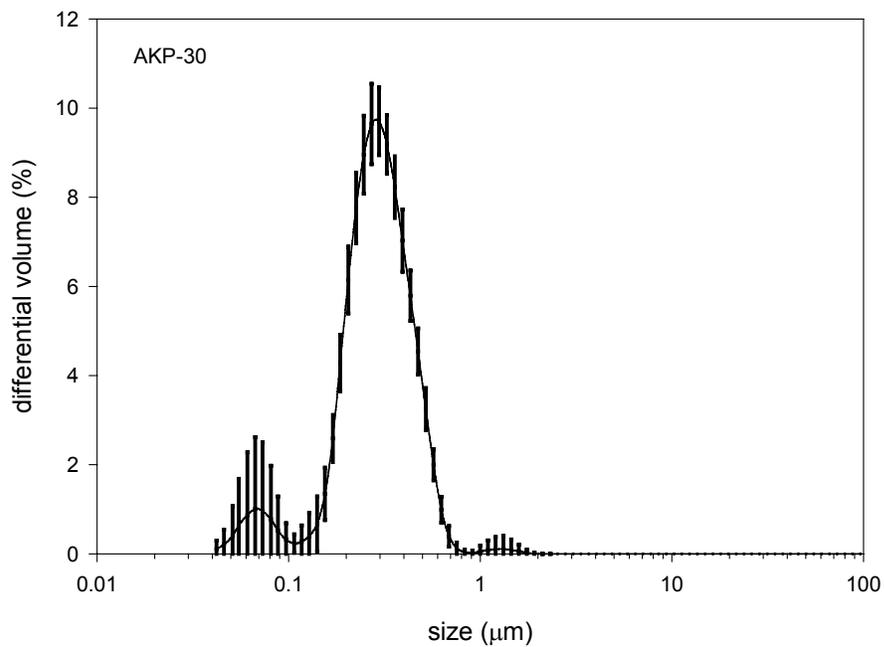
Figure 28. Differential volume PSD for AKP-30 aluminum oxide in aqueous medium.
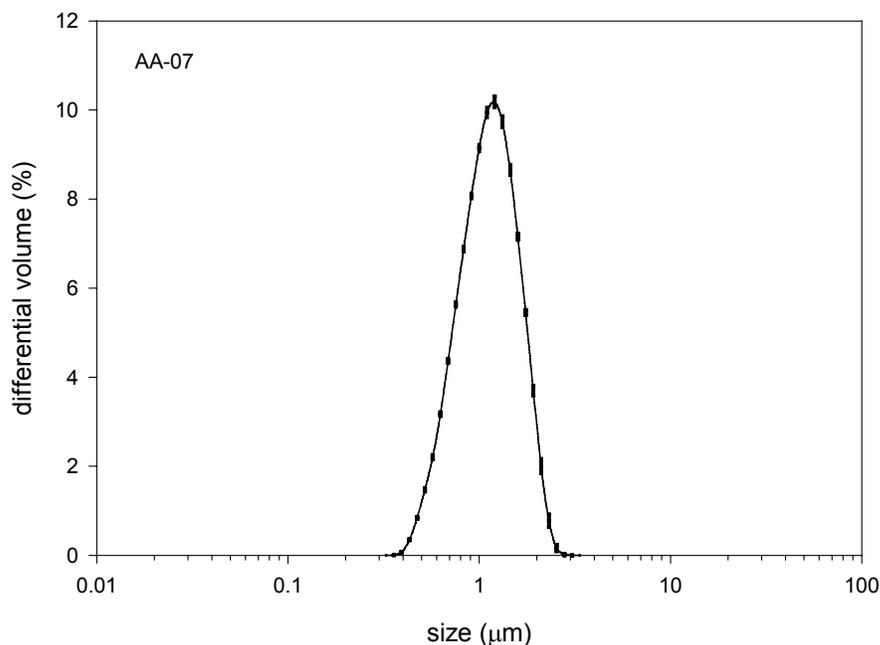
Figure 29. Differential volume PSD for AA-07 aluminum oxide in aqueous medium.

34

Figure 30. Differential volume PSD for AA-2 aluminum oxide in aqueous medium.

Figure 31. Differential volume PSD for AA-5 aluminum oxide in aqueous medium.

Figure 32. Differential volume PSD for AA-10 aluminum oxide in aqueous medium.

Figure 33. Comparison of cumulative volume PSDs for aluminum oxide in aqueous media.

Figure 34. Calculated standard deviation of PSD plotted collectively as a function of particle size for all aluminum oxide powders in aqueous media. Solid line is a second order polynomial regression fit to data. Dotted lines represent the 99 % confidence intervals for the fit.
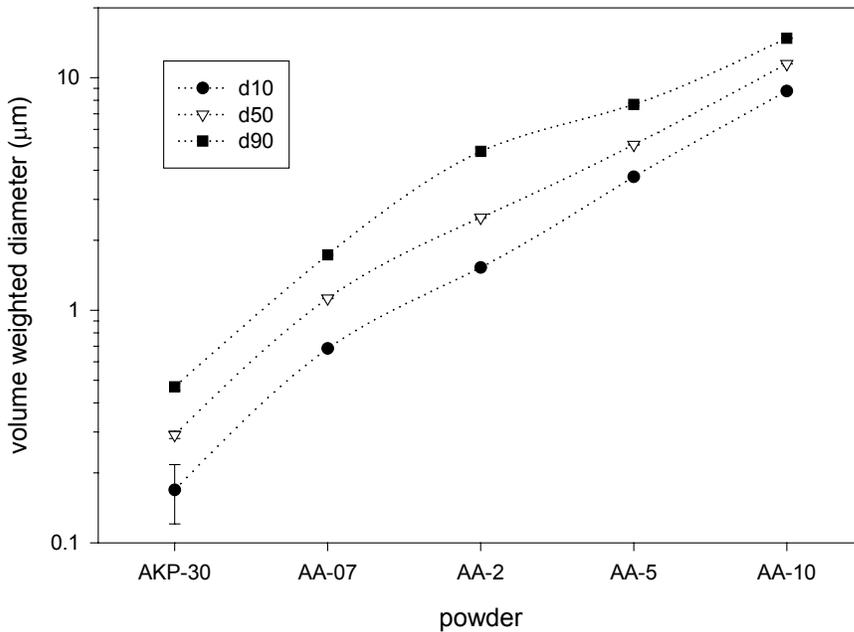
Figure 35. Comparison of mean volume-weighted percentile diameters for aluminum oxide in aqueous media.
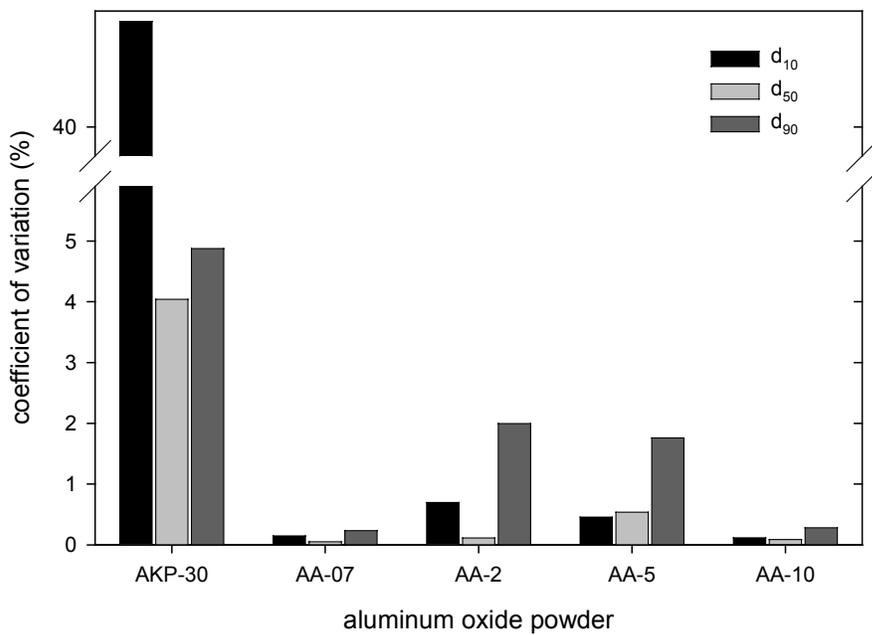
Figure 36. Precision (run-to-run) of volume-weighted percentile diameters measured for aluminum oxide in aqueous media: sample 1.
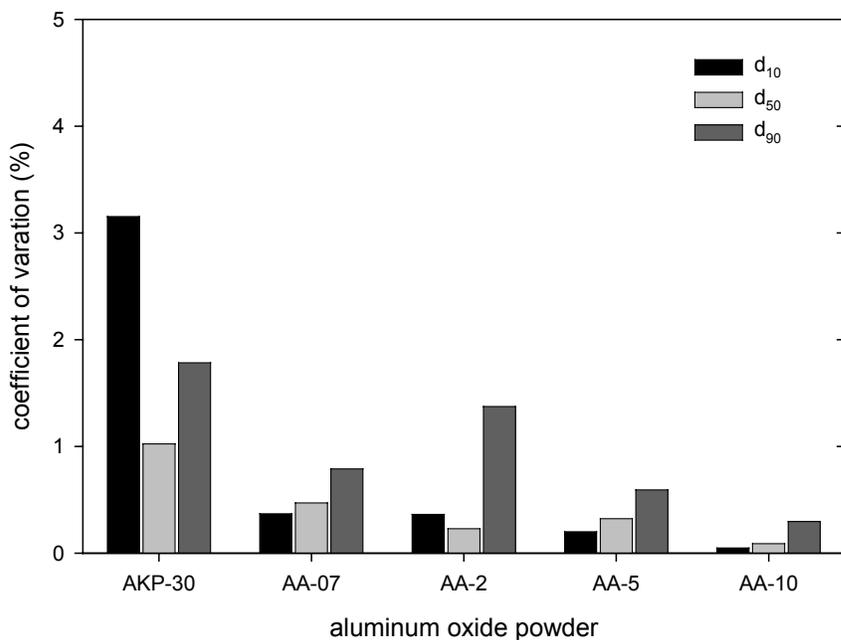
Figure 37. Precision (run-to-run) of volume-weighted percentile diameters measured for aluminum oxide in aqueous media: sample 2.

Figure 38. Repeatability (sample-to-sample) of volume-weighted percentile diameters measured for aluminum oxide in aqueous media.

Wet dispersion method - alcohol data

The following data were obtained for dispersions of aluminum oxide in IPA, using the standard (Mie) optical model with PIDS analysis. PSD data represents the mean (symbol) and standard deviation (error bar) calculated from the analysis of 3 individual subsamples (one run each) from each of 2 separately prepared samples, for a total of 6 measurements (runs). Error bars represent the effect of subsample variation in combination with sample-to-sample variation, unless otherwise noted. Individual differential volume PSDs are shown for each powder, followed by a single graph comparing the cumulative volume PSDs for all powders. Also shown is the calculated standard deviation (all powders plotted collectively) as a function of particle size, and the mean volume-weighted percentile diameters (d_{10}, d_{50} and d_{90}) for each powder. The CV for each percentile diameter is calculated for each powder based on the run-to-run and sample-to-sample variations, thus yielding a measure of precision and repeatability, respectively. Finally, the effect of ultrasonic treatment on the value of d_{50} is examined.

All powders except AKP-30 (Figure 39) exhibit a log-normal primary mode with a coarse-side shoulder at a low multiple of the primary modal size (size ratio range of 2:1 to 4:1). In contrast, AKP-30 shows a well defined bimodal PSD with a very minute fine-side shoulder near 0.07 µm. However, the error associated with the shoulder is such that it can not be considered statistically significant. The primary modes for AKP-30 are located at about 0.3 µm and 1.5 µm (size ratio of ≈ 5:1). The coarse-side shoulder in AA-07 (Figure 40) is significant enough to also suggest a bimodal distribution for this powder, with a size ratio close to 4:1.

Analysis of the absolute error as a function of size plotted collectively on a log-log basis for all powders (Figure 45) shows a roughly hyperbolic distribution with a maximum near 1 μm. There is a significant narrowing of the spread in the mean percentile diameters with increasing nominal particle size, as shown from left to right in Figure 46. The run-to-run CV of the percentile diameters for both samples (Figure 47 and Figure 48) exceeds 5 % for all three characteristic diameters in the case of AKP-30, and for d_{90} in the case of AA-07. The percentile diameters for the remaining powders exhibit relative errors under 3 %. There is an overall trend toward decreasing uncertainty with increasing nominal size. Sample-to-sample repeatability is high for the two coarser powders (Figure 49), with CVs under 1 %. Whereas, each of the three finer powders (AKP-30, AA-07 and AA02) exhibit at least one percentile diameter with a CV exceeding 5 %. Surprisingly, AKP-30 had good repeatability but poor precision, again indicating the importance of averaging multiple runs or subsamples. The poorest repeatability occurred with AA-07.

The impact of ultrasonic treatment on the measured PSD was assessed for the two finest powders, AKP-30 and AA-07, using d_{50} as a metric. The results are summarized in Figure 50. Statistically, ultrasonication has no significant effect on the measured PSD for AKP-30. For AA-07, the impact of ultrasonication is quite large compared to the absence of treatment. There is some apparent dependence on the duration of treatment, although the results for 2 min versus 4 min duration fall within the range of uncertainty determined from multiple averaged runs.
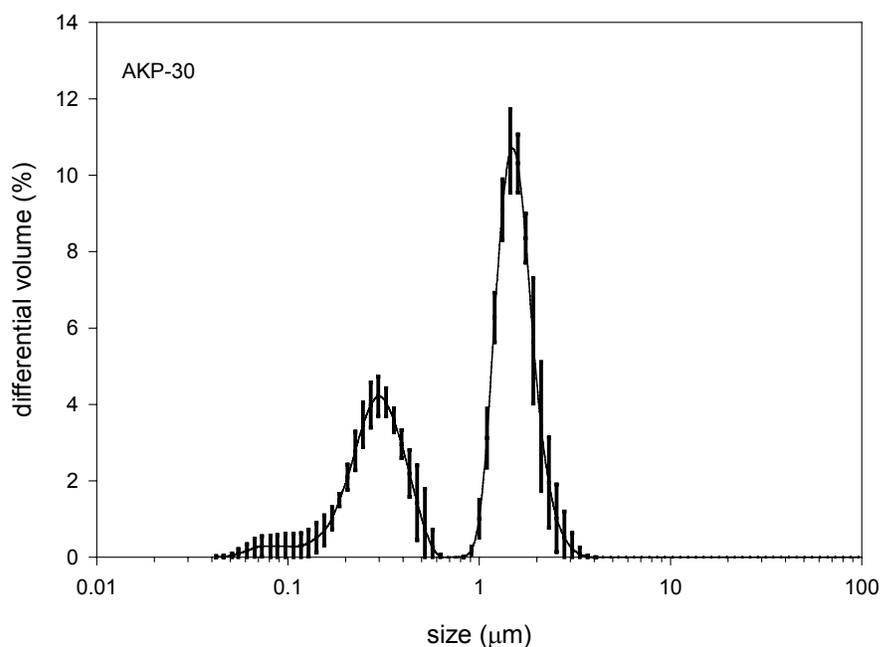
Figure 39. Differential volume PSD for AKP-30 aluminum oxide in IPA.
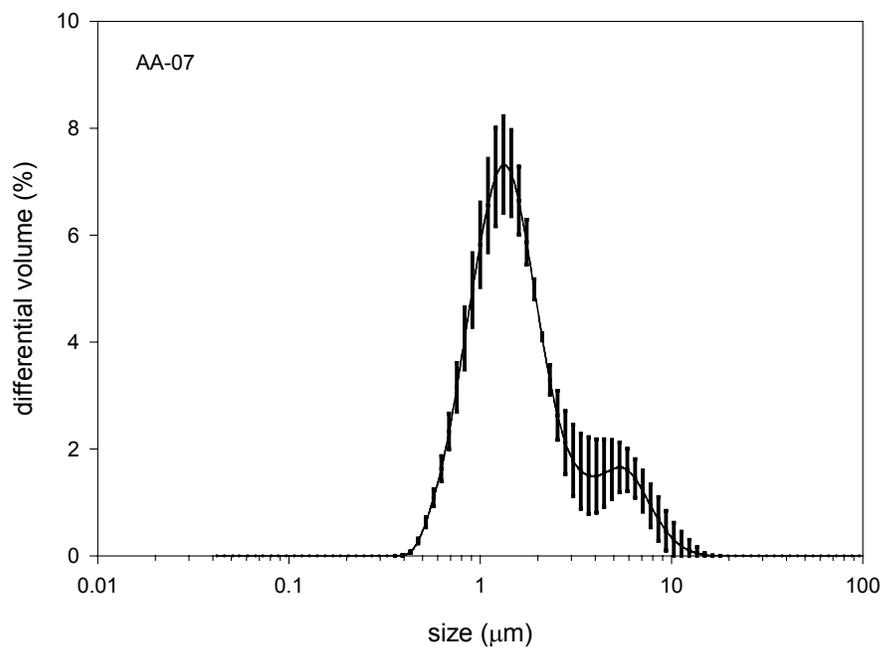
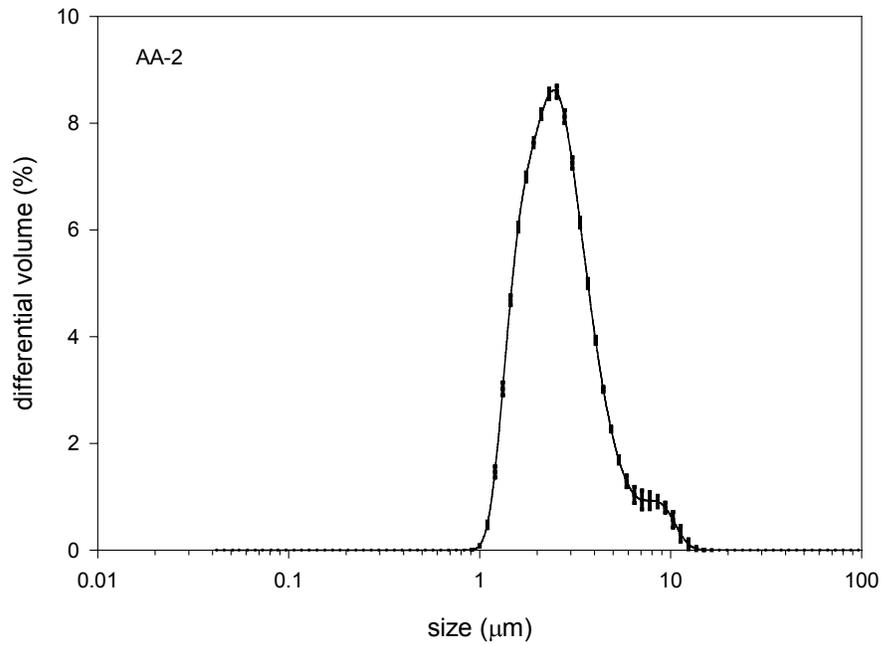**Figure 40. Differential volume PSD for AA-07 aluminum oxide in IPA.**
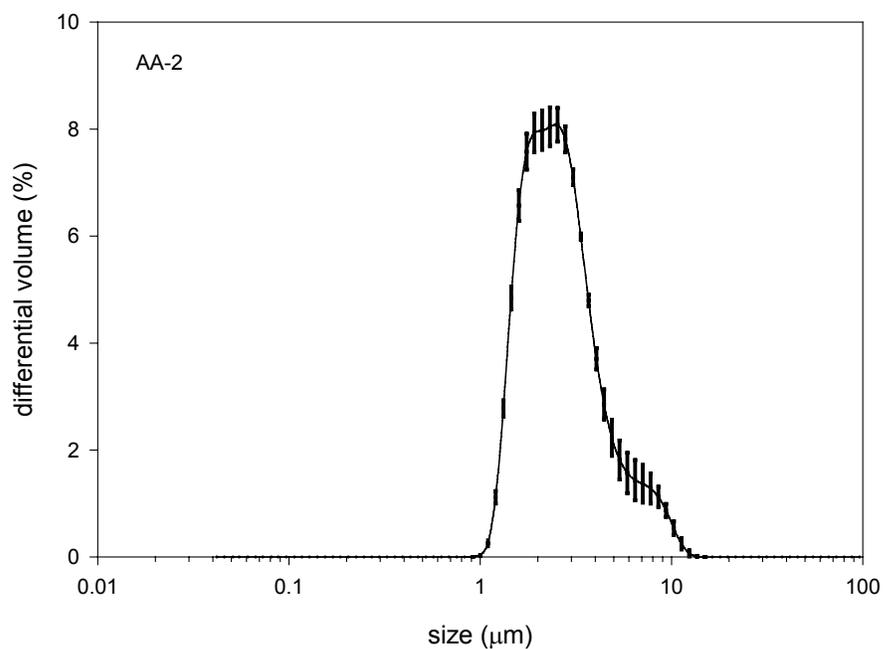
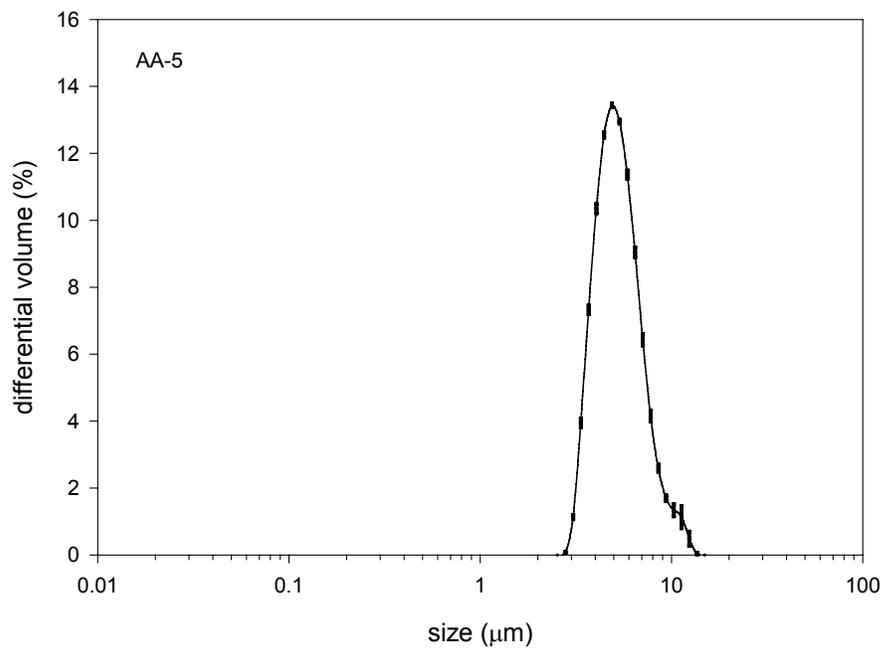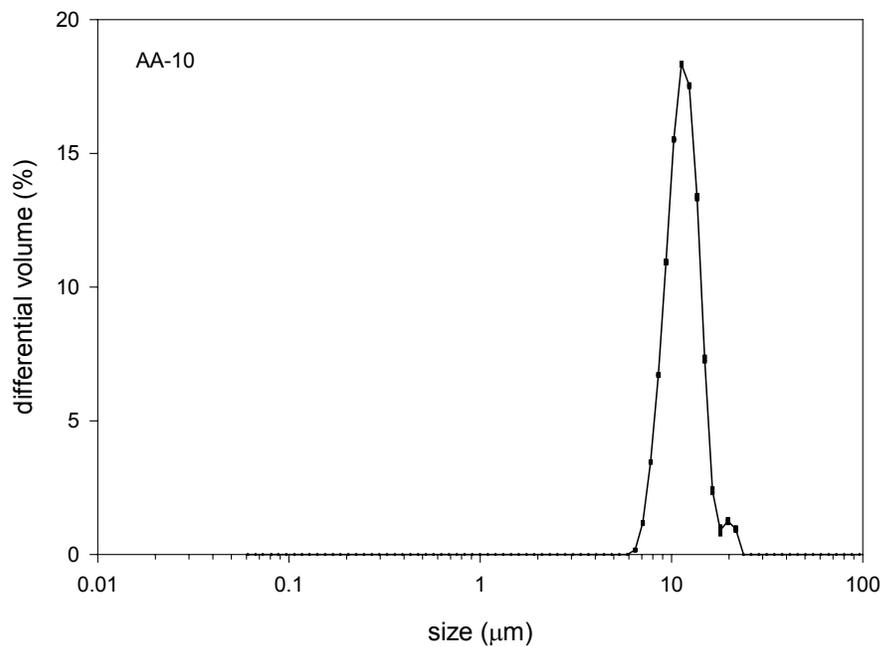**Figure 41. Differential volume PSD for AA-2 aluminum oxide in IPA.**

41
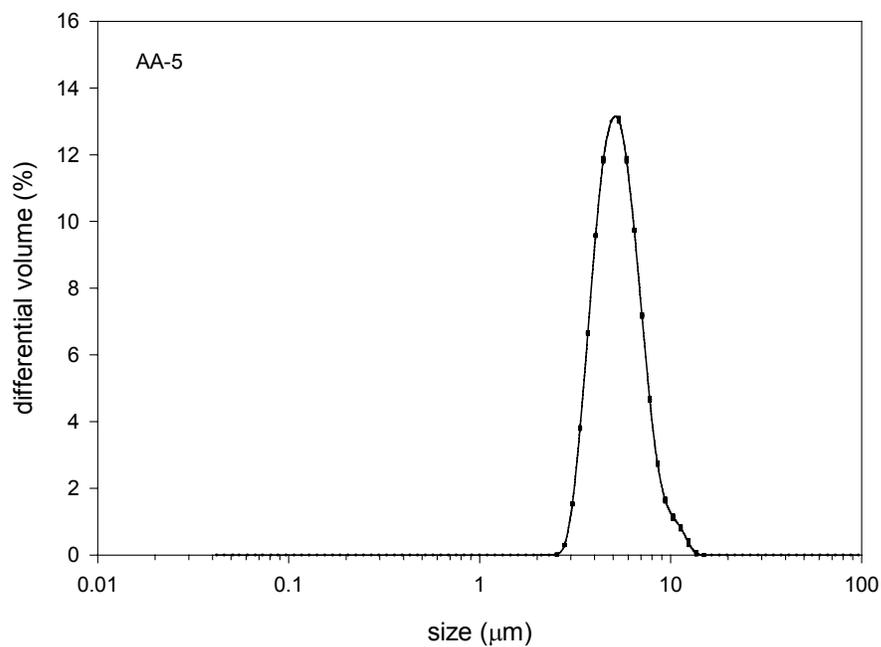
Figure 42. Differential volume PSD for AA-5 aluminum oxide in IPA.
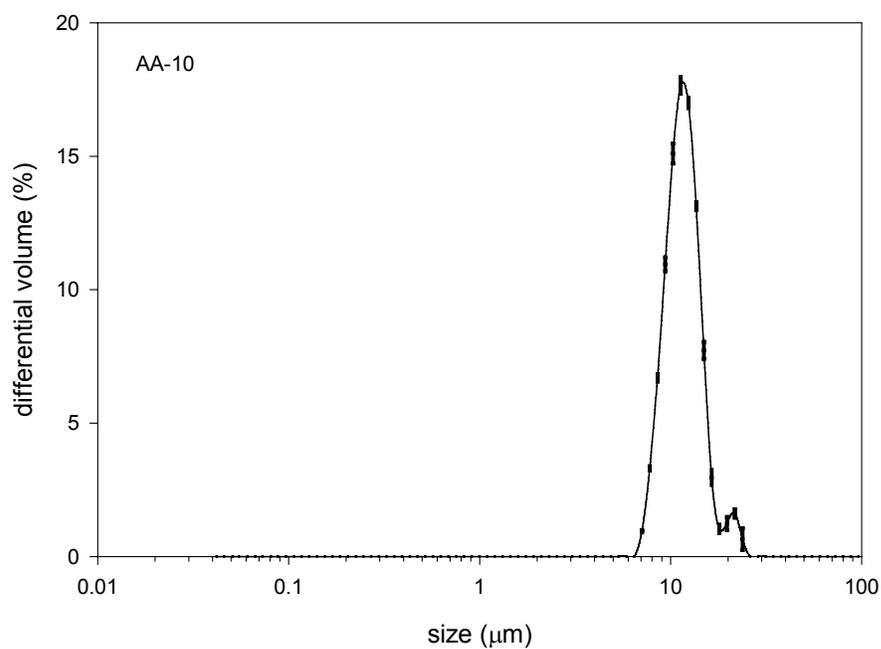
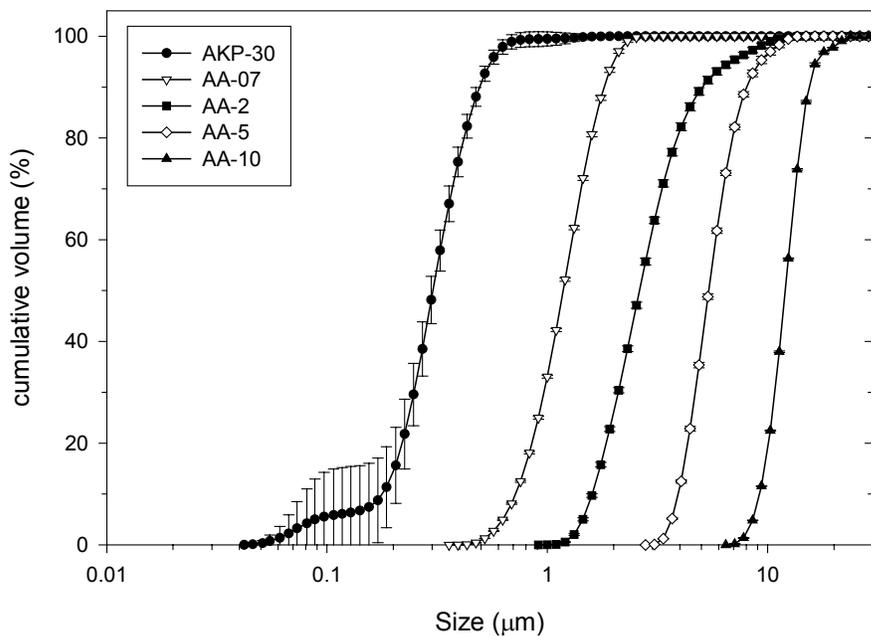**Figure 43. Differential volume PSD for AA-10 aluminum oxide in IPA.**
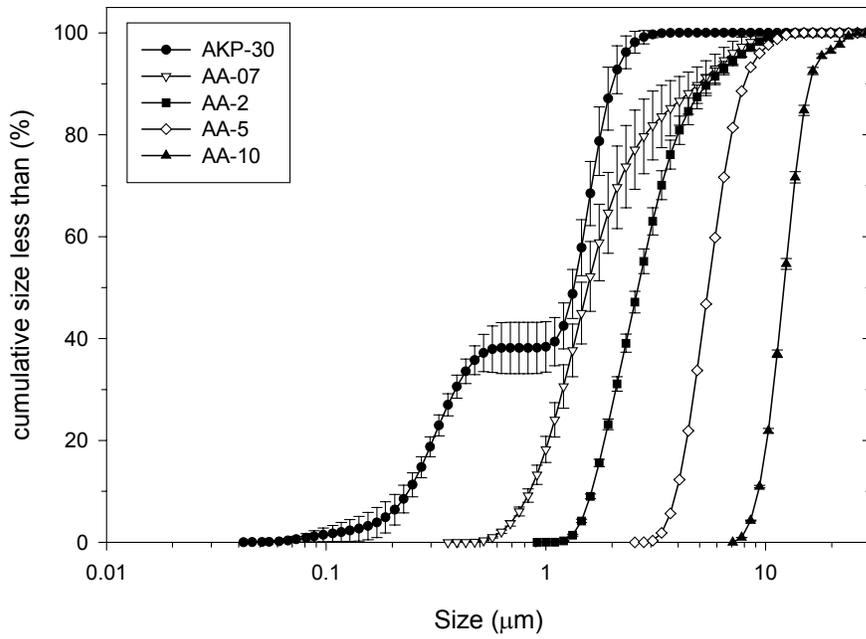
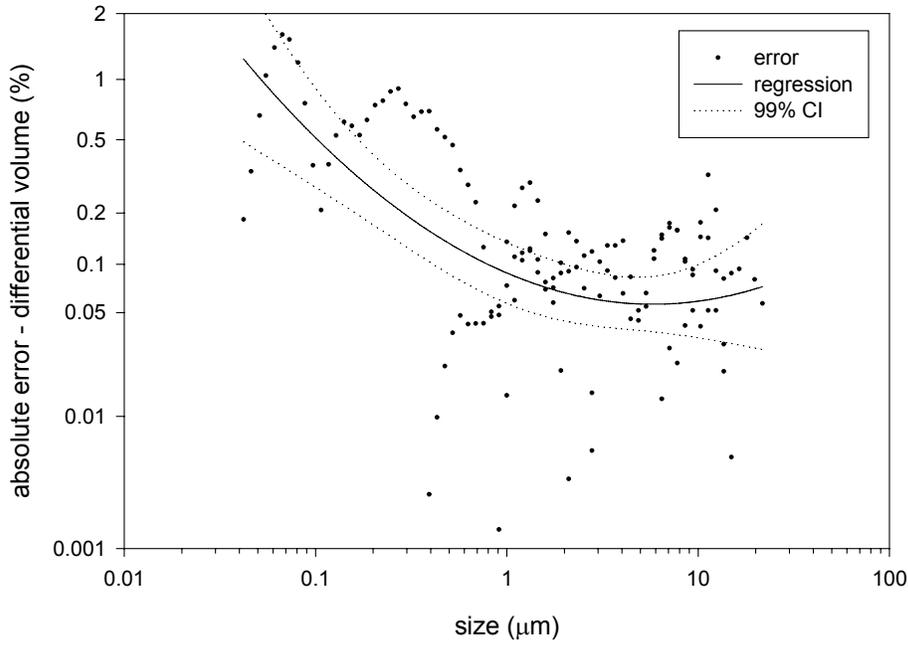**Figure 44. Comparison of cumulative volume PSDs for aluminum oxide in IPA.**
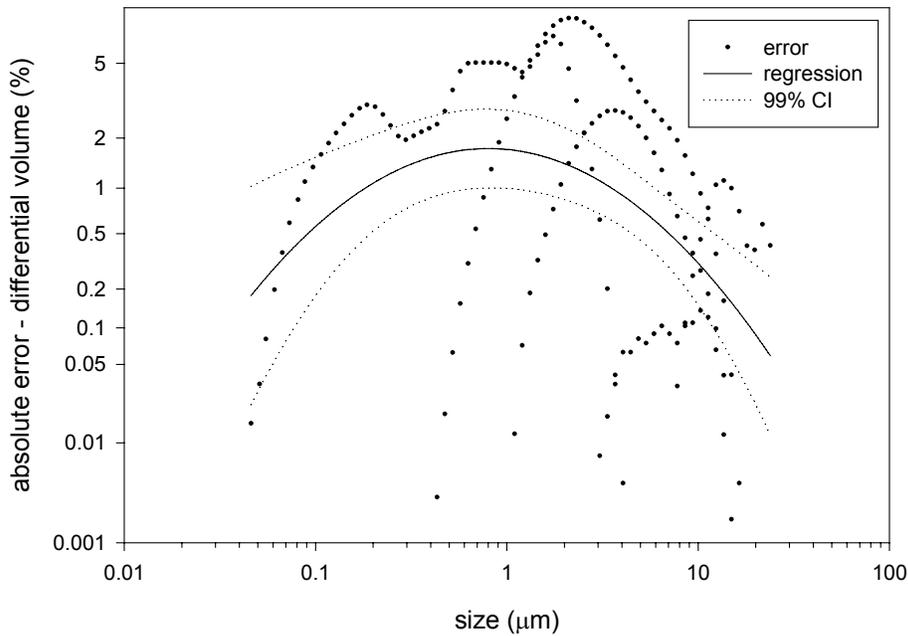

Figure 45. Calculated standard deviation of PSD plotted collectively as a function of particle size for all aluminum oxide powders in IPA. Solid line is a second order polynomial regression fit to data. Dotted lines represent the 99 % confidence intervals for the fit.
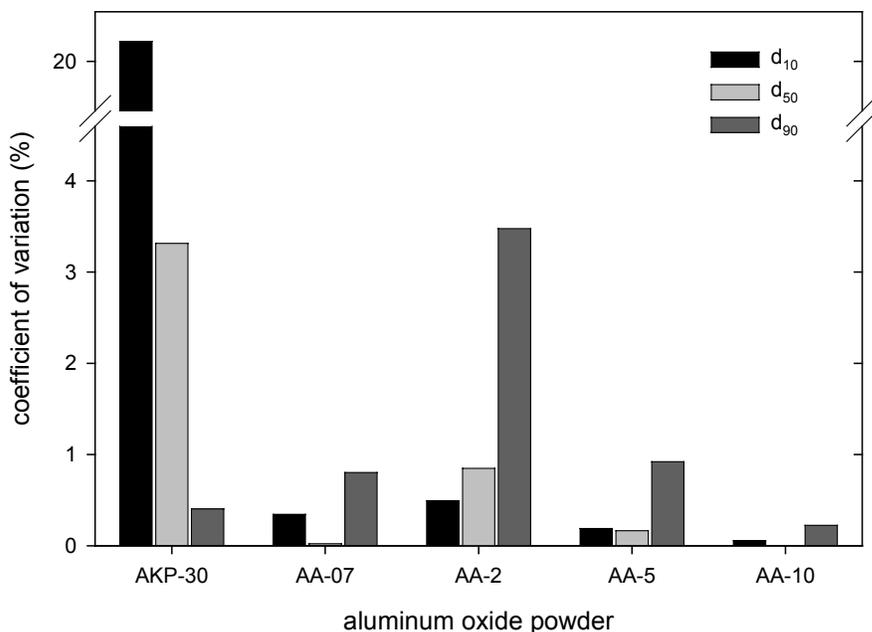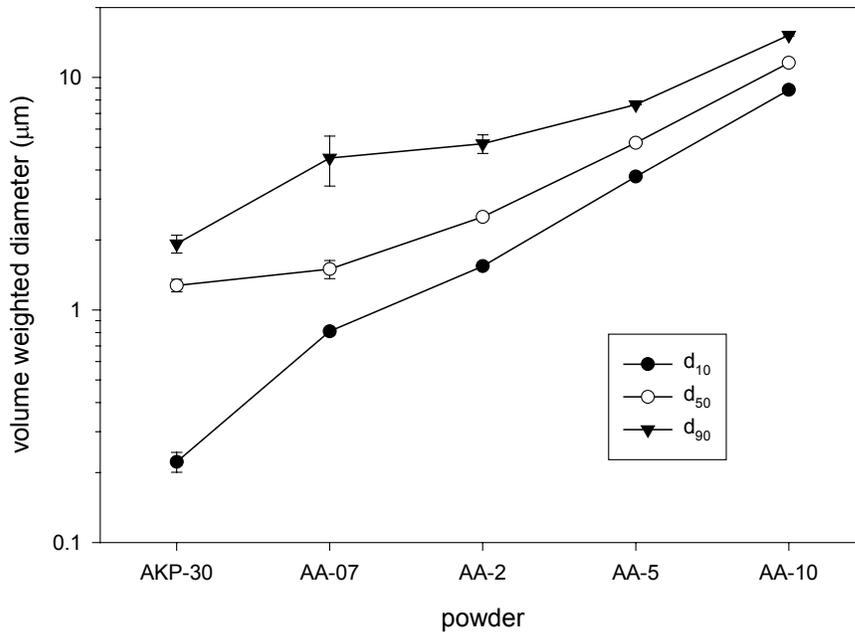
Figure 46. Comparison of mean volume-weighted percentile diameters for aluminum oxide in IPA.
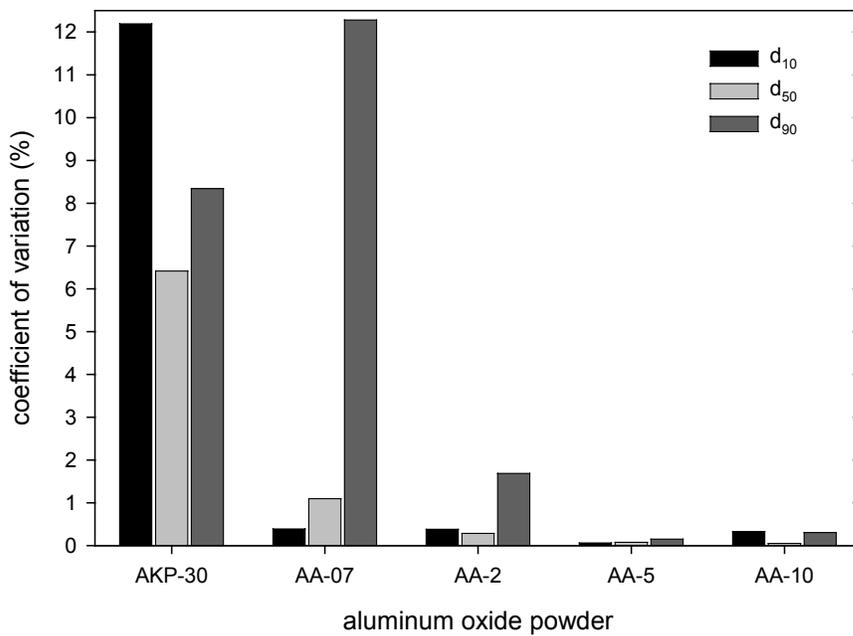
Figure 47. Precision (run-to-run) of volume-weighted percentile diameters measured for aluminum oxide in IPA: sample 1.
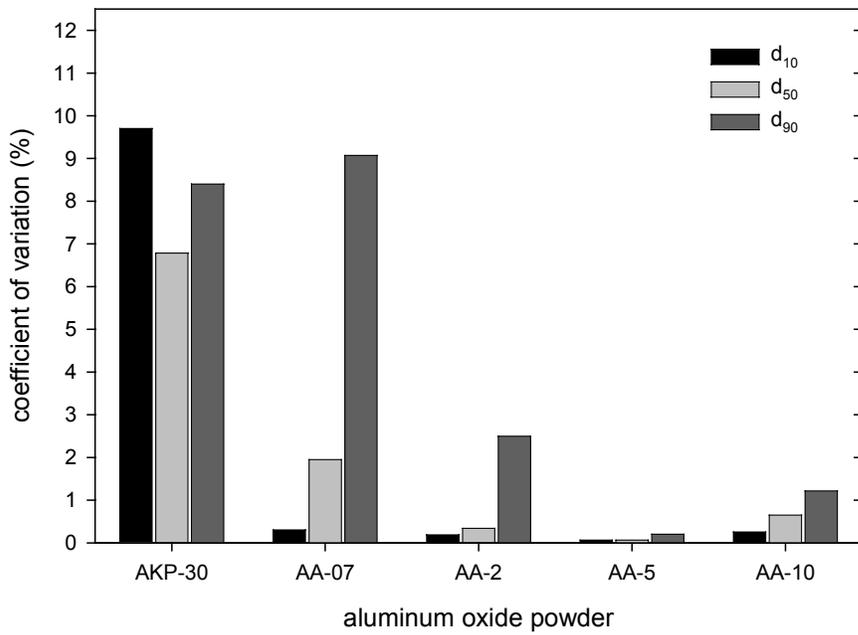
Figure 48. Precision (run-to-run) of volume-weighted percentile diameters measured for aluminum oxide in IPA: sample 2.
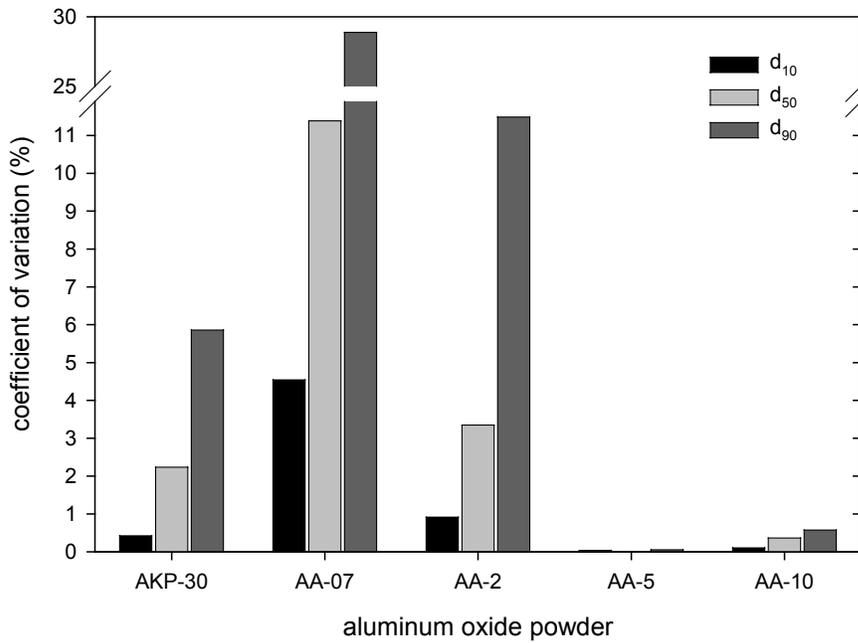
Figure 49. Repeatability (sample-to-sample) of volume-weighted percentile diameters measured for aluminum oxide in IPA.
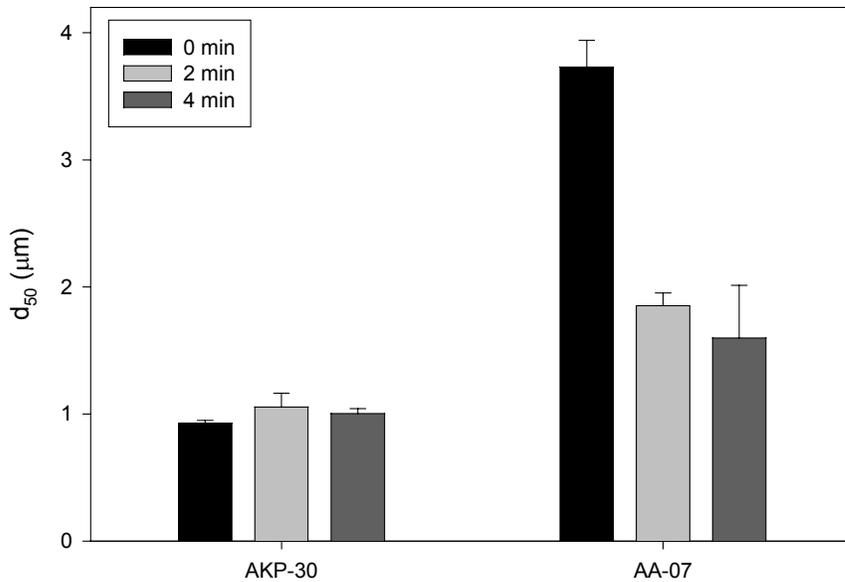
Figure 50. Effect of ultrasonic treatment time on the measured d_{50} value for aluminum oxide powders.

Dry method data

The following data were obtained for dry powder (air) dispersion of aluminum oxide, using the standard (Mie) optical model. PSD data represents the mean (symbol) and standard deviation (error bar) calculated from the analysis of 3 individual runs of a single powder sample. Error bars represent the effect of run-to-run variation. Individual differential volume PSDs are shown for each powder, followed by a single graph comparing the cumulative volume PSDs for all powders. Also shown is the calculated standard deviation (all powders plotted collectively) as a function of particle size, and the mean volume-weighted percentile diameters (d_{10}, d_{50} and d_{90}) for each powder. The CV for each percentile diameter is calculated for each powder based on run-to-run variations, thus yielding a measure of precision..

All powders except AKP-30 (Figure 51) exhibit a single log-normal mode. In contrast, AKP-30 exhibits a multimodal PSD, characterized by a broad fine-side shoulder centered at 0.7 μm, a primary log-normal mode at 8 μm and a very broad mode centered near 220 μm. The coarse mode yields a size ratio of almost 30:1 relative to the primary mode and more than 300:1 relative to the finest mode, indicating an extremely high degree of agglomeration. A comparison of cumulative volume PSDs (Figure 56) clearly shows that AKP-30 deviates in form from the other powders. For the remaining powders, AA-07 (Figure 52), AA-2 (Figure 53), AA-5 (Figure 31) and AA-10 (Figure 55), the PSD can be fit by a 4-parameter log-normal function with a R^2 value in excess of 0.999.

Analysis of the absolute error as a function of size plotted collectively on a log-log basis for all powders (Figure 57) indicates a strong dependence on size. There is a systematic narrowing of the spread in the mean percentile diameters with increasing nominal particle size, as shown from left to right in Figure 58, although AKP-30 clearly deviates in magnitude from the trend. The CV for the percentile diameters (Figure 59) exceeds 3 % only for d_{10} of AKP-30. In fact, with the exception of AKP-30, all percentile diameters exhibit a CV of about 1 % or less, indicating a very high degree of precision. There is also a strong inverse dependence of the CV on the nominal powder size (left to right in Figure 59).

46
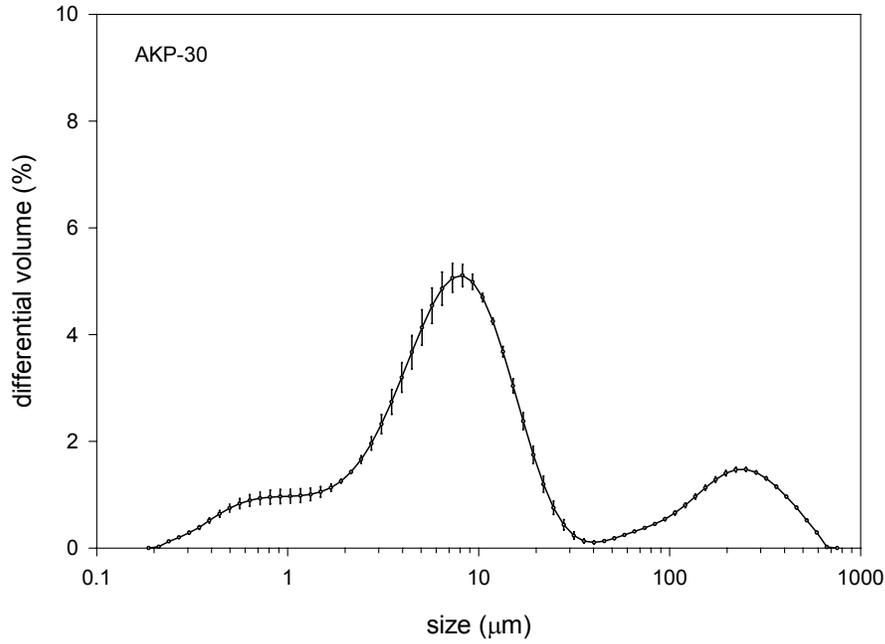
Figure 51. Differential volume PSD for AKP-30 aluminum oxide dispersed as a dry powder.
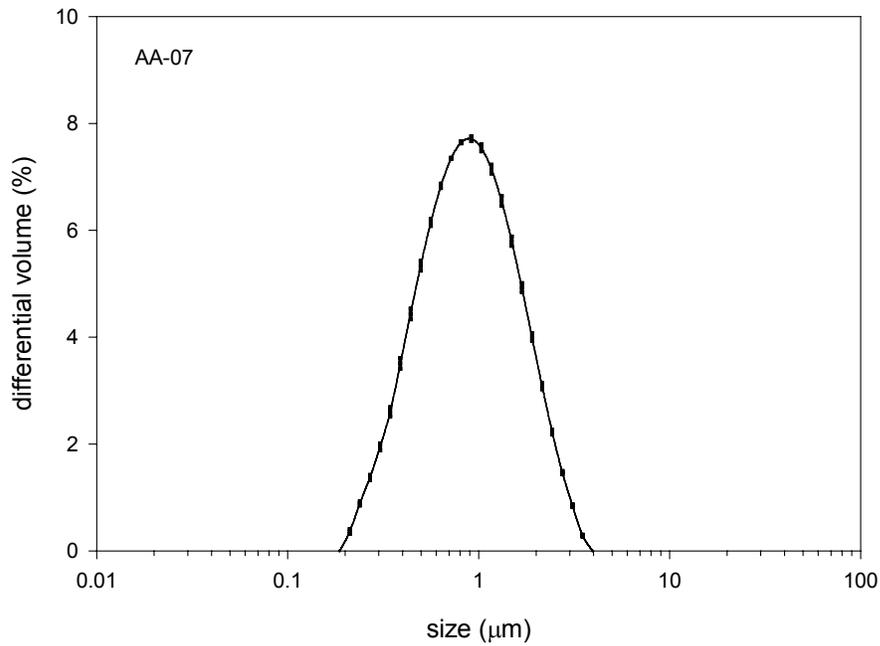
Figure 52. Differential volume PSD for AA-07 aluminum oxide dispersed as a dry powder.
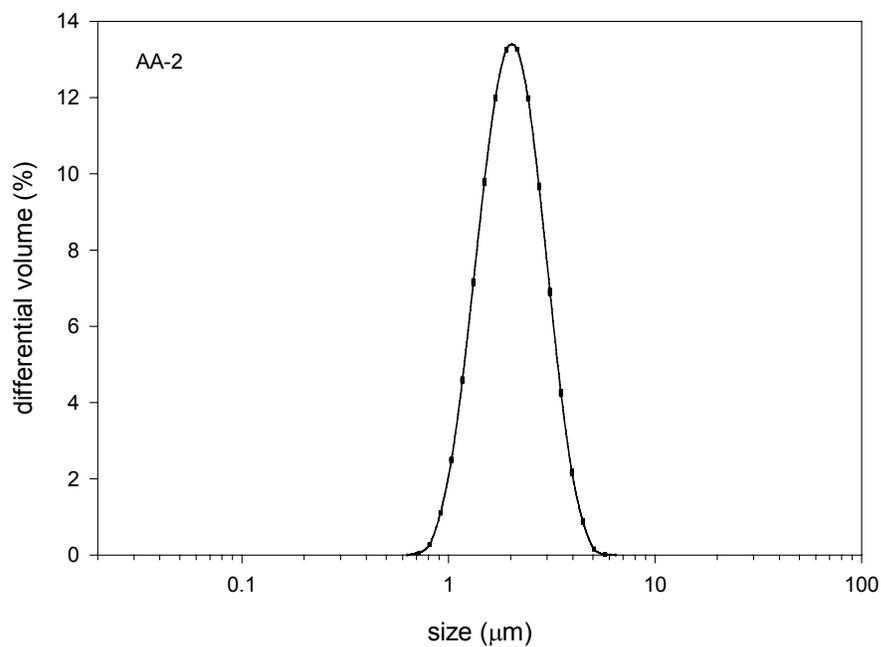
Figure 53. Differential volume PSD for AA-2 aluminum oxide dispersed as a dry powder.
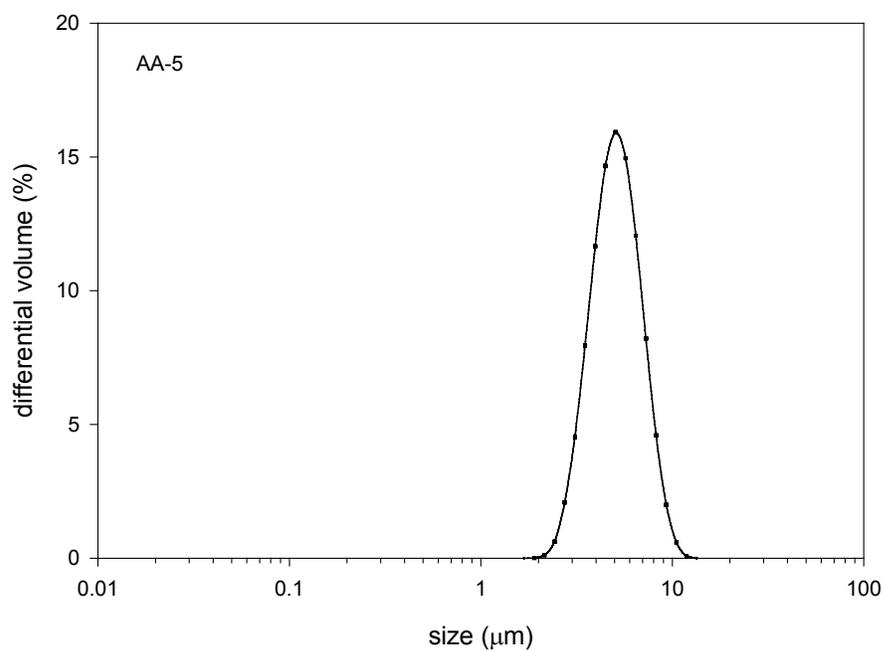
Figure 54. Differential volume PSD for AA-5 aluminum oxide dispersed as a dry powder.
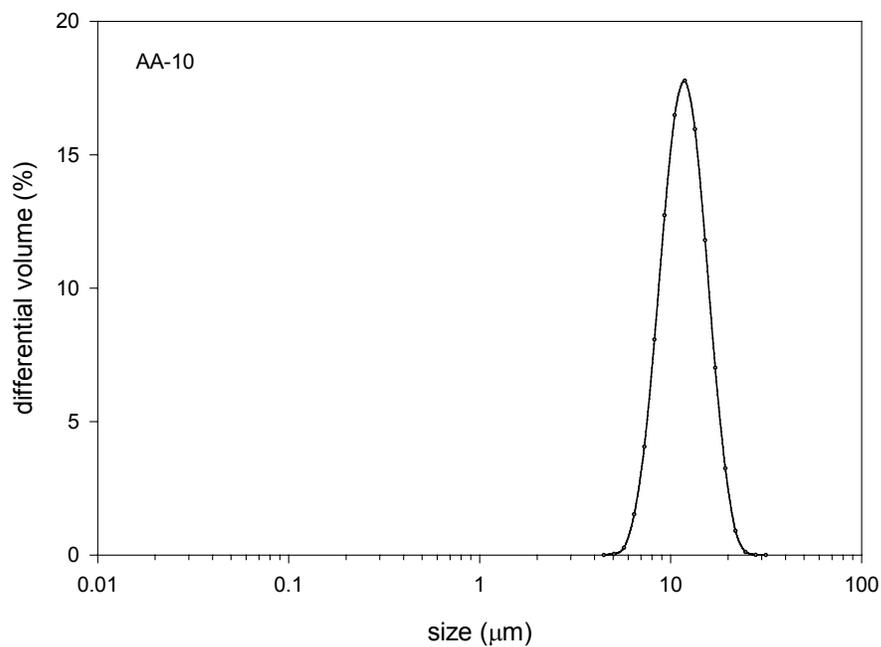
Figure 55. Differential volume PSD for AA-10 aluminum oxide dispersed as a dry powder.
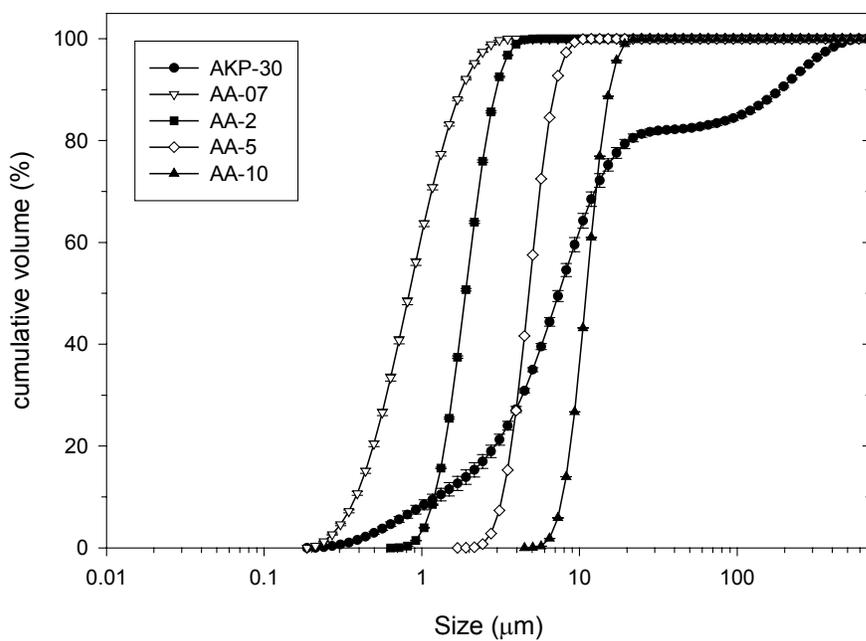
Figure 56. Comparison of cumulative volume PSDs for aluminum oxide dispersed as dry powders.
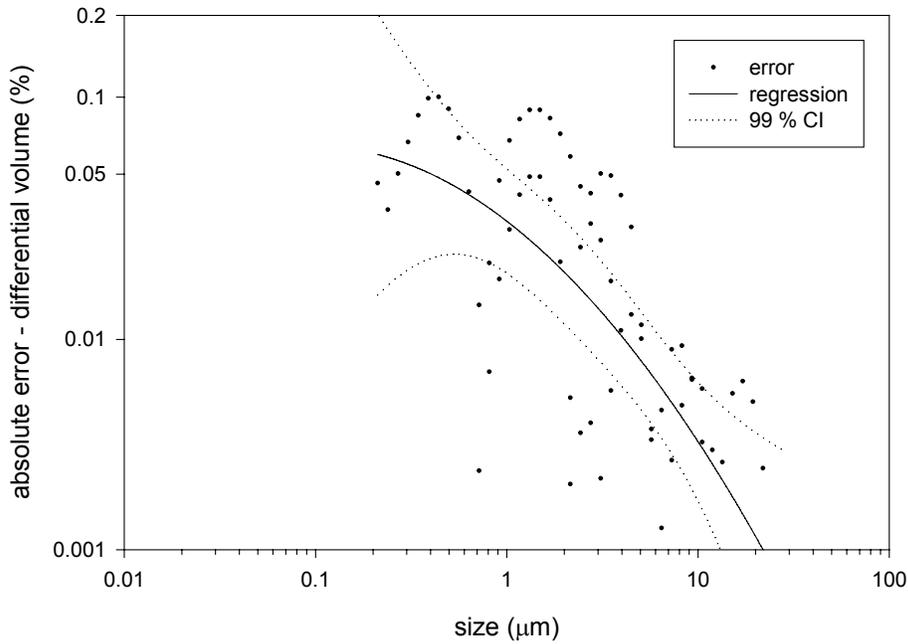
Figure 57. Calculated standard deviation of PSD plotted collectively as a function of particle size for all aluminum oxide powders dispersed in dry form. Solid line is a second order polynomial regression fit to data. Dotted lines represent the 99 % confidence intervals for the fit.
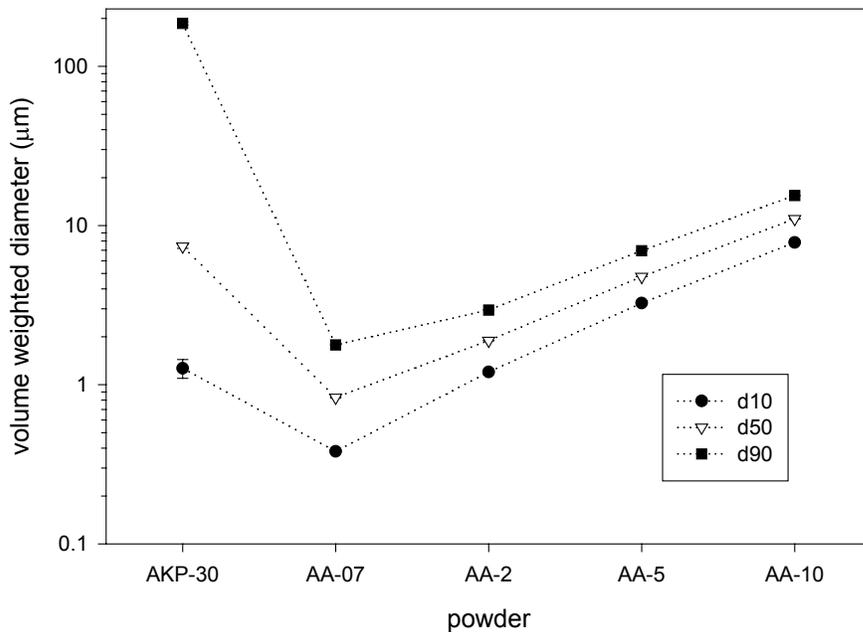
Figure 58. Comparison of mean volume-weighted percentile diameters for aluminum oxide dispersed in dry form.
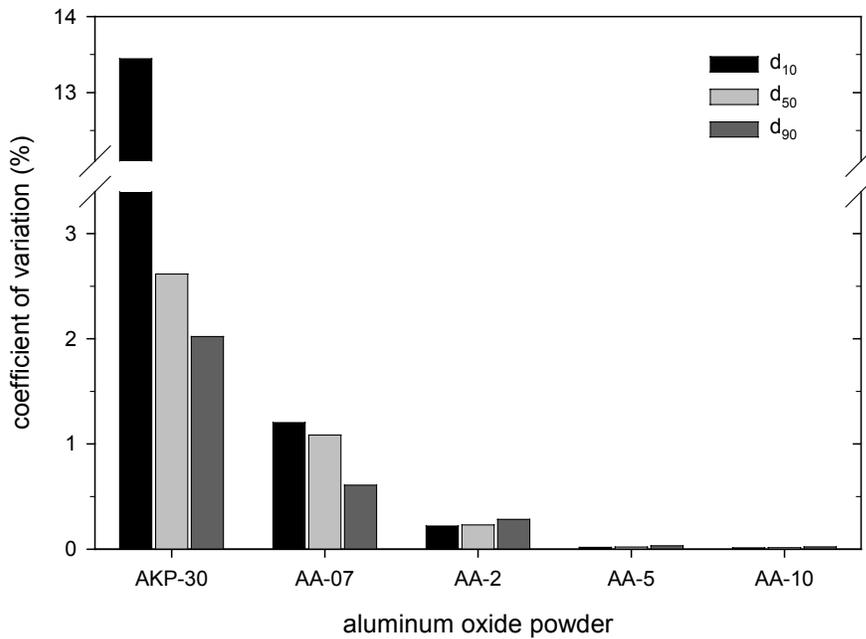
Figure 59. Precision (run-to-run) of volume-weighted percentile diameters measured for aluminum oxide dispersed in dry form.

Method comparison

Head-to-head comparisons of the mean percentile diameters determined for each powder in the three different media are shown in Figure 60, Figure 61 and Figure 62, for d_{10}, d_{50} and d_{90}, respectively. This data can be used to quickly assess the degree to which wet-IPA method and dry method reproduce the PSD measured in an optimum aqueous medium.

PSDs measured in IPA for powders having a nominal size greater than AA-07 (i.e., > 1 μm) are statistically identical to their aqueous counterparts, indicating that equal states of dispersion are attained in both media. From this we infer that alcohol should be an effective dispersion medium for the coarse particle fraction in cement above ≈ 1 μm. Comparing the dry method data, it is seen that only AA-5 and AA-10, the two coarsest powders, yield PSDs that are close to being statistically identical with both IPA and aqueous media data. In both cases, the modal diameters (peak centers) match, but the small shoulder evident in the wet method PSDs is absent from the dry PSDs (see for example Figure 63). For AA-2, the dry method yields a modal diameter that is slightly smaller compared to aqueous dispersion, and again the coarse shoulder apparent in the wet method is absent from the dry dispersion PSD. This could be interpreted to mean that air dispersion is slightly more effective for coarse particles, breaking up the residual agglomerates that persist in the wet dispersions, though this is speculation. In any case, and despite possible differences in resolution and optical model algorithms between the two instruments, the wet and dry results for the coarser powders above 1 μm are highly coherent.

At the other end of the size spectrum, large differences are noted for AKP-30 between the PSDs determined by the three methods (see figures comparing the percentile diameters and Figure 64 for a direct comparison of the PSDs). Clearly, submicrometer particles are not effectively dispersed by either the wet-alcohol or dry method. Dispersion in IPA yields the same modal diameters found in the aqueous dispersion for AKP-30, but the relative differential volumes associated with the coarser

modes in IPA are greatly enhanced at the expense of the finer modes. This indicates an incomplete deagglomeration in IPA. In the dry method, extremely large agglomerates persist well into the macroscopic range above 100 μm. Therefore, we conclude that neither the dry nor the wet-IPA method is appropriate for resolving the ultrafine submicrometer fraction in cement. As a consequence, the coarse fraction will be overestimated due to the persistence of large agglomerates.

AA-07 (nominal diameter 1 μm) represents a transition size range, where significant differences between aqueous and IPA media first become apparent. This is also the point at which the dry method yields a broader PSD relative to wet-aqueous dispersion, although the modal diameter is the same in both cases. One can conclude that alcohol is somewhat less effective than water as a dispersion medium for micrometer size particles. The effectiveness of the dry method is less clear, since it accurately resolves the modal size, though slightly overestimates both the fine and coarse bounds of the PSD. We can conclude that neither dry nor wet-alcohol dispersion is completely effective below ≈ 2 μm.

It is interesting to note that only low-multiple agglomerates (i.e., those with size ratios of 4:1 or less relative to the primary particle modal size) seem to persist after dispersion in IPA (see AKP-30 and AA-07). Furthermore, primary particles larger than ≈ 2 μm (see AA-5 and AA-10) appear to disperse well in IPA. From this we infer that agglomerates larger than about 10 μm will not be found in wet media. In contrast, dry dispersion, which seems to be more effective than either wet method for breaking up primary particles with sizes above ≈ 1 μm, can nevertheless result in residual agglomerates with sizes well above 10 μm if the primary size is ultrafine. This phenomenon can be attributed to the extremely high surface-to-volume ratio associated with colloidal phase particles, which results in strong interparticle attractive forces that oppose dispersion. In an aqueous medium, these particles are charged, and a situation can be created where mutual repulsion enables particles to separate and remain stable toward agglomeration. This is not possible in a dry air stream.

An analysis of precision for the three methods, using the percentile diameters as a metric, yields a complicated picture. Although precision in general tends to improve (lower CV) with increasing nominal size of the powder (for all methods), this trend is continuous and systematic only for the dry dispersion data (see Figure 59). The dry method also produced the strongest dependence of the absolute error (in the measured PSD) on particle size (see Figure 57). Except for AKP-30, the largest CV (run-to-run) is most often associated with d_{90} (i.e., the coarse fraction of the PSD) in both aqueous and IPA dispersions. One wonders if this is due to the presence of agglomerates, rather than being associated with the coarse primary constituents. In the dry method, the CV is greatest in the d_{10} percentile (i.e., the fine fraction of the PSD) for powders below a nominal size of 2 μm, and about even with the other percentiles for nominally larger powders.

Table 6 lists the d_{50} and d_{90} coefficients of variation for all powders and dispersion media. For wet-method PSDs, the magnitude of the d_{90} CV is highly sensitive to the presence of a coarse secondary peak or shoulder, suggesting that large errors in d_{90} may be associated with residual agglomerates; for example, a CV exceeding 2 % could be considered an indication of poor dispersion. On the other hand, the corresponding d_{50} CV more closely correlates with the residual agglomerate peak height, but is less sensitive to this factor. These relationships do not seem to apply in the case of dry method measurements, where a high degree of precision can be associated with a poorly deagglomerated sample (as in the case of AKP-30).

Table 6. Coefficients of variation for the characteristic diameters d_{50} and d_{90} determined for each aluminum oxide powder: comparison of LDS methods.[¶]

medium	d_{50} coefficient of variation (%)				
	AKP-30	**AA-07**	**AA-2**	**AA-5**	**AA-10**
aqueous	2.5	0.09	0.4	0.2	0.3
IPA	6.6	1.5	0.3	0.1	0.4
air	2.6	1.1	0.2	0.02	0.01

medium	d_{90} coefficient of variation (%)				
	AKP-30	**AA-07**	**AA-2**	**AA-5**	**AA-10**
aqueous	3.3	0.5	1.7	1.2	0.3
IPA	8.4	10.7	2.1	0.2	0.8
air	2.0	0.6	0.3	0.03	0.02

[¶] For aqueous and IPA, values are the average of run-to-run coefficients for each of two samples.

In comparison to precision, the (sample-to-sample) repeatability CV is less clearly correlated to the presence of residual agglomerates. In IPA, the poorest repeatability occurred with AA-07. We attribute this to the intermediate nature of AA-07, which makes it highly sensitive to small changes in dispersion conditions. In contrast, coarse powders (i.e., non-colloidal fraction > 2 µm) are much more easily dispersed in IPA, and therefore are less subject to minor variations in dispersion conditions. Similarly, submicrometer particles are so difficult to disperse in IPA, that small changes in dispersion and/or measurement conditions have little impact on the measured PSD. As a result, the worst repeatability occurs in the intermediate-sized powders (AA-07 and AA-2). Repeatability and precision are not separable in the case of dry method measurements, so no comparison is possible.
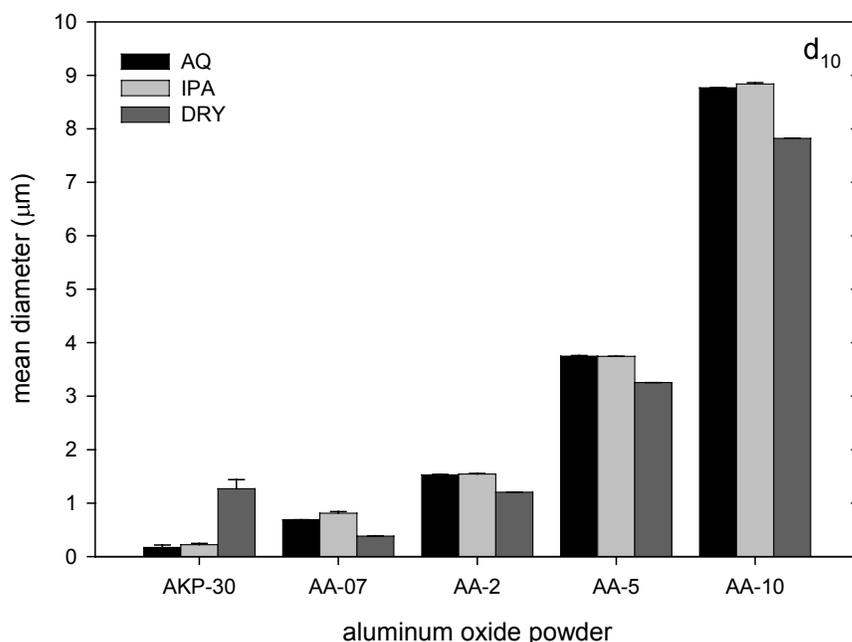
Figure 60. Comparison of d_{10} values for each powder measured by different methods: AQ, wet-aqueous method; IPA, wet-alcohol method; DRY, dry (air dispersion) method.
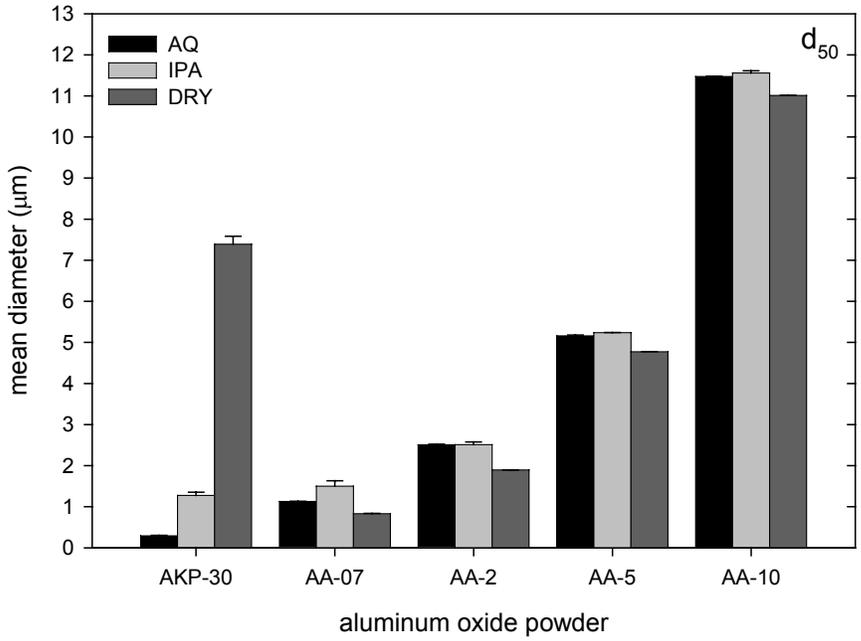
Figure 61. Comparison of d$_{50}$ values for each powder measured by different methods: AQ, wet-aqueous method; IPA, wet-alcohol method; DRY, dry (air dispersion) method.
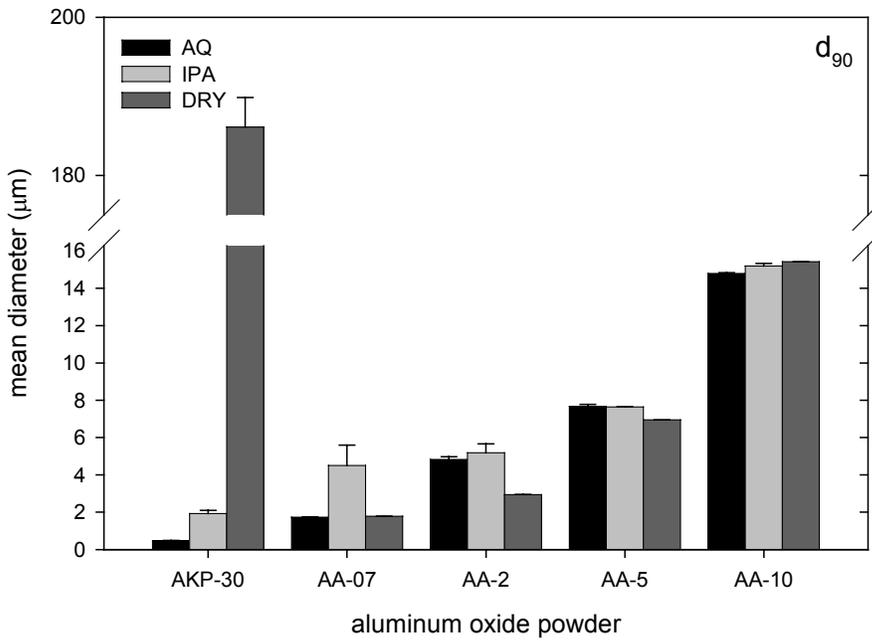
Figure 62. Comparison of d$_{90}$ values for each powder measured by different methods: AQ, wet-aqueous method; IPA, wet-alcohol method; DRY, dry (air dispersion) method.
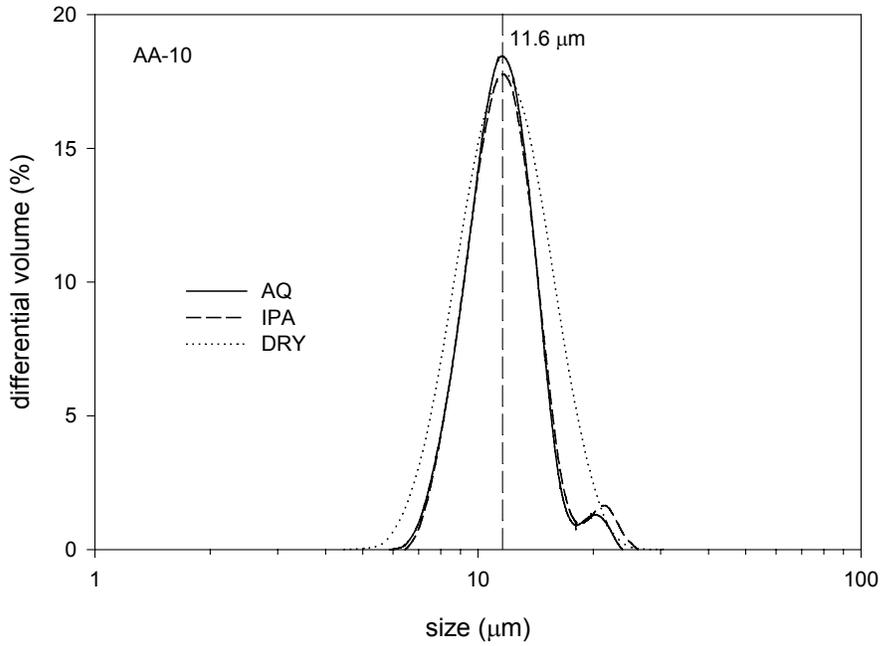
Figure 63. Overlay of differential volume PSDs for AA-10 aluminum oxide: AQ, wet-aqueous method; IPA, wet-alcohol method; DRY, dry (air dispersion) method. The modal diameter is noted.
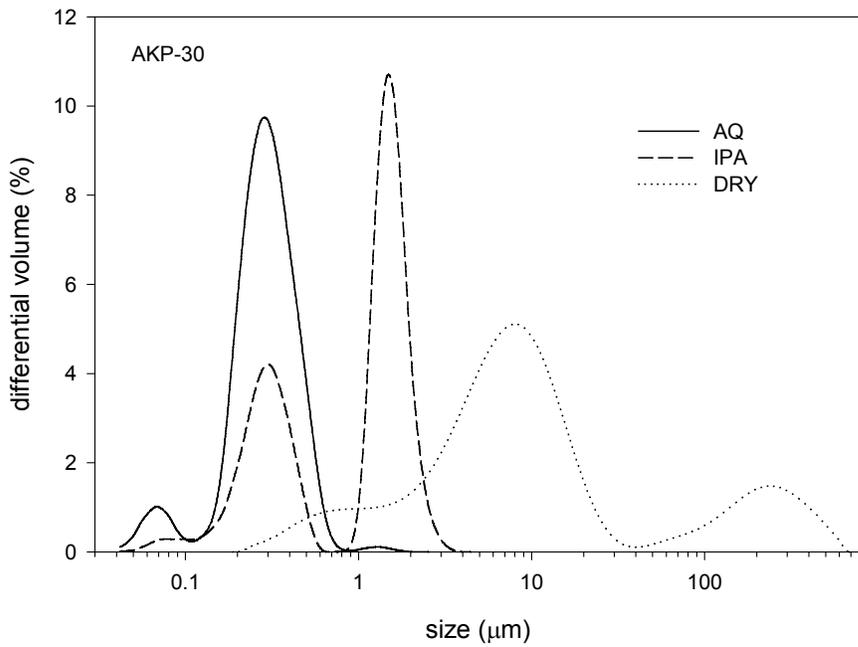
Figure 64. Overlay of differential volume PSDs for AKP-30 aluminum oxide: AQ, wet-aqueous method; IPA, wet-alcohol method; DRY, dry (air dispersion) method.

Choice of optical model: Fraunhofer versus Mie

The Fraunhofer approximation is commonly applied for cementitious materials, where the refractive index is unknown or is in doubt, since this approximation does not require knowledge of the optical constants. Indeed, its use is recommended in cases where samples contain mixtures of different materials.[2] The choice of Fraunhofer over Mie is therefore a choice of convenience in most cases, and this choice is often reinforced by the misleading observation of good precision and repeatability. However, it is important to understand the limitations of this optical model, and the ramifications of its use beyond those limits.

First of all, in the application of Fraunhofer diffraction theory it is implicitly assumed the particles are both opaque and much larger than the wavelength of light (i.e., only edge scattering can occur). In practice, only the smallest (forward) scattering angles are considered. The Fraunhofer optical model is strictly valid only for very large particles (diameter $\approx 40x$ the wavelength or larger) and somewhat smaller particles that are opaque (strongly absorptive) or have a high value of n (> 1.1). ISO standard 13320-1:1999(E), *Particle size analysis - Laser diffraction methods - Part 1: General principles*, provides the following guidelines for the choice of optical model:[2]

- For all particle larger than ≈ 50 μm, Fraunhofer works well and gives accurate PSDs.
- For particles smaller than ≈ 50 μm, Mie theory is generally the best choice if the optical constants are known.
- For intermediate sized particles in the range ≈ 1 μm to 50 μm, with $n_R > 1.1$ and/or k (particle) > 0.05, Fraunhofer usually gives good results.
- In all cases where Mie is used, good values for the optical constants must be provided.

Incorrect application of the Fraunhofer approximation can result in the creation of "apparent" fines, frequently called "ghost" particles. This occurs when a significant fraction of transparent fines (i.e., particles smaller than a few μm with k less than ≈ 0.05) exist, and results in an overestimation of the calculated fine fraction.

Since we are working with a material (aluminum oxide) that is well defined both optically and morphologically (i.e., they are roughly spherical in shape), and for which we therefore can apply the Mie model with a high degree of confidence, this permits us to then examine the effect of using the Fraunhofer approximation with powders varying nominally in size.

Figure 65 shows the differential volume PSDs for the same measured diffraction spectrum of AKP-30 calculated by both Mie and Fraunhofer optical models. The Fraunhofer approximation yields a population of virtual particles that do not exist in reality, and does a poor job of resolving the primary mode accurately. Clearly, the Fraunhofer approximation is inappropriate for quantifying PSDs with largely submicrometer size fractions, and in this case the Mie theory should be applied if the refractive index values are known or a reasonable estimate can be made. Without good values for the refractive index, Mie is likely to produce equally biased results, in which case LDS may not be an appropriate choice.

Figure 66 shows a similar analysis for nominally coarser AA-2 aluminum oxide, which contains no significant submicrometer fraction. In this case, the Fraunhofer model is able to correctly position the primary mode (≈ 2 μm) and its shoulder (≈ 9 μm), but creates a substantial population of virtual particles below 0.7 μm. Additionally, the integrated volume of the primary mode (including the shoulder) is underestimated by 36 % in using Fraunhofer rather than Mie. So, there is improvement over the submicrometer case, but the Fraunhofer approximation still produces significant errors for aluminum oxide particles in the 1 to 10 μm range.

Finally, Figure 67 shows a comparison of the optical models for the coarsest aluminum oxide powder, AA-10. Further improvement is noted in regard to the analysis of the primary mode and its

shoulder for these nominally coarser particles, but Fraunhofer still produces a 20 % lower integrated volume for the primary mode, while generating a moderate population of virtual submicrometer particles. So, even for powders containing size fractions in the 6 µm to 23 µm range, the problem of underestimation of the coarse fraction and the generation of "ghost" particles persists, albeit to a lesser degree than for particles under 6 µm.

In this study, we did not examine powders with constituents coarser than about 23 µm, but the trend seems obvious, and our results correspond fairly closely with the applicability limits outlined in ISO 13320-1:1999(E). The exact meaning of "good results" in regard to intermediate size particles with a high refractive index (conditions corresponding to AA-2 and AA-10 in the present case), in the ISO document, is unclear and thus open to interpretation. In our case, volumetric errors exceeding 20 % coupled with a substantial population of virtual particles would seem somewhat less than good. Presumably, one could simply disregard any secondary submicrometer modes that appear in the application of the Fraunhofer model, so long as the sample is known to be coarse in nature. Then one would contend only with the absolute volumetric error in the primary modes. Of course, this approach only works with powders containing relatively narrow PSDs. In the case of cement, it is conceivable that the moderate absorptive properties would further decrease the errors due to use of Fraunhofer (i.e., by reducing transparency and thus refractive effects). Regardless, the current results should provide at least an order of magnitude estimate of the errors to be expected in applying the Fraunhofer model to portland cement containing intermediate and submicrometer size fractions.
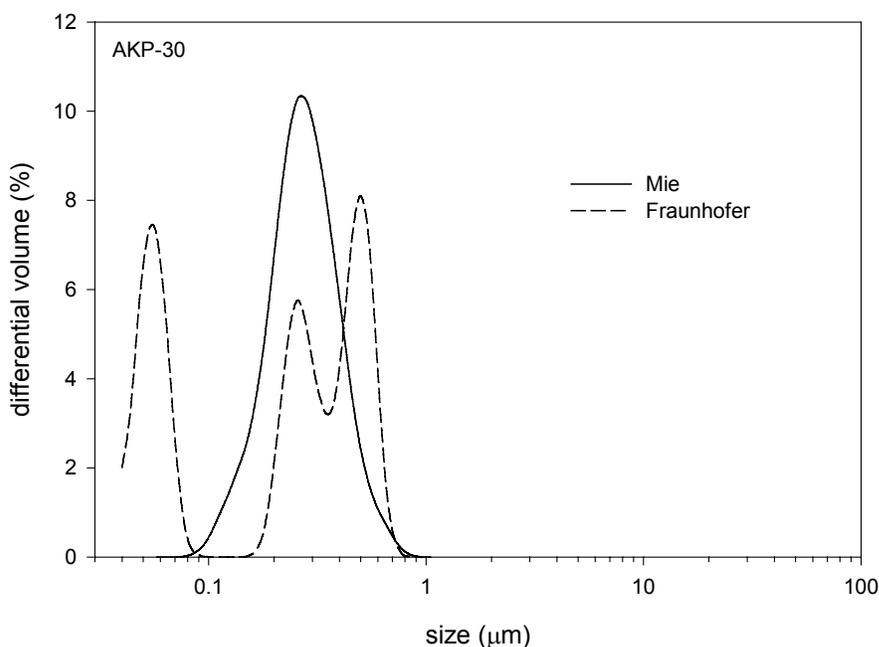
Figure 65. Effect of using the Fraunhofer approximation versus the Mie model in the calculation of the differential volume PSD for AKP-30 aluminum oxide.
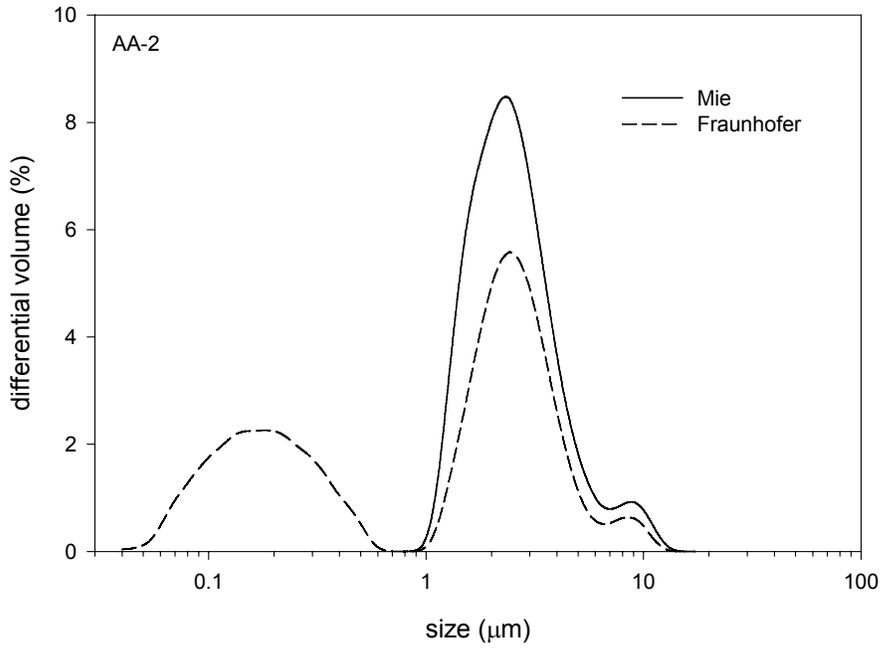
Figure 66. Effect of using the Fraunhofer approximation versus the Mie model in the calculation of the differential volume PSD for AA-2 aluminum oxide.
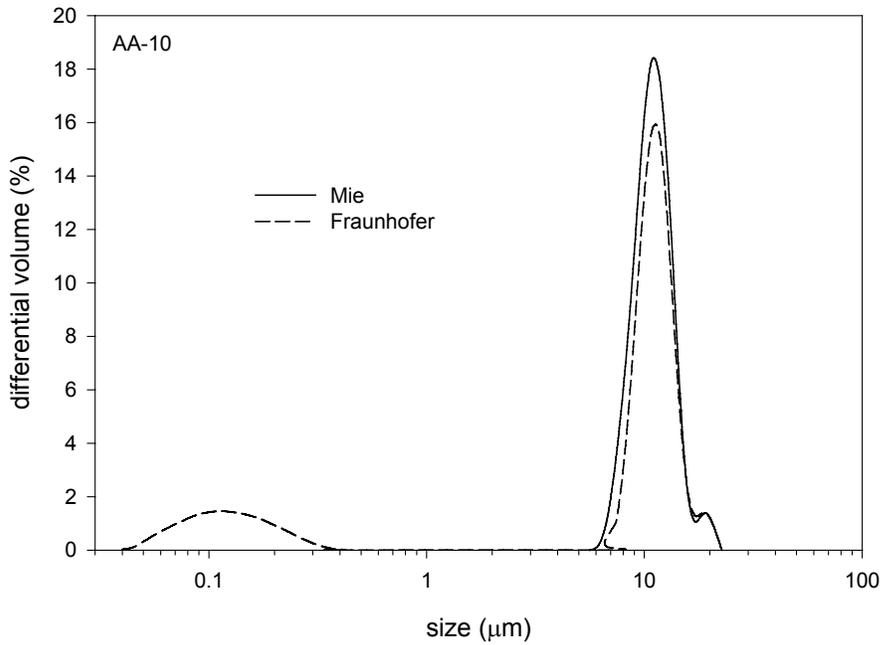
Figure 67. Effect of using the Fraunhofer approximation versus the Mie model in the calculation of the differential volume PSD for AA-10 aluminum oxide.

GLOBAL SUMMARY AND CONCLUSIONS

A number of factors that impact particle size distribution analysis of cementitious powders by laser diffraction spectrometry were examined in the course of two studies. The first study employed a typical portland cement (CCRL 135) as a test material, while the second study focused on a series of high-purity discrete size-fractionated aluminum oxide powders. In particular, sample preparation and the choice of optical model were identified as key factors and examined in some detail. Wet and dry LDS methods were compared in the case of aluminum oxide. A detailed assessment of measurement precision and repeatability (i.e., sample-to-sample precision) was provided for a wide range of material/experimental conditions. The following conclusions regarding the analysis of cementitious powders by LDS are drawn from this work.

In regard to sample preparation, the choice of medium can have a profound but complex impact on the resulting PSD. For coarse particle sizes greater than about 2 µm, both wet (alcohol or aqueous) and dry methods produce highly coherent results. In this case, the choice of medium appears more or less inconsequential. In fact, the dry method appears to be slightly more effective than the wet methods in dispersing the coarser fractions above 2 µm, though this difference could just as easily be attributed to variations inherent in the use of two different instruments for wet and dry measurements (e.g., dissimilar size intervals used in the calculation of differential volume PSDs; see Appendix A). On the other hand, for submicrometer particles the dry method is clearly inappropriate, and will yield strongly biased PSDs that greatly underestimate the fines and overestimate the coarse fraction. To a lesser degree, dispersion in an alcohol medium may also produce biased PSDs due to possible incomplete deagglomeration of submicrometer fines. The ability of the dry method to accurately assess the PSD in the transition range around 1 µm to 2 µm, though suspect, is less clear. The implication for the analysis of cement powders with a broad range of particle sizes is that neither the dry nor the wet-alcohol method will likely yield the "correct" PSD, though they may produce precise and repeatable results.

It is impractical to improve dispersion in the dry method, as the method is primarily designed for the analysis of coarse powders. One way to improve the wet-alcohol method would be to use surfactants designed specifically for the cement-alcohol system in order to facilitate deagglomeration of the fines. However, the application of a widely used surfactant, like AOT, did not consistently improve results in alcohol. An alternative would be to use a chemical admixture at saturation concentration levels to disperse the cement powder in an aqueous medium, while at the same time inhibiting the hydration reaction. We evaluated this approach using a naphthalene sulfonate admixture, but the resulting PSD indicated poorer dispersion relative to IPA, so alcohol may in fact be the best practical medium for cement analysis.

A comparison of alcohols in the series methyl, ethyl, 2-propyl (IPA) and n-butyl, showed that PSDs with a more substantial fine fraction could be obtained using alcohols other than IPA, but that IPA yields the best combination of precision and repeatability. Ethyl alcohol, for instance, gives a mean PSD that is finer relative to IPA, but subsample precision is very poor. Run-to-run precision is very high and of similar magnitude for all four alcohol media, but subsample-to-subsample precision within the same sample appears to track closely with alcohol viscosity. Methyl alcohol, with a viscosity of 0.6 mPa·s, has less than half the viscosity of IPA, and exhibits extremely poor subsample precision. Therefore, it appears that the decrease in precision is due to a sampling error during transfer and dilution of the low-viscosity stock suspension prior to measurement. We also conclude that the small sampling volume used for the dilution of stock suspension (only a few drops of 20 % stock suspension are necessary to obtain the optimum obscuration level on the instrument) may contribute to these sampling errors. Any segregation or settling of material that occurs during transfer (e.g., in the disposable pipette) will be greatly magnified during analysis because of the small volume transferred. We suggest that to improve the statistics and to reduce the possibility of

sampling error during transfer of stock suspension, the solids concentration in the stock should be lowered by a factor of at least 4 (i.e., from 20 % mass fraction to 5 % mass fraction). This will quadruple the volume of stock transferred during dilution, which should help improve the subsample precision and sample-to-sample statistics. On the other hand, if less powder is used in the preparation of the stock suspension, then this will increase the likelihood of sampling errors at this stage. To compensate, the total volume of the stock suspension could be increased or rifling techniques used to insure homogeneity in the dry powder. A lower solids concentration in the stock will also probably mean that less ultrasonic energy is required to achieve the same level of dispersion.

High-energy ultrasonic treatment of the stock cement suspension using an immersible transducer causes a measurable improvement in dispersion (i.e., reduction in the differential volume of larger particle sizes with a concurrent increase at smaller sizes), but this effect is relatively moderate in alcohol. It was also found that a treatment time exceeding about 1 min did not provide further improvement in the level of deagglomeration in alcohol dispersions. Therefore, minimal ultrasonic treatment might be used to achieve a better dispersed state and more consistent results, but a bath-type ultrasonicator probably would not be sufficiently powerful to provide this improvement if applied to the more concentrated stock suspension.

An analysis of precision for the wet (IPA) and dry methods, using the characteristic percentile diameters (d_{10}, d_{50}, d_{90}) as metrics, yields a complicated picture. The precision of replicate sequential measurements (runs) within a single subsample proved to be very high for the wet-alcohol method, with CVs near 1 % for all three characteristic diameters. The subsample-to-subsample and sample-to-sample variations are similar in magnitude, with CVs ranging from about 5 % for d_{10} up to 16 % for d_{90}. This seems to indicate that the most significant contribution to uncertainty in the measured PSDs arises during the process of diluting the stock sample prior to analysis. The CV values generally increase with increasing characteristic diameter for the wet methods, indicating that the poorest precision is associated with the coarser fractions. This may be due to the lower frequency of large particles that contribute to the measured signal in the sensing zone, or it may be due to particle segregation due to variations in the stir rate or sampling technique prior to dilution on the instrument. Dry measurement precision depends strongly on the particle size, with excellent precision (CV < 1 %) for particles above 2 μm. Precision rapidly deteriorates as the particle size falls below about 1 μm.

We have determined that the most significant factor, post-sample-preparation, that impacts PSD determination is the choice of optical model used for the inversion of the measured diffraction spectrum. For $n \geq 1.6$ (i.e., fairly refractive materials), the model is not very sensitive to the choice of n for weakly absorbing or transparent materials (i.e., $k < 0.1$). It is only moderately sensitive at $k = 0.1$. The Fraunhofer model generates a PSD that is nearly equivalent to the Mie calculation if the optical constants are set at $n = 1.6$ and $k = 0.1$ in the latter model. For $n \geq 1.7$ and for any value of k, the Fraunhofer model by comparison greatly overestimates the submicrometer fraction while slightly underestimating the 2μm to 40 μm size range. The magnitude of the calculated submicrometer fraction depends on the choice of k, with the dependence becoming stronger as n becomes smaller. The portion of the PSD above 1 μm is largely insensitive to the value of k for values of $n \geq 1.7$. Therefore, the greatest uncertainty for the analysis of cement, with a value of n near 1.7, probably results from the selection of k. Since this value is not known with any degree of certainty, the best practice might be to simply fix the value for analysis of portland cements.

Although not specifically addressed in this report, it is important to stress that particle shape may be a significant factor for particle sizing in cementitious powders using LDS. A published study on photocentrifugation sizing of ground quartz, for instance, concluded that the sensitivity of the fine end of the PSD is impacted by the presence of non-spherical quartz geometries.[18]

Overall, our results correspond fairly closely with the applicability guidelines set out in ISO 13320-1:1999(E)[2] pertaining to the selection of an appropriate optical model. These guidelines are summarized below:

- For all particle larger than $\approx$ 50 µm, Fraunhofer works well and gives accurate PSDs.
- For particles smaller than $\approx$ 50 µm, Mie theory is generally the best choice if the optical constants are known.
- For intermediate sized particles in the range $\approx$ 1 µm to 50 µm, with $n > 1.1$ and/or $k > 0.05$, Fraunhofer usually gives good results.
- In all cases where Mie is used, good values for the optical constants must be provided.

In regard to the so-called "intermediate" size fraction, the standard for "good results" is arguable. Our studies on discrete size fractions of aluminum oxide indicate that, if Fraunhofer is used in place of Mie (assuming correct optical constants are known), one can expect volumetric errors exceeding 20 % for coarse particles in the 2 µm to 20 µm range and the appearance of a significant population of submicrometer virtual particles. Virtual particles are an artifact caused by refraction of light through small transparent particles that the Fraunhofer model then interprets as arising from diffraction by very small particles, since Fraunhofer does not take refractive effects into account. We would argue that this constitutes fairly poor reproduction of the actual PSD.

In conclusion, a generic standard for the analysis of cementitious materials by LDS would have to address the selection of a dispersion medium, the selection of an optical model, the selection of optical constants in the case that the Mie model is applied, and a dispersion procedure in the case of wet-method measurements (dry method does not appear applicable to cement powders with a substantial ultrafine fraction). If these factors are fixed, or a logical protocol devised for their selection, we believe that consistent and reproducible PSDs could be obtained by different users on a variety of commercially available instruments.

APPENDIX A

Differential Volume Particle Size Distribution

The density distribution for a collection of particles can be defined as:

$$p(r) = \frac{\mathrm{d}P(r)}{\mathrm{d}r} \tag{A1}$$

where $P(r)$ is the cumulative frequency of particles smaller than size r expressed as a fraction of the total population. The function $p(r)$ is the derivative of the cumulative frequency with respect to size. In practice, a series of finite size intervals are used to approximate the derivative, such that:

$$p(r) = \frac{P(r_{i+1}) - P(r_i)}{r_{i+1} - r_i} \tag{A2}$$

where r_{i+1} and r_i represent the upper and lower bounds of size interval i. It is common to use the volume-weighted frequency, where V is the fractional volume of particles smaller than size r:

$$p(r) = \frac{\Delta V}{\Delta r} = \frac{V(r_{i+1}) - V(r_i)}{r_{i+1} - r_i} \tag{A3}$$

However, one often encounters data presented as the differential volume fraction (or percentage), ΔV, plotted as a function of r. Here r is the characteristic size associated with an interval (typically the upper, lower, or center diameter). The trouble with this practice, widely adopted by instrument manufacturers, is that the magnitude of ΔV is dependent on the width of the chosen interval Δr; as the interval increases, ΔV increases. This complicates the comparison of differential volume PSDs determined on different instruments that may use different interval widths.

Sommer[19] demonstrates in clear terms that the proper method for constructing a "differential" volume PSD is to normalize the differential volume by the corresponding size interval, as shown in Eq.(A3). In this way, the function becomes independent of the interval width, and a straightforward comparison is possible. The distribution function $p(r)$ carries units of 1/size (ΔV is expressed as a unitless fraction or percentage).

The instruments used in the present work provide an *unnormalized* differential volume PSD, and therefore care must be taken when comparing these data with data from other instruments. The intervals used in the two instruments involved in our studies are of roughly the same width, and thus the PSDs for the coarser powders are in very close correspondence. However, the presence or absence of a secondary peak or shoulder in some PSDs determined on different instruments (e.g., dry method vs. wet method data in the present case) could potentially be an artifact related to differences in the interval widths used by the two instruments.

Sommer also points out that semi-logarithmic plots, such as those generated by many commercial instruments (including those used in the present work), can lead to misinterpretation or artifacts. In this case, it is the density distribution of the *logarithm* of the characteristic size $p(\log r)$ that is plotted, not $p(r)$, and interval widths are typically varied logarithmically in order to accommodate the semi-logarithmic ordinate. Again, this can complicate the comparison of data between different instruments.

The interval width and the use of semi-logarithmic plots will not impact data presented as a cumulative frequency distribution: e.g., $V(r)$ versus r.

APPENDIX B

CCRL 135 Property Data

CCRL Proficiency Sample Program
Portland Cement Proficiency Sample No. 135
Final Report - Physical Results - March 24, 2000

Test		#Labs	Average	S.D.	C.V.
N.C. Water	prcnt	220	24.81	2.4	9.85
N.C. Water	prcnt	* 212	24.90	0.34	1.36
Vicat TS Initial	min	211	168	18.5	11.0
Vicat TS Initial	min	* 204	168	15.9	9.49
Vicat TS Final	min	209	279	40.6	14.5
Vicat TS Final	min	* 208	278	39.4	14.2
Gillmore TS Initial	min	172	197	27.3	13.8
Gillmore TS Initial	min	* 169	196	24.1	12.3
Gillmore TS Final	min	172	304	41.9	13.8
Gillmore TS Final	min	* 166	302	35.9	11.9
False Set	prcnt	184	65.8	12.8	19.5
False Set	prcnt	* 182	66.3	12.1	18.3
Autoclave Expan	prcnt	205	0.022	0.055	244
Autoclave Expan	prcnt	* 196	0.021	0.012	58.7
Air Content	prcnt	202	8.84	1.7	19.3
Air Content	prcnt	* 198	8.77	1.0	12.0
AC Mix Water	prcnt	203	68.37	5.6	8.16
AC Mix Water	prcnt	* 198	68.78	2.4	3.56
AC Flow	prcnt	202	87.1	3.4	3.91
AC Flow	prcnt	* 201	87.0	3.3	3.82
Comp Str 28-day	psi	170	5898	401.6	6.81
Comp Str 28-day	psi	* 167	5885	358.8	6.10
CS Flow	prcnt	183	147.5	415.9	282
CS Flow	prcnt	* 173	118.4	8.2	6.97
Fineness AP	sqcm/g	216	3932	117.8	3.00
Fineness AP	sqcm/g	* 201	3928	79.0	2.01
Fineness WT	sqcm/g	38	2042	389.5	19.1
Fineness WT	sqcm/g	* 36	2122	129.6	6.11
45μm Sieve	prcnt	201	95.161	1.00	1.05
45μm Sieve	prcnt	* 196	95.218	0.70	0.736

CCRL Proficiency Sample Program
Portland Cement Proficiency Sample No. 135
Final Report - Chemical Results - March 24, 2000

Test		#Labs	Average	S.D.	C.V.
Silicon Dioxide	prcnt	146	21.440	0.32	1.49
Silicon Dioxide	prcnt	* 141	21.449	0.21	0.988
Aluminum Oxide[1]	prcnt	128	4.442	0.26	5.94
Aluminum Oxide[1]	prcnt	* 123	4.454	0.16	3.65
[1](P_2O_5 & TiO_2 not included)					
Ferric Oxide	prcnt	145	3.062	0.13	4.31
Ferric Oxide	prcnt	* 138	3.068	0.061	1.98
Calcium Oxide	prcnt	144	63.812	0.44	0.688
Calcium Oxide	prcnt	* 140	63.805	0.36	0.564
Free Lime	prcnt	145	0.644	0.20	31.4
Free Lime	prcnt	* 142	0.638	0.18	27.9
Magnesium Oxide	prcnt	143	2.426	0.22	8.96
Magnesium Oxide	prcnt	* 136	2.417	0.118	4.90
Sulfur Trioxide	prcnt	149	2.457	0.136	5.53
Sulfur Trioxide	prcnt	* 143	2.460	0.075	3.04
Loss on Ignition	prcnt	179	0.810	0.10	12.6
Loss on Ignition	prcnt	* 162	0.809	0.066	8.11
Insoluble Residue	prcnt	165	0.192	0.23	122.2
Insoluble Residue	prcnt	* 158	0.156	0.073	46.8
Sodium Oxide	prcnt	123	0.197	0.038	19.6
Sodium Oxide	prcnt	* 115	0.199	0.023	11.8
Potassium Oxide	prcnt	125	0.829	0.045	5.40
Potassium Oxide	prcnt	* 119	0.834	0.022	2.59
Phosphorus Pent	prcnt	67	0.106	0.021	19.9
Phosphorus Pent	prcnt	* 60	0.106	0.013	11.99
Titanium Dioxide	prcnt	75	0.207	0.038	18.2
Titanium Dioxide	prcnt	* 68	0.215	0.016	7.39

64

CCRL Proficiency Sample Program
Portland Cement Proficiency Sample No. 135
Final Report - Heat of Hydration Results - March 24, 2000

Test		#Labs	Average	S.D.	C.V.
Heat Solution Dry	cal/g	22	607.0	11.7	1.94
Heat Solution Dry	cal/g *	20	604.8	8.1	1.339
Heat Sol 7-day	cal/g	22	529.2	9.6	1.80
Heat Sol 7-day	cal/g *	21	527.8	7.3	1.39
Heat Sol 28-day	cal/g	14	523.2	5.1	0.979
Heat Sol 28-day	cal/g *	13	522.2	3.7	0.714
Heat Hyd 7-day	cal/g	22	78.0	5.2	6.69
Heat Hyd 28-day	cal/g	15	86.1	4.6	5.33

Note: 1 cal = 4.184 J

REFERENCES

[1] V.A. Hackley and C.F. Ferraris, "Use of Nomenclature in Dispersion Science and Technology," *NIST Recommended Practice Guide 960-3*, National Institute of Standards and Technology, Gaithersburg, MD, 2001.

[2] ISO 13320-1:1999(E), Particle size analysis — LASER diffraction methods — Part 1: General principles.

[3] ASTM C204-96a, Standard Test Method for Fineness of Hydraulic Cement by Air Permeability Apparatus.

[4] Standard Reference Material 114p, Portland Cement Fineness Standard, National Institute of Standards and Technology, Gaithersburg, MD.

[5] C.F. Ferraris, V.A. Hackley and A.I. Avilés, "Measurement of Particle Size Distribution in Portland Cement Powder: Analysis of ASTM Round-Robin Studies," accepted for publication, *Cem. Concr. Aggr*.

[6] C.F. Ferraris, V.A. Hackley, A.I. Avilés and C.E. Buchanan, "Analysis of the ASTM Round-Robin Test on Particle Size Distribution of Portland Cement: Phase I" NISTIR 6883, National Institute of Standards and Technology, 2002.

[7] C.F. Ferraris, V.A. Hackley, A.I. Avilés and C.E. Buchanan, "Analysis of the ASTM Round-Robin Test on Particle Size Distribution of Portland Cement: Phase II" NISTIR 6931, National Institute of Standards and Technology, 2002.

[8] M. Cyr, and A. Tagnit-Hamou, "Particle size distribution of fine powders by LASER diffraction spectrometry. Case of cementitious materials," *Mater. Structur.*, **34**, 342-350 (2000).

[9] D.P. Bentz, E.J. Garboczi, C.J. Haecker and O.M. Jensen, "Effects of Cement Particle Size Distribution on Performance Properties of Portland Cement-Based Materials," *Cem. Concr. Res.*, **29**, 1663-1671 (1999).

[10] D.P. Bentz, "Effects of Cement PSD on Porosity Percolation and Self-Desiccation," pp 127-134 in *Self-Desiccation and Its Importance in Concrete Technology*, Proceedings of the 2nd International Research Seminar, June 18, 1999, Lund, Sweden. (Edited by B. Persson and G. Fagerlund) 1999.

[11] E.J. Garboczi, D.P. Bentz, K.A. Snyder, N.S. Martys, P.E. Stutzman, C.F. Ferraris and J.W. Bullard, "Modeling and Measuring the Structure and Properties of Cement-Based Materials," electronic monograph, National Institute of Standards and Technology (http://ciks.cbt.nist.gov/monograph), 2003.

[12] C.F. Bohren and D.R. Huffman, *Absorption and Scattering of Light by Small Particles*, John Wiley & Sons, New York, NY, 1983.

[13] *Handbook of Optical Constants of Solids*, edited by E.D. Palik, Academic Press, New York, NY, 1985; *Handbook of Optical Constants of Solids II*, edited by E.D. Palik, Academic Press, New York, NY, 1991.

[14] Handbook of Chemistry and Physics, 62nd Edition, 1981-82, CRC Press, Boca Raton, FL.

[15] J. Catalán, V. López, P. Pérez, "Solvent Dipolarity/Polarizability (SPP) of Alcoholic Solvents," *Liebigs Ann.* 793-795 (1995).

[16] B. Grobety and A. Mocellin, "Preparation of AlN-TiO$_2$ Powder Compacts using Colloidal Methods," *Ceram. Int.*, **15**[5], 271-279 (1989).

[17] V.A. Hackley, J. Patton, L.H. Lum, R. Wäsche, H. Abe, M. Naito, Y. Hotta and H. Pendse, "Analysis of the Isoelectric Point in Moderately Concentrated Alumina Suspensions by Electroacoustic and Streaming Potential Methods", *J. Dispersion Sci. Tech.*, **23**[5], 601-617 (2002).

[18] P. Bowen, C. Hérard, R. Humphry-Baker and E. Sato, "Accurate Submicron Particle-Size Measurement of Alumina and Quartz Powders using a Cuvette Photocentrifuge," *Powder Tech.*, **81**[3], 235-240 (1994).

[19] K. Sommer, "40 Years of Presentation Particle Size Distributions – Yet Still Incorrect?," *Part. Part. Syst. Charact.*, **18**, 22-25 (2001).